doi.org/10.26434/chemrxiv.12444908.v1

A Modular, Self-Assembling Metallaphotocatalyst for Cross Couplings Using the Full Visible-Light Spectrum

Susanne Reischauer, Volker Strauss, Bartholomäus Pieber

Submitted date: 08/06/2020 • Posted date: 09/06/2020

Citation information: Reischauer, Susanne; Strauss, Volker; Pieber, Bartholomäus (2020): A Modular, Self-Assembling Metallaphotocatalyst for Cross Couplings Using the Full Visible-Light Spectrum. ChemRxiv. Preprint. https://doi.org/10.26434/chemrxiv.12444908.v1

The combination of nickel- and photocatalysis has unlocked a variety of cross couplings. These protocols rely on a few photocatalysts that can only convert a small portion of visible light (<500 nm) into chemical energy. Many dyes that absorb a much broader spectrum of light are not applicable due to their short-lived excited states. Here we describe a self-assembling catalyst system that overcomes this limitation. The modular approach combines nickel catalysis with dye-sensitized titanium dioxide and can be used to catalyze various bond formations.

A modular, self-assembling metallaphotocatalyst for cross couplings using the full visible-light spectrum

Authors: Susanne Reischauer,[1,2] Volker Strauss,[3] Bartholomäus Pieber[1]*

Affiliations:

[1]Department of Biomolecular Systems, Max Planck Institute of Colloids and Interfaces, Am Mühlenberg 1, 14476 Potsdam, Germany

[2]Department of Chemistry and Biochemistry, Freie Universität Berlin, Arnimalle 22, 14195 Berlin, Germany

[3]Department of Colloid Chemistry, Max Planck Institute of Colloids and Interfaces, Am Mühlenberg 1, 14476 Potsdam, Germany

*Correspondence to: bartholomaeus.pieber@mpikg.mpg.de

Abstract: The combination of nickel- and photocatalysis has unlocked a variety of cross couplings. These protocols rely on a few photocatalysts that can only convert a small portion of visible light (<500 nm) into chemical energy. Many dyes that absorb a much broader spectrum of light are not applicable due to their short-lived excited states. Here we describe a self-assembling catalyst system that overcomes this limitation. The modular approach combines nickel catalysis with dye-sensitized titanium dioxide and can be used to catalyze various bond formations.

The combination of photo- and nickel catalysis (metallaphotocatalysis) has emerged as a powerful strategy for carbon–carbon and carbon–heteroatom cross couplings (Fig. 1A) (*1-3*). Key to the success are redox or photosensitization events between a nickel- and a photocatalyst (PC). Applicable PCs are iridium and ruthenium polypyridyl complexes (*2*), or carbazolyl dicyanobenzenes (*4*), with tailored redox potentials or triplet energies, and long-lived excited states (Fig. 1B). These PCs are limited to short excitation wavelengths that can cause unwanted side-reactions (*5*). These could be avoided in a metallaphotocatalytic system that harvests longer wavelengths. Current approaches towards photocatalysis with low photon energies require complex catalytic cocktails that enable photon upconversion (*6*), osmium complexes as PCs (*7*), or multi-photon excitation processes (*5*).

The use of abundant dyes that absorb broadly across the visible-light spectrum is highly desirable. The redox potentials and triplet energies of many commodity chemicals, such as fluorescein, rose bengal, or coumarins are in theory suitable for metallaphotocatalysis (*8*), but their short excited state lifetime render a diffusion-limited interaction with a nickel catalyst in a homogeneous solution unlikely (Fig. 1B). These dyes are, however, able to sensitize metal oxide semiconductors, such as TiO_2, in dye-sensitized solar cells (DSSCs) (*9*), or dye-sensitized photocatalysts (DSPs) for light-driven H_2 production (*10*). The carboxylic acid groups of the dyes bind to the surface hydroxyl groups of TiO_2. This facilitates electron injection into the conduction band of the semiconductor upon photoexcitation. This results in a charge-separated species that is sustained for several microseconds (*11*).

We wondered whether immobilization of a suitable nickel complex on dye-sensitized TiO_2 accesses a bifunctional material that serves as metallaphotocatalyst (Fig. 1 C). We hypothesized that such a system overcomes limitations related to short excited state lifetimes and diffusion-controlled energy or single electron transfer events due to the close spatial proximity between the PC and the nickel catalyst. The proposed, modular design of dye-sensitized metallaphotocatalysts (DSMPs) allows selecting dyes/wavelengths and nickel complexes depending on the respective application.

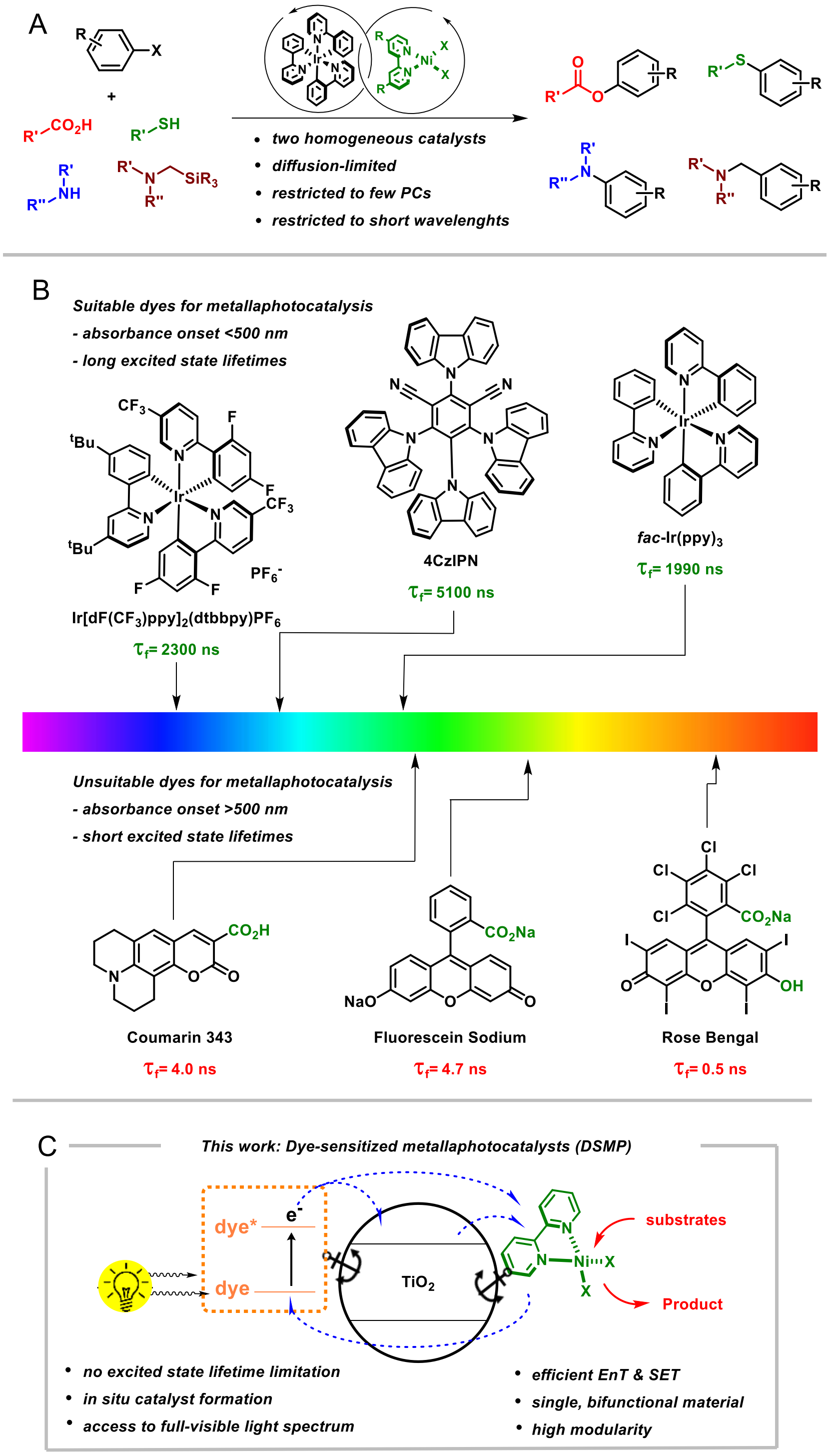

Fig. 1. Working hypothesis towards a modular, heterogeneous metallaphotocatalyst. Cross-coupling reactions using homogeneous metallaphotocatalysis (**A**). Onset of absorption of photocatalysts. The suitability for homogeneous metallaphotocatalysis depends on excited state lifetime (**B**). Dye-sensitized metallaphotocatalysts (DSMP) are proposed to overcome excited state lifetime limitations (**C**).

Our investigations started with the *O*-arylation of carboxylic acids that was reported using the PC Ir(ppy)$_3$ (ppy = 2-phenylpyridine) and a nickel bipyridine complex. The cross-coupling proceeds *via* an energy transfer (EnT) mechanism (*12*), and is feasible using semiconductors that absorb blue light (*13, 14*), but does not work using simple organic dyes (*4*). We first tested if anchoring of a nickel complex on TiO$_2$ P25 results i) in an active, heterogeneous metallaphotocatalyst, and ii) improves the reaction yield due to permanent spatial proximity of the PC and the nickel catalyst using near-UV light. A ligand equipped with carboxylic acid groups (dcbpy = 2,2′-bipyridine-4,4′-dicarboxylic acid) indeed gave a higher yield of the C–O cross coupling product **1** than a ligand that lacks functionalities capable of binding to the semiconductor's surface (dtbbpy = 4,4′-di-*tert*-butyl-2,2′-dipyridyl) (Fig. 2A). Next, dyes that contain a suitable anchoring group were studied as sensitizers using green light (525 nm). Fluorescein sodium (NaFluo) showed the best results (see Supplementary Information). The C–O coupling was also feasible at higher wavelengths (666 nm) using the ruthenium dye N3 that has an excited state lifetime of 20 ns (*9*). The DSMPs self-assemble *in situ*. An *ex situ* preparation of the DSMPs was carried out to characterize the bifunctional materials (Fig. 2B). The UV–Vis spectra of the materials confirmed immobilization of the dyes on the metal oxide, and inductively coupled plasma - optical emission spectrometry (ICP-OES) corroborated anchoring of the nickel complex.

Optimization of all reaction parameters using the *in situ* DSMP approach resulted in a highly selective formation of **1** using blue (440 nm), green (525 nm), or red (666 nm) light (Fig. 2C). The highest activities were obtained when the amount of dye (1.25 mol%) and NiCl$_2$·dcbpy (10 mol%) exceeded the loading that was determined using *ex situ* DSMP preparation. This is rationalized by a dynamic equilibrium between immobilized and unbound NiCl$_2$·dcbpy as well as dye molecules, which also contribute to productive catalysis in the course of the bulk experiment (*10*). No product formation was observed in the absence TiO$_2$ P25, the dye, dcbpy, nickel salt, or light.

The DSMP approach also enabled metallaphotocatalyzed C–S (*15*), C–N (*16*), and C–C (*17*) bond formations that proceed *via* single electron transfer processes (SET) (Fig. 2D). The modular design principle and the self-assembling strategy facilitated a straightforward optimization of dyes, nickel salts, and ligands resulting in selective cross-couplings using blue (440 nm), green (525 nm), and red (666 nm) light. With regards to the C–C coupling, 68% of the desired product (**4**) were obtained using blue light, which is similar to the homogeneous metallaphotocatalysis system (*17*). Reactions at higher wavelengths, not accessible with the original, homogeneous approach, resulted in a higher selectivity.

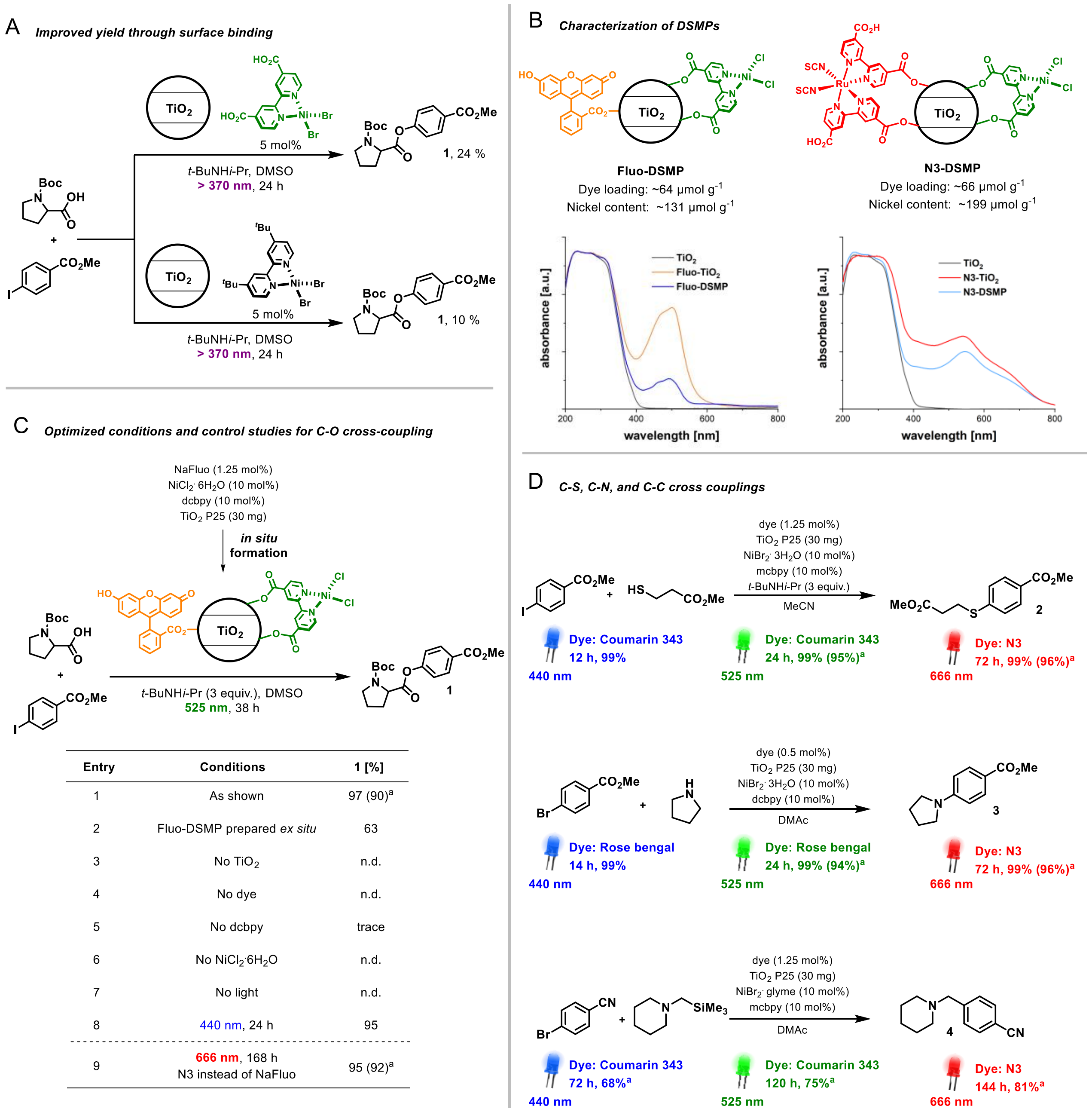

Entry	Conditions	1 [%]
1	As shown	97 (90)^a
2	Fluo-DSMP prepared *ex situ*	63
3	No TiO$_2$	n.d.
4	No dye	n.d.
5	No dcbpy	trace
6	No NiCl$_2$·6H$_2$O	n.d.
7	No light	n.d.
8	440 nm, 24 h	95
9	666 nm, 168 h N3 instead of NaFluo	95 (92)^a

Fig. 2. Self-assembling, modular metallaphotocatalysts enable cross-couplings using the entire visible-light spectrum. Anchoring of nickel complexes on TiO$_2$ P25 improves yield due to permanent spatial proximity (**A**). UV–Vis spectra and nickel/dye loadings of two representative DSMPs (**B**). Optimized conditions and control experiments for the *O*-arylation of carboxylic acids using DSMPs. (**D**) C–S, C–N, and C–C cross coupling catalyzed by DSMPs using blue, green, or red light. Yields were determined by ^{1}H-NMR using 1,3,5-trimethoxybenzene as internal standard if not stated otherwise. ^{a}Isolated yields. DSMP = dye-sensitized metallaphotocatalyst n.d. = not detected. dcbpy = 2,2′-bipyridine-4,4′-dicarboxylic acid. mcbpy = 4'-methyl-2,2'-bipyridine-4-carboxylic acid. glyme = 1,2-dimethoxyethane. NaFluo = fluorescein sodium

The dynamic equilibrium between immobilized and unbound molecules is responsible for leaching of nickel and fluorescein during catalyst recycling studies and caused a gradual decrease of the yield of **1** (Fig. 3A). Addition of either NaFluo or the nickel salt restored the catalytic activity. This indicated that the amount of immobilized dye molecules and nickel complexes have to be above a certain limit to observe catalytic activity. We therefore questioned if only the close proximity of the dye molecules and the nickel complex is responsible for productive catalysis, and TiO_2 P25 only acts as support. In other words, an “on-particle” rather than a “through-particle” mechanism could be responsible for overcoming the short excited state lifetime (Fig. 3B). To test this hypothesis, we substituted TiO_2 P25 with the insulating metal oxides (MO) SiO_2 and Al_2O_3 that only enable binding of the dye and the nickel complex and observed product formation for all cross-couplings, but with significantly lower efficiency compared to TiO_2 P25 (Fig. 3C). A second set of experiments was carried out using a nickel complex that is not able to bind to the surface of metal oxides. Here, only experiments with the semiconductor TiO_2 P25 gave productive catalysis. This confirms that dye sensitization leads to a charge-separated species that is sufficiently long-lived to turn over a homogeneous nickel catalyst in a semi-heterogeneous, diffusion-controlled reaction. Spectrophotometric titrations unveiled the electronic communication between the excited dye and the immobilized nickel complex “through” a semiconductor. Static fluorescence quenching of fluorescein-sensitized TiO_2 P25 was observed with a nickel complex that binds to the semiconductor’s surface ($NiCl_2$·dcbpy). $NiCl_2$·dtbbpy showed solely dynamic quenching (Fig. 3D). Titration experiments with fluorescein bound to SiO_2 instead of TiO_2 P25 displayed dynamic quenching behavior in case of both nickel complexes, and significantly lower quenching rates. Taking all results together, we assumed that a combination of “on-particle” and “through-particle” processes is responsible for the high catalytic activity of DSMPs with TiO_2 P25.

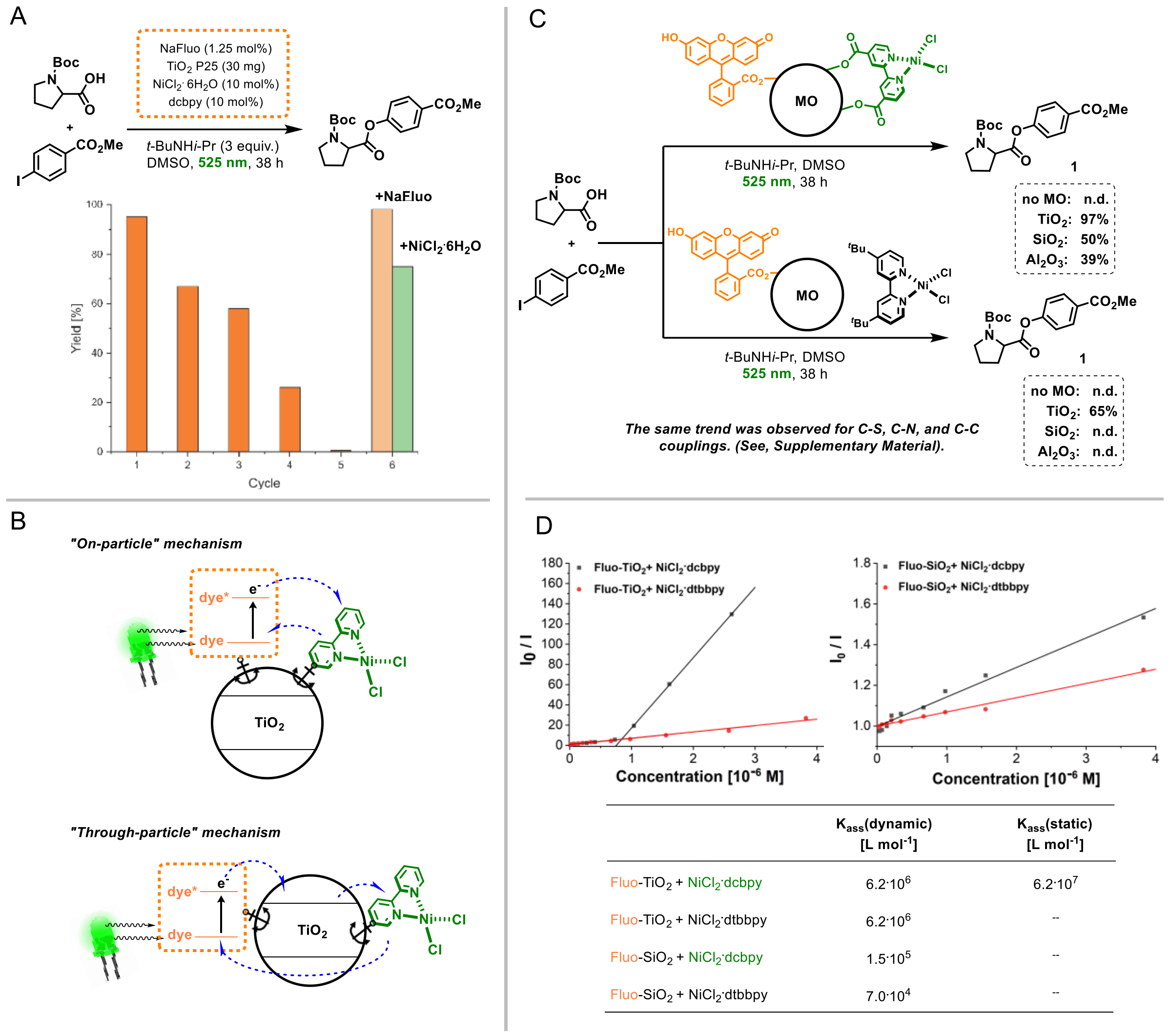

	K_{ass}(dynamic) [L mol^{-1}]	K_{ass}(static) [L mol^{-1}]
Fluo-TiO_2 + $NiCl_2$·dcbpy	$6.2 \cdot 10^6$	$6.2 \cdot 10^7$
Fluo-TiO_2 + $NiCl_2$·dtbbpy	$6.2 \cdot 10^6$	--
Fluo-SiO_2 + $NiCl_2$·dcbpy	$1.5 \cdot 10^5$	--
Fluo-SiO_2 + $NiCl_2$·dtbbpy	$7.0 \cdot 10^4$	--

Fig. 3. Mechanistic investigations. (**A**) Recycling experiments showed that catalytic inactive materials still contain nickel complexes and dye molecules. (**B**) DSMPs might work *via* an “on-particle” and/or “through-particle” mechanism. (**C**) Experiments using insulating metal oxides and diffusion controlled metallaphotocatalysis. (**D**) Spectrophotometric titrations show static quenching for DSMPs, whereas solely dynamic quenching was observed in other systems. MO = metal oxide. dcbpy = 2,2′-bipyridine-4,4′-dicarboxylic acid. dtbbpy = 4,4'-di-*tert*-butyl-2,2'-bipyridine. Fluo = fluorescein.

In addition, we sought to compare the selectivity of DSMPs with homogenous metallaphotocatalysis systems in the C–O arylation of (*E*)-cinnamic acid with 4-iodobenzotrifluoride (Figure 4). The resulting coupling product (***E*-5**) is prone to subsequent photocatalytic isomerization or cycloadditions that could lead to low selectivities (*18, 19*). We indeed observed significant amounts of the undesired Z-isomer (***Z*-5**) when Ir(ppy$_3$) was used as PCs using 440 nm irradiation. Other Ir complexes gave even worse results (see Supplementary Information). Control experiments showed that ***E*-5** is also slowly converted to ***Z*-5** at 440 nm in the absence of a PC (see Supplementary Information). The selectivity was, however, not improved using Ir(ppy3) and 525 nm irradiation, because the triplet energy of the PC is not wavelength-dependent. The *E*-*Z* isomerization was also observed when the reaction was catalyzed by a DSMP at 440 nm, but was totally suppressed by switching to higher wavelengths, resulting in a selective formation of ***E*-5**.

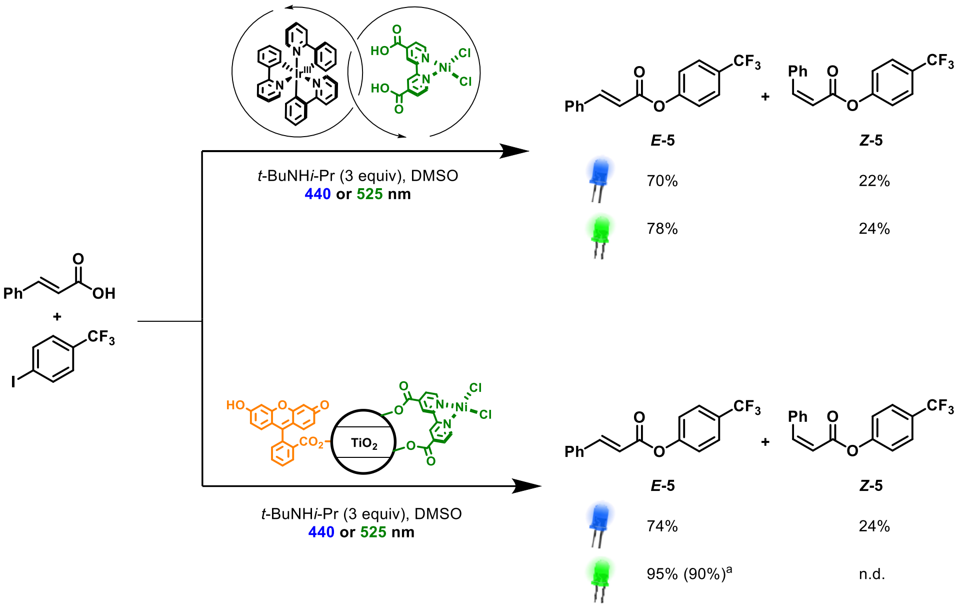

Figure 4. C–O arylation of (*E*)-cinnamic acid with 4-iodobenzotrifluoride with different metallaphotocatalyst systems. Yields were determined by ^{1}H-NMR using 1,3,5-trimethoxybenzene as internal standard if not stated otherwise. ^{a}Isolated yield in parentheses.

The DSMP concept overcomes the constraint of long excited state lifetimes of PCs for metallaphotocatalysis and unlocks the potential of many dyes that were previously unsuitable. Many cross couplings can be carried out using the entire visible light spectrum and selectivity issues can be tackled strategically. The simplicity and modularity of DSMPs suggest that the present approach will complement existing methods.

Acknowledgments: We gratefully acknowledge the Max-Planck Society for generous financial support. S.R. and B.P. thank the German Chemical Industry Fund (Fonds der Chemischen Industrie, FCI) for funding through a Liebig Fellowship. B.P. thanks the Deutsche Forschungsgemeinschaft (DFG, German Research Foundation) under Germany´s Excellence Strategy – EXC 2008 – 390540038 – UniSysCat for financial support. We thank our colleagues Prof. Peter H. Seeberger, Dr. Jamal Malik, Dr. Martina Delbianco, Dr. Kerry Gilmore, Dr. Lukas Zeininger, Cristian Cavedon, Silvia Fürstenberg, Jessica Brandt and Katharina ten Brummelhuis (all MPIKG), for scientific, technical and analytical support.

References:

1. J. A. Milligan, J. P. Phelan, S. O. Badir, G. A. Molander, Alkyl Carbon-Carbon Bond Formation by Nickel/Photoredox Cross-Coupling. *Angew. Chem. Int. Ed.* **58**, 6152-6163 (2019).
2. J. Twilton *et al.*, The merger of transition metal and photocatalysis. *Nat. Rev. Chem.* **1**, 1-18 (2017).
3. C. Cavedon, P. H. Seeberger, B. Pieber, Photochemical Strategies for Carbon–Heteroatom Bond Formation. *Eur. J. Org. Chem.* **10**, 1379-1392 (2020).
4. J. Lu *et al.*, Donor–Acceptor Fluorophores for Energy-Transfer-Mediated Photocatalysis. *J. Am. Chem. Soc.* **140**, 13719-13725 (2018).
5. F. Glaser, C. Kerzig, O. S. Wenger, Multi-Photon Excitation in Photoredox Catalysis: Concepts, Applications, Methods. *Angew. Chem. Int. Ed.* **59**, 2-21 (2020).
6. B. D. Ravetz *et al.*, Photoredox catalysis using infrared light via triplet fusion upconversion. *Nature.* **565**, 343-346 (2019).
7. B. D. Ravetz *et al.*, *https://doi.org/10.26434/chemrxiv.12124215.v1*. (2020).
8. N. A. Romero, D. A. Nicewicz, Organic Photoredox Catalysis. *Chem. Rev.* **116**, 10075-10166 (2016).
9. A. Hagfeldt, G. Boschloo, L. Sun, L. Kloo, H. Pettersson, Dye-Sensitized Solar Cells. *Chem. Rev.* **110**, 6595-6663 (2010).
10. J. Willkomm *et al.*, Dye-sensitised semiconductors modified with molecular catalysts for light-driven H2 production. *Chem. Soc. Rev.* **45**, 9-23 (2016).
11. A. Hagfeldt, M. Graetzel, Light-Induced Redox Reactions in Nanocrystalline Systems. *Chem. Rev.* **95**, 49-68 (1995).
12. E. R. Welin, C. Le, D. M. Arias-Rotondo, J. K. McCusker, D. W. C. MacMillan, Photosensitized, energy transfer-mediated organometallic catalysis through electronically excited nickel(II). *Science* **355**, 380-385 (2017).
13. X. Zhu *et al.*, Lead halide perovskites for photocatalytic organic synthesis. *Nat. Commun.* **10**, 2843 (2019).
14. B. Pieber *et al.*, Semi-heterogeneous Dual Nickel/Photocatalysis using Carbon Nitrides: Esterification of Carboxylic Acids with Aryl Halides. *Angew. Chem. Int. Ed.* **58**, 9575-9580 (2019).
15. M. S. Oderinde, M. Frenette, D. W. Robbins, B. Aquila, J. W. Johannes, Photoredox Mediated Nickel Catalyzed Cross-Coupling of Thiols With Aryl and Heteroaryl Iodides via Thiyl Radicals. *J. Am. Chem. Soc.* **138**, 1760-1763 (2016).
16. E. B. Corcoran *et al.*, Aryl amination using ligand-free Ni(II) salts and photoredox catalysis. *Science* **353**, 279-283 (2016).
17. C. Remeur, C. B. Kelly, N. R. Patel, G. A. Molander, Aminomethylation of Aryl Halides Using α-Silylamines Enabled by Ni/Photoredox Dual Catalysis. *ACS Catalysis* **7**, 6065-6069 (2017).
18. T. Lei *et al.*, General and Efficient Intermolecular [2+2] Photodimerization of Chalcones and Cinnamic Acid Derivatives in Solution through Visible-Light Catalysis. *Angew. Chem. Int. Ed.* **56**, 15407-15410 (2017).
19. P. Shu *et al.*, Synthesis of (Z)-Cinnamate Derivatives via Visible-Light-Driven E-to-Z Isomerization. *SynOpen* **03**, 103-107 (2019).

Supplementary Materials for

A modular, self-assembling metallaphotocatalyst for cross couplings using the full visible-light spectrum

Susanne Reischauer, Volker Strauss, Bartholomäus Pieber*

Corresponding author. Email: bartholomaeus.pieber@mpikg.mpg.de

Contents

1. General remarks

Substrates, reagents, and solvents were purchased from commercial suppliers and used without further purification. Titanium dioxide Aeroxide P25 (Acros), silicon dioxide (10-20 nm particle size; Aldrich), and aluminum oxide, basic (50-200 µm, 60Å; Acros) were used. 2,2'-Bipyridine-4,4'-diphosphonic acid (*20*), 4,4′-di(p-carboxyphenyl)-2,2′-bipyridine (*21*), *N-tert*-butylisopropylamine (BIPA) (*22*), and 1-((trimethylsilyl)methyl)piperidine (*17*) were prepared according to literature procedures. LED lamps for photocatalytic experiments were purchased from Kessil Lightning (*23*). ^{1}H-, ^{13}C-, and ^{19}F spectra were recorded on a Varian 400 spectrometer (400 MHz, Agilent), a Ascend^{TM} 400 spectrometer (400 MHz, cryoprobe, Bruker) and a Varian 600 spectrometer (600 MHz, Agilent) at 298 K, and are reported in ppm relative to the residual solvent peaks. Peaks are reported as: s = singlet, d = doublet, t = triplet, q = quartet, m = multiplet or unresolved, with coupling constants in Hz. Analytical thin layer chromatography (TLC) was performed on pre-coated TLC-sheets, ALUGRAM Xtra SIL G/UV$_{254}$ sheets (Macherey-Nagel) and visualized with 254 nm light or staining solutions followed by heating. Purification of final compounds was carried out by flash chromatography on the Reveleris X2 Flash Chromatography System from GRACE using prepacked columns with 40 µm silica gel. Silica 60 M (0.04-0.063 mm) silica gel (Sigmal Aldrich) was used for dry loading of the crude compounds on the flash chromatography system. Centrifugation was carried out using an Eppendorf 5430 centrifuge. UV/Vis spectra of liquid samples were recorded using a UV-1900 spectrometer (Shimadzu). Diffuse reflectance UV/Vis spectra of powders were recorded on a Shimadzu UV-2600 spectrometer equipped with an integrating sphere. Inductively coupled plasma - optical emission spectrometry (ICP-OES) was carried out using a Horiba Ultra 2 instrument equipped with a photomultiplier tube detection system. FTIR spectra were recorded on a Thermo Scientific Nicolet iD5 spectrometer. High-resolution mass spectral data were obtained using a Waters XEVO G2-XS 4K spectrometer with the XEVO G2-XS QTOF capability kit (ESI) and a Micromass GC-TOF micro (Water Inc.) (EI). Spectrophotometric titrations were carried out in 10 mm OS cuvettes. Prior to the measurements, the optical density of the TiO_2 or SiO_2 dispersions were adjusted to ~0.1 at 505 nm for comparability and to reduce the influence of inner filter effects. UV-vis-NIR absorption measurements were performed with a Specord 210 plus from Analytik Jena. Fluorescence measurements were performed with a Fluoromax 4 from Horiba.

1.1 440 nm setup

Experiments using blue light were carried out using a Kessil PR160-440 LED (Fig. S1). Two sealed reaction vessels were placed on a stirring plate 4.5 cm away from a single lamp. To avoid heating of the reaction mixture, a fan was used for cooling. All reactions were performed with maximum stirring speed. The LED also emits light below 400 nm, which enabled the excitation of pure titanium dioxide Aeroxide P25 for initial experiments (see Fig. 2A in the manuscript)

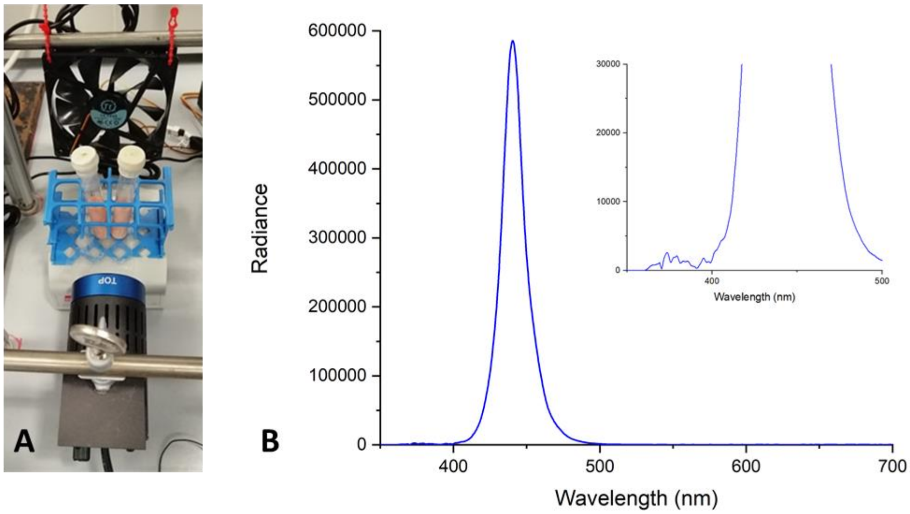

Fig. S1. Setup for blue light experiments (**A**). Emission spectra of the Kessil PR160-440 (**B**)

1.2 525 nm setup

Experiments using green light were carried out using a Kessil PR160-525 LED (Fig. S2). Two sealed reaction vessels were placed on a stirring plate 4.5 cm away from a single lamp. To avoid heating of the reaction mixture, a fan was used for cooling. All reactions were performed with maximum stirring speed.

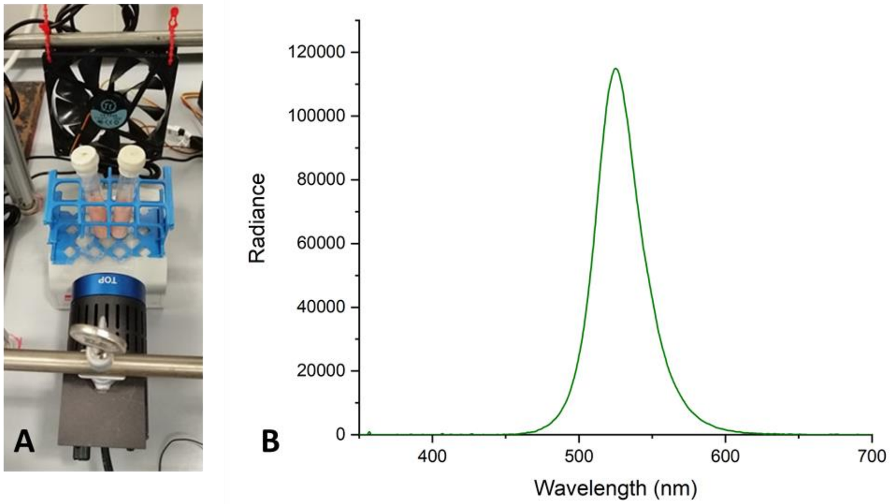

Fig. S2. Setup for green light experiments (**A**). Emission spectra of the Kessil PR160-525 (**B**).

1.3 666 nm setup

Experiments using red light were carried out using a Kessil H160 Tuna Flora LED in “red” mode (Fig. S3). Two sealed reaction vessels were placed between two lamps on a stirring plate (4.5 cm distance from each lamp). To avoid heating of the reaction mixture, a fan was used for cooling. All reactions were performed with maximum stirring speed.

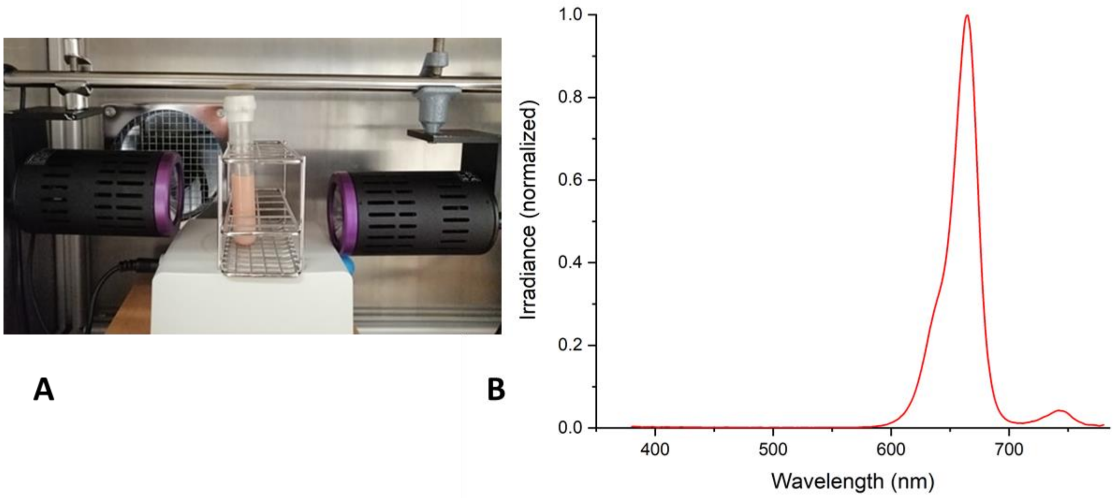

Fig. S3. A Setup for red light experiments (**A**). Emission spectra of the Kessil H160 Tuna Flora LED in “red” mode (**B**).

2 *Ex situ* preparation and characterization of DSMPs

General experimental procedure for the *ex situ* preparation of DSMPs. TiO_2 Aeroxide P25 (30 mg) was dispersed in 3 mL DMSO and sonicated for 5 min. The respective dye (2.4 µmol), $NiCl_2 \cdot 6H_2O$ (19.0 µmol) and 2,2′-bipyridine-4,4′-dicarboxylic acid (dcbpy, 19.0 µmol) were added and the mixture was again sonicated for 10 min. The mixture was stirred overnight and the solid material was separated by centrifugation. After washing with DMSO and separation by centrifugation (2x), the DMSP was lyophilized overnight.

The experimental procedure was also modified to immobilize only the dye (dye-TiO_2), or the nickel complex (TiO_2-$NiCl_2 \cdot$dcbpy) on TiO_2 Aeroxide P25.

2.1 Fluo-TiO_2-$NiCl_2 \cdot$dcbpy

Fluorescein sodium (NaFluo) was used as dye (Fig. S4). The amount of immobilized fluorescein (Fluo, ~64 µmol g^{-1}) was determined by UV/Vis spectrometry. The solution of the dye in DMSO was measured before and after (supernatant) the immobilization process and the amount of immobilized dye was determined using a calibration curve.

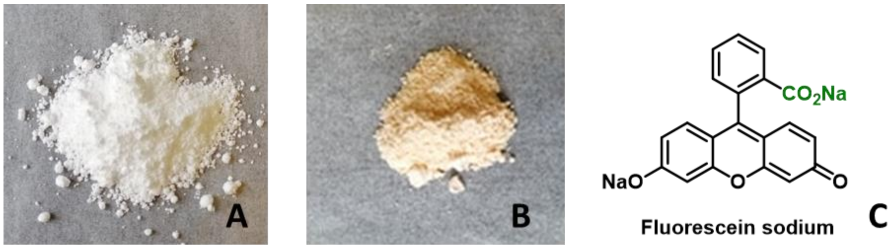

Fig. S4. Fluo-TiO_2-$NiCl_2 \cdot$dcbpy. Unfunctionalized TiO_2 Aeroxide P25 (**A**) and Fluo-TiO_2-$NiCl_2 \cdot$dcbpy (**B**). Structure of fluorescein sodium (**C**). The functionalities that bind to the surface hydroxyl groups of TiO_2 are marked in green.

Table S1. Nickel content of Fluo-TiO_2-$NiCl_2$·dcbpy and reference samples determined by ICP-OES analysis

Sample	Ni [mg/g catalyst]
Fluo-TiO_2-$NiCl_2$·dcbpy	6.50
TiO_2	0.02
TiO_2-$NiCl_2$·dcbpy	5.45

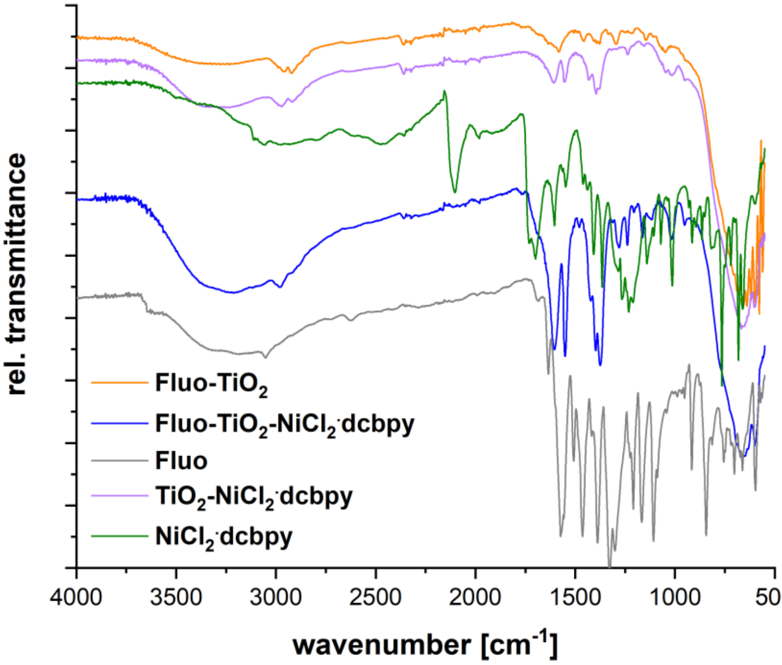

Fig. S5. FTIR spectra of Fluo-TiO_2-$NiCl_2$·dcbpy and reference samples.

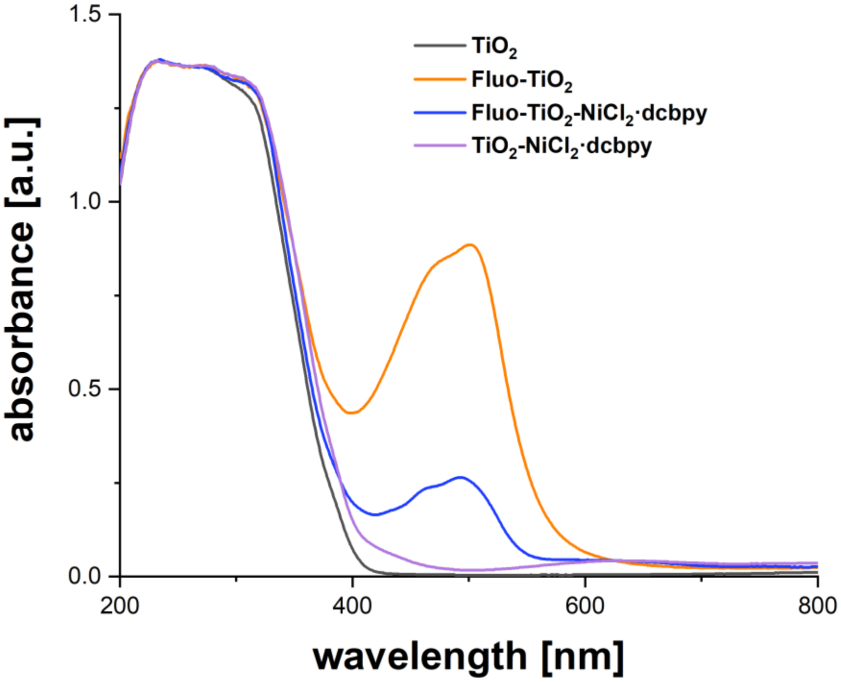

Fig. S6. Diffuse reflectance UV/Vis spectra of Fluo-TiO_2-$NiCl_2$·dcbpy and reference samples.

2.2 N3-TiO_2-$NiCl_2$·dcbpy

The ruthenium complex N3 was used as dye (Fig. S7). The amount of immobilized N3 (~66 µmol g^{-1}) was determined by UV/Vis spectrometry. The solution of the dye in DMSO was measured before and after (supernatant) the immobilization process and the amount of immobilized dye was determined using a calibration curve.

Fig. S7. N3-TiO_2-$NiCl_2$·dcbpy. Unfunctionalized TiO_2 Aeroxide P25 (**A**) and N3-TiO_2-$NiCl_2$·dcbpy (**B**). Structure of N3 (**C**). The functionalities that bind to the surface hydroxyl groups of TiO_2 are marked in green.

Table S2. Nickel content of N3-TiO_2-$NiCl_2$·dcbpy and reference samples determined by ICP-OES analysis

Sample	Ni [mg/g catalyst]
N3-TiO_2-$NiCl_2$·dcbpy	11.3
TiO_2	0.02
TiO_2-$NiCl_2$·dcbpy	5.45

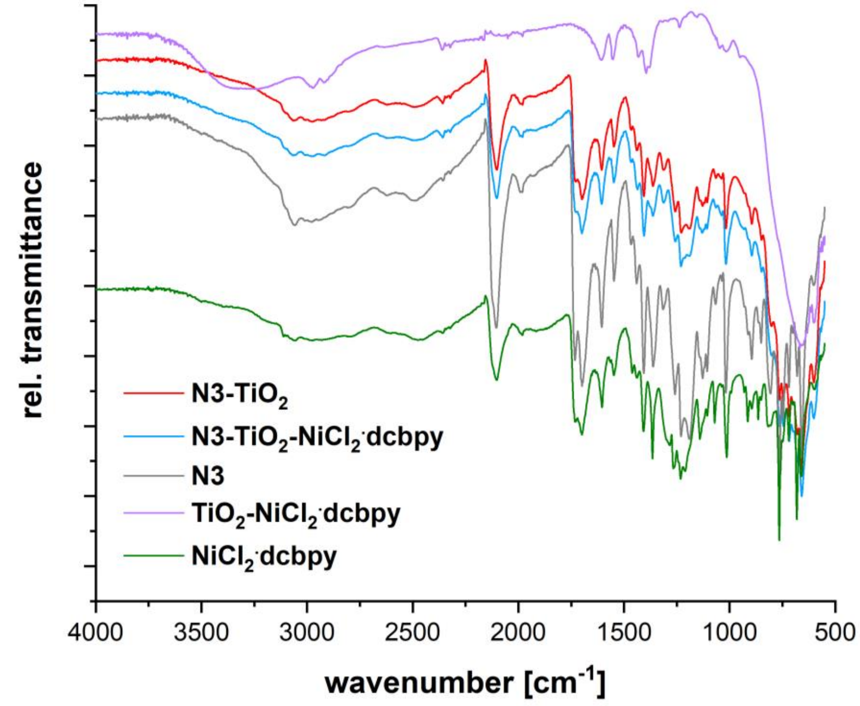

Fig. S8. FTIR spectra of N3-TiO_2-$NiCl_2$·dcbpy and reference samples.

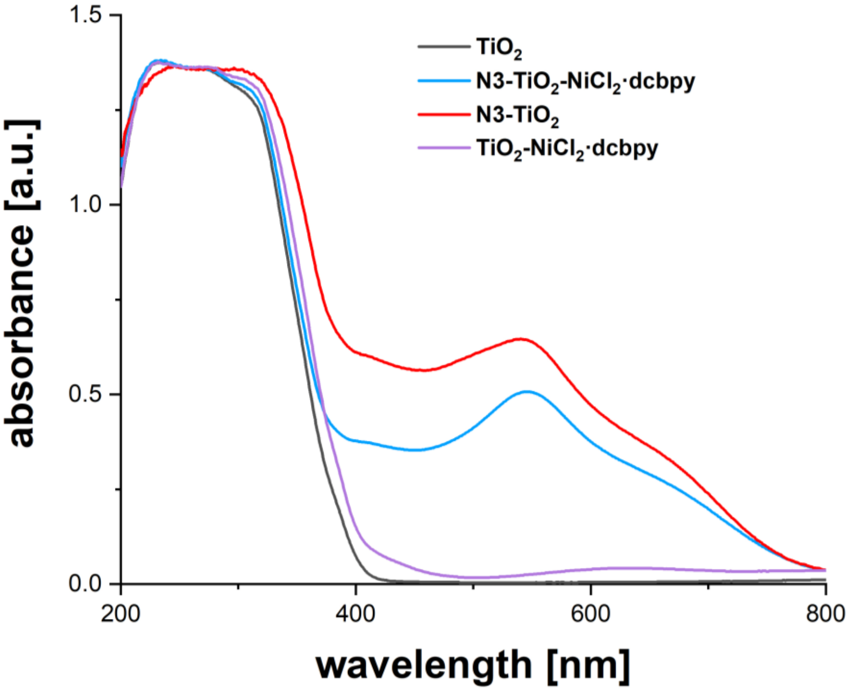

Fig. S9. Diffuse reflectance UV/Vis spectra of N3-TiO_2-$NiCl_2$·dcbpy and reference samples.

3 C-O cross-coupling

3.1 Optimization studies using *in situ* generated DSMPs.

General experimental procedure for screening experiments *via in situ* DSMP preparation. An oven dried vial (19 x 100 mm) equipped with a stir bar was charged with TiO_2 P25, methyl 4-iodobenzoate, *N*-Boc proline (*N*-(*tert*-Butoxycarbonyl)-L-proline), a dye, a Ni^{II} salt and the ligand. Subsequently, the solvent (anhydrous, 3 mL) and *N*-*tert*-butylisopropylamine were added and the vial was sealed with a septum and Parafilm. The reaction mixture was sonicated for 5-10 min followed by stirring for 5 minutes to obtain a fine dispersion. The mixture was then degassed by bubbling argon for 10 min. The mixture was irradiated with the respective LED lamps with rapid stirring (1400 rpm). After the respective reaction time, one equivalent of 1,3,5-trimethoxybenzene was added. An aliquot of the reaction mixture (~200 µL) was filtered, diluted with DMSO-d_6 and subjected to ^{1}H-NMR analysis. For a representative NMR spectrum, see Fig. S10.

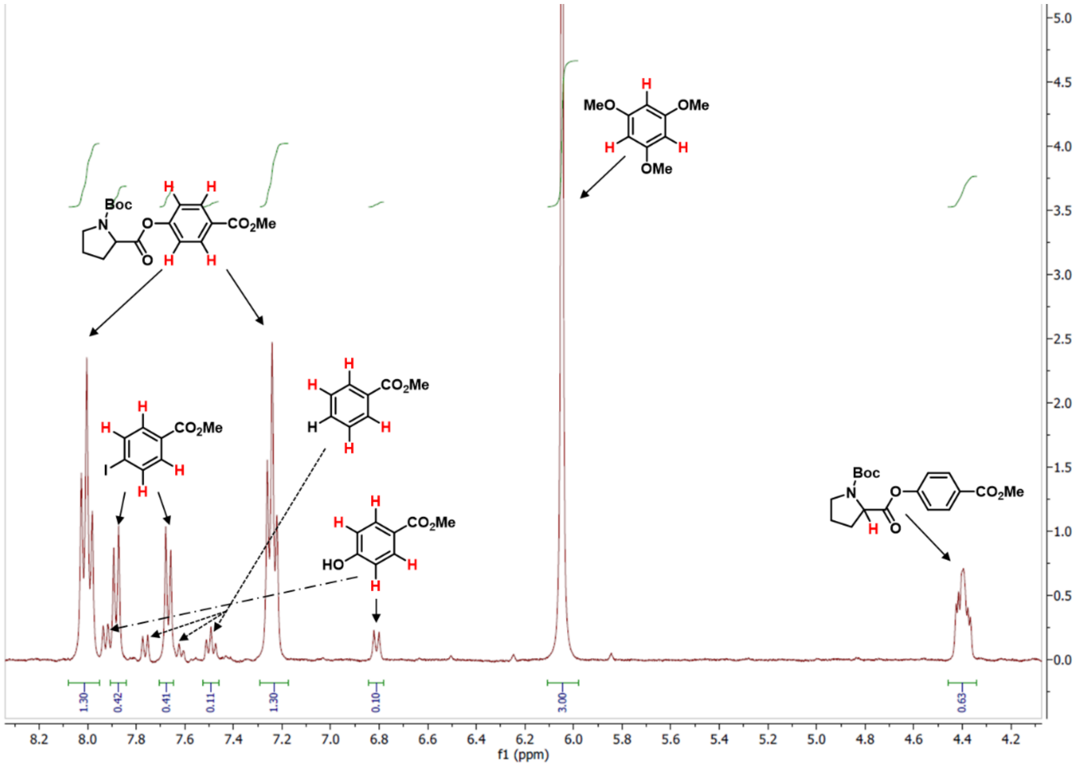

Fig. S10. Representative ^{1}H-NMR spectrum of a crude reaction mixture for determining NMR yields in the DSMP catalyzed C-O arylation.

Table S3· Ligand screening in absence of a dye using the 440 nm LED setup.[a]

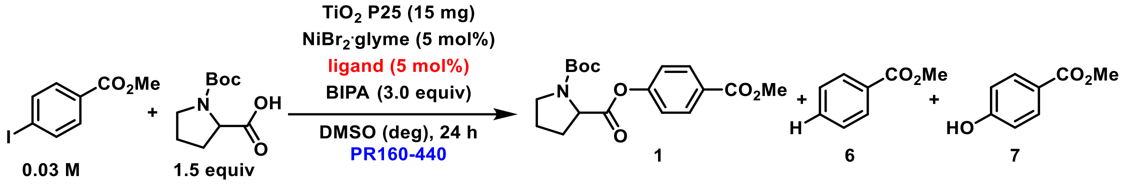

Entry	Ligand	Conversion [%][b]	1 [%][c]	6 [%][c]	7 [%][c]
1	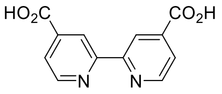	29	24	n.d.	n.d.
2	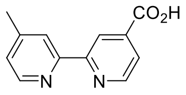	17	8	n.d.	n.d.
3	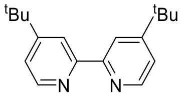	16	12	n.d.	n.d.
4	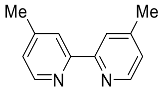	12	7	n.d.	n.d.
5	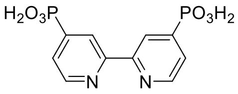	10	0	n.d.	n.d.
6	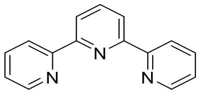	8	0	n.d.	n.d.

[a]Reaction conditions: methyl 4-iodobenzoate (95.1 µmol), *N*-Boc proline (140.7 µmol), $NiBr_2$·glyme (4.6 µmol), ligand (4.6 µmol), BIPA (285.4 µmol), TiO_2 (15 mg), DMSO (anhydrous, 3 mL), 440 nm LED (50% power), 24 h. [b]Conversion of methyl 4-iodobenzoate determined by ^{1}H-NMR using 1,3,5-trimethoxybenzene as internal standard. [c]NMR yields determined by ^{1}H-NMR using 1,3,5-trimethoxybenzene as internal standard. n.d. = not detected. BIPA = *N*-*tert*-butylisopropylamine. glyme = 1,2-dimethoxyethane. deg = degassed

Table S4. Dye screening using the 440 nm LED setup.[a]

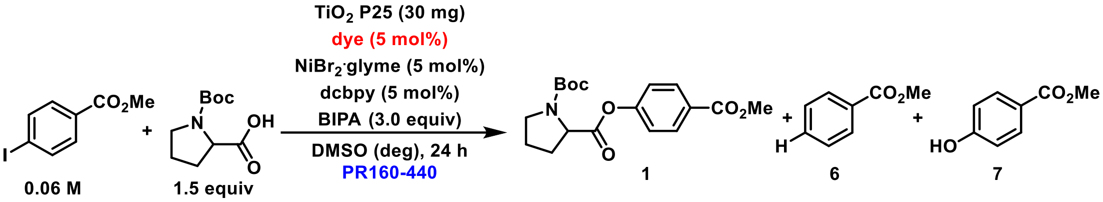

Entry	Dye	Conversion [%][b]	1 [%][c]	6 [%][c]	7 [%][c]
1	--	37	33	n.d.	traces
2	Fluorescein sodium	76	48	16	traces
3	Rose bengal	42	25	9	traces
4	Brilliant blue R	29	5	18	n.d.
5	Rhodamin B	26	traces	12	n.d.
6	Coumarin 343	15	n.d.	10	n.d.
7	Alizarin red S	9	n.d.	4	n.d.
8	Bromophenol blue	6	n.d.	n.d.	traces
9	Congo red	3	n.d.	n.d.	n.d.
10	Catechol	0	n.d.	n.d.	n.d.
11	Methyl orange	0	n.d.	n.d.	n.d.

[a] Reaction conditions: methyl 4-iodobenzoate (190.3 µmol), *N*-Boc proline (285.4 µmol), dye (9.5 µmol), $NiBr_2$·glyme (9.5 µmol), dcbpy (9.5 µmol), BIPA (570.8 µmol), TiO_2 (30 mg), DMSO (anhydrous, 3 mL), 440 nm LED (50% power), 24 h. [b] Conversion of methyl 4-iodobenzoate determined by ^{1}H-NMR using 1,3,5-trimethoxybenzene as internal standard. [c] NMR yields determined by ^{1}H-NMR using 1,3,5-trimethoxybenzene as internal standard. dcbpy = 2,2′-bipyridine-4,4′-dicarboxylic acid. n.d. = not detected. BIPA = *N*-*tert*-butylisopropylamine. glyme = 1,2-dimethoxyethane. deg = degassed

Table S5. Dye screening using the 525 nm LED setup.[a]

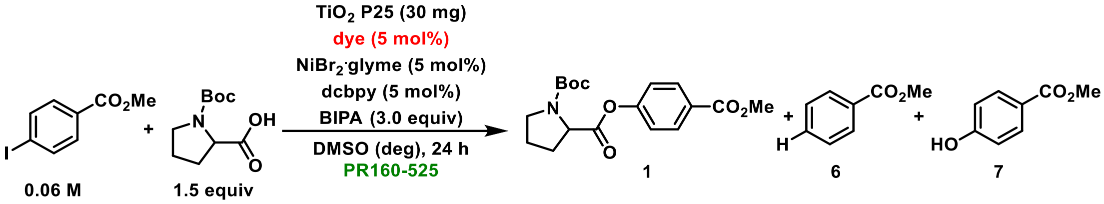

Entry	Dye	Conversion [%][b]	1 [%][c]	6 [%][c]	7 [%][c]
1	--	0	n.d.	n.d.	n.d.
2	Fluorescein sodium	47	29	12	1
3	Rhodamin B	23	9	10	n.d.
4	Rose bengal	21	7	10	n.d.
5	Coumarin 343	7	traces	traces	n.d.
6	Congo red	1	n.d.	n.d.	n.d.
7	Methyl orange	0	n.d.	n.d.	n.d.
8	Alizarin red S	0	n.d.	n.d.	n.d.
9	Brilliant blue R	0	n.d.	n.d.	n.d.
10	Catechol	0	n.d.	n.d.	n.d.
11	Bromophenol blue	0	n.d.	n.d.	n.d.

[a]Reaction conditions: methyl 4-iodobenzoate (190.3 µmol), *N*-Boc proline (285.4 µmol), dye (9.5 µmol), NiBr$_2$·glyme (9.5 µmol), dcbpy (9.5 µmol), BIPA (570.8 µmol), TiO$_2$ (30 mg), DMSO (anhydrous, 3 mL), 525 nm LED (50% power), 24 h. [b]Conversion of methyl 4-iodobenzoate determined by ^{1}H-NMR using 1,3,5-trimethoxybenzene as internal standard. [c]NMR yields determined by ^{1}H-NMR using 1,3,5-trimethoxybenzene as internal standard. dcbpy = 2,2′-bipyridine-4,4′-dicarboxylic acid. n.d. = not detected. BIPA = *N-tert*-butylisopropylamine. glyme = 1,2-dimethoxyethane. deg = degassed

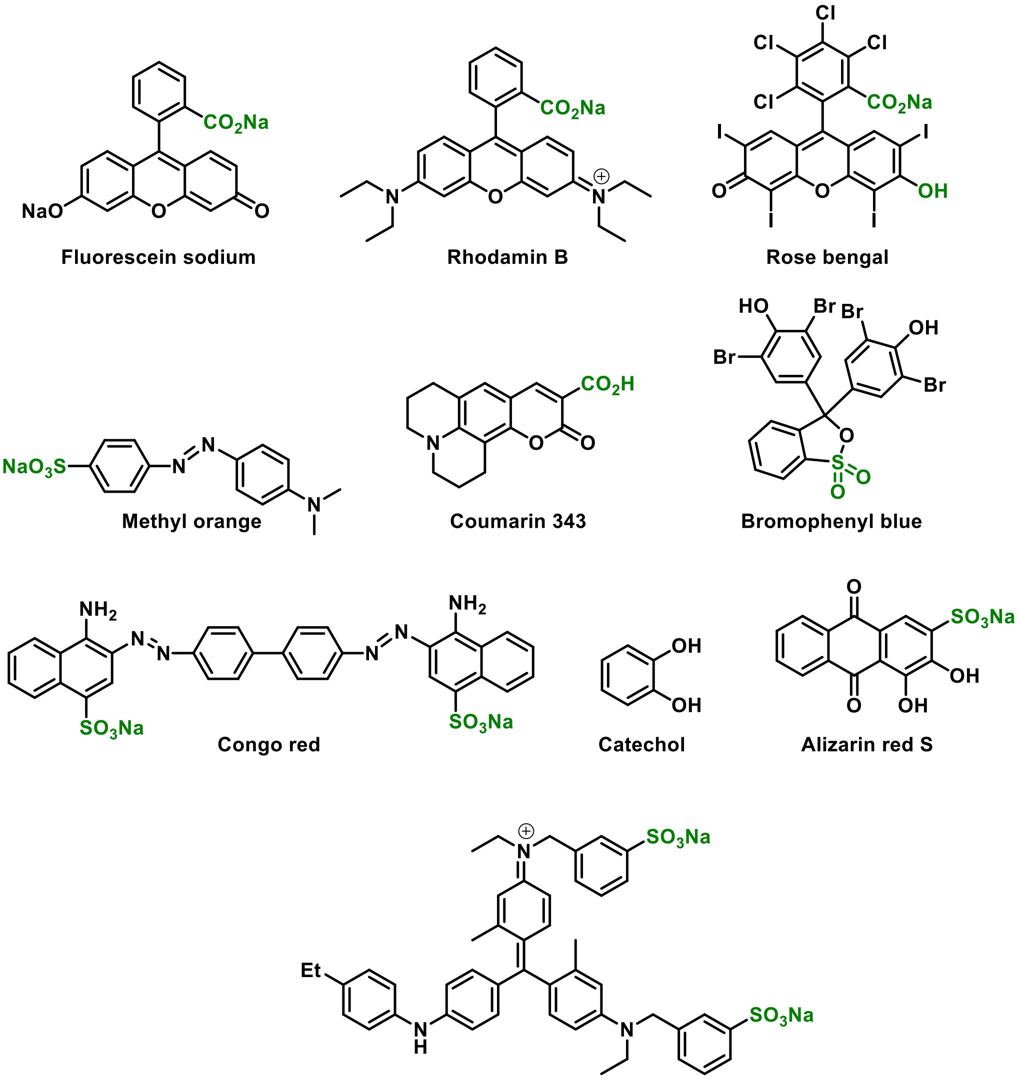

Fluorescein sodium

Rhodamin B

Rose bengal

Methyl orange

Coumarin 343

Bromophenyl blue

Congo red

Catechol

Alizarin red S

Brilliant blue

Fig. S11. Structures of dyes that were tested for experiments using the 440 and 525 nm setup. The functionalities that bind to the surface hydroxyl groups of TiO_2 are marked in green.

Table S6. Screening of Ni^{II} salts using the 525 nm LED setup.[a]

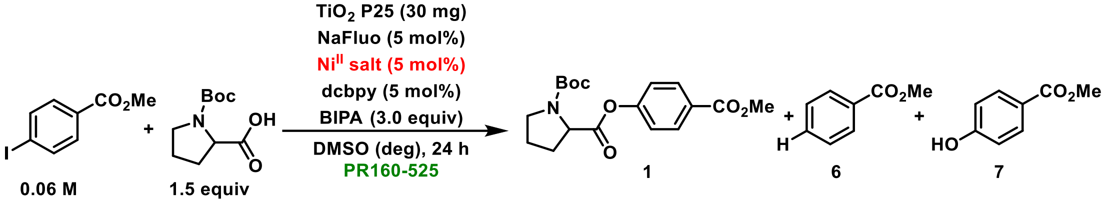

Entry	Ni^{II} source	Conversion [%][b]	1 [%][c]	6 [%][c]	7 [%][c]
1	$NiBr_2$·glyme	40	20	11	traces
2	$NiCl_2$·glyme	38	19	12	traces
3	$Ni(OAc)_2·4H_2O$	38	14	10	traces
4	$NiCl_2·6H_2O$	32	15	10	traces
5	$NiBr_2·3H_2O$	12	n.d.	8	n.d.

[a] Reaction conditions: methyl 4-iodobenzoate (190.3 µmol), *N*-Boc proline (285.4 µmol), Fluorescein sodium (9.5 µmol), $NiBr_2$·glyme (9.5 µmol) and dcbpy (9.5 µmol) in DMSO (anhydrous, 3 mL), BIPA (570.8 µmol), TiO_2 (30 mg), 525 nm LED (50% power), 24 h. [b] Conversion of methyl 4-iodobenzoate determined by ^{1}H-NMR using 1,3,5-trimethoxybenzene as internal standard. [c] NMR yields determined by ^{1}H-NMR using 1,3,5-trimethoxybenzene as internal standard. NaFluo = Fluorescein sodium. dcbpy = 2,2′-bipyridine-4,4′-dicarboxylic acid. n.d. = not detected. BIPA = *N*-*tert*-butylisopropylamine. glyme = 1,2-dimethoxyethane. deg = degassed

Although $NiBr_2$·glyme and $NiCl_2$·glyme showed best results, $NiCl_2·6H_2O$ was used for further experiments. This nickel source is significantly cheaper and more convenient to handle, as $NiBr_2$·glyme and $NiCl_2$·glyme are hygroscopic. Methyl 4-acetoxybenzoate was occasionally observed in case of $Ni(OAc)_2·4H_2O$ as side-product. This resulted from the C-O arylation of the aryl iodide with the acetate anion of $Ni(OAc)_2·4H_2O$.

Table S7. Solvent screening using the 525 nm LED setup.[a]

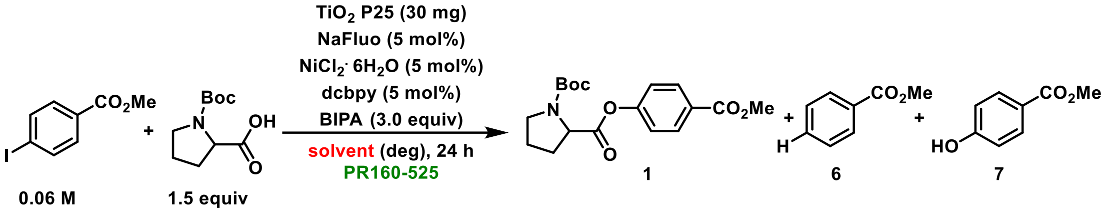

Entry	Solvent	Conversion [%][b]	1 [%][c]	6 [%][c]	7 [%][c]
1	DMSO	52	27	13	traces
2	DMAc	50	24	12	traces
3	MeCN	10	6	3	traces
4	Diglyme	10	7	3	n.d.
5	THF	9	3	traces	traces
6	Dioxane	8	4	4	n.d.
7	DCM	6	n.d.	n.d.	n.d.
8	Acetone	2	n.d.	n.d.	n.d.

[a]Reaction conditions: methyl 4-iodobenzoate (190.3 µmol), *N*-Boc proline (285.4 µmol), Fluorescein sodium (9.5 µmol), $NiCl_2 \cdot 6H_2O$ (9.5 µmol) and dcbpy (9.5 µmol) in solvent (anhydrous, 3 mL), BIPA (570.8 µmol), TiO_2 (30 mg), 525 nm LED (50% power), 24 h. [b]Conversion of methyl 4-iodobenzoate determined by ^{1}H-NMR using 1,3,5-trimethoxybenzene as internal standard. [c]NMR yields determined by ^{1}H-NMR using 1,3,5-trimethoxybenzene as internal standard. NaFluo = Fluorescein sodium. dcbpy = 2,2′-bipyridine-4,4′-dicarboxylic acid. n.d. = not detected. BIPA = *N*-*tert*-butylisopropylamine. glyme = 1,2-dimethoxyethane. deg = degassed

Table S8. Optimization of lamp power using the 525 nm LED setup.[a]

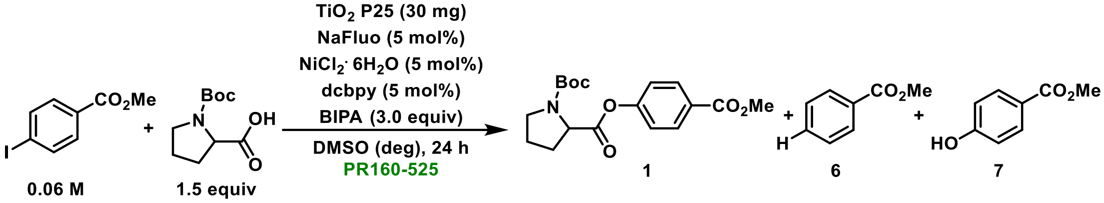

Entry	Lamp power [%]	Conversion [%][b]	1 [%][c]	6 [%][c]	7 [%][c]
1	50	52	27	13	traces
2	25	43	27	9	traces

[a] Reaction conditions: methyl 4-iodobenzoate (190.3 µmol), *N*-Boc proline (285.4 µmol), Fluorescein sodium (9.5 µmol), $NiCl_2 \cdot 6H_2O$ (9.5 µmol) and dcbpy (9.5 µmol) in solvent (anhydrous, 3 mL), BIPA (570.8 µmol), TiO_2 (30 mg), 525 nm LED, 24 h. [b] Conversion of methyl 4-iodobenzoate determined by ^{1}H-NMR using 1,3,5-trimethoxybenzene as internal standard. [c] NMR yields determined by ^{1}H-NMR using 1,3,5-trimethoxybenzene as internal standard. NaFluo = Fluorescein sodium. dcbpy = 2,2′-bipyridine-4,4′-dicarboxylic acid. n.d. = not detected. BIPA = *N*-*tert*-butylisopropylamine. deg = degassed

Table S9. Optimization of the equivalents of *N*-Boc proline using the 525 nm LED setup.[a]

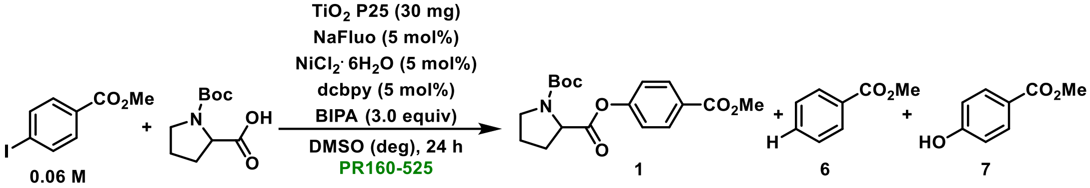

Entry	*N*-Boc proline [equiv]	Conversion [%][b]	1 [%][c]	6 [%][c]	7 [%][c]
1	1.0	30	20	7	traces
2	1.5	30	17	8	traces
3	2.0	22	13	8	traces
4	2.5	22	10	8	n.d.

[a]Reaction conditions: methyl 4-iodobenzoate (190.3 µmol), *N*-Boc proline, Fluorescein sodium (9.5 µmol), $NiCl_2 \cdot 6H_2O$ (9.5 µmol) and dcbpy (9.5 µmol) in DMSO (anhydrous, 3 mL), BIPA (570.8 µmol), TiO_2 (30 mg), 525 nm LED (25% power), 24 h. [b]Conversion of methyl 4-iodobenzoate determined by ^{1}H-NMR using 1,3,5-trimethoxybenzene as internal standard. [c]NMR yields determined by ^{1}H-NMR using 1,3,5-trimethoxybenzene as internal standard. NaFluo = Fluorescein sodium. dcbpy = 2,2′-bipyridine-4,4′-dicarboxylic acid. n.d. = not detected. BIPA = *N*-*tert*-butylisopropylamine. deg = degassed

Table S10. Optimization of the amount of fluorescein sodium using the 525 nm LED setup.[a]

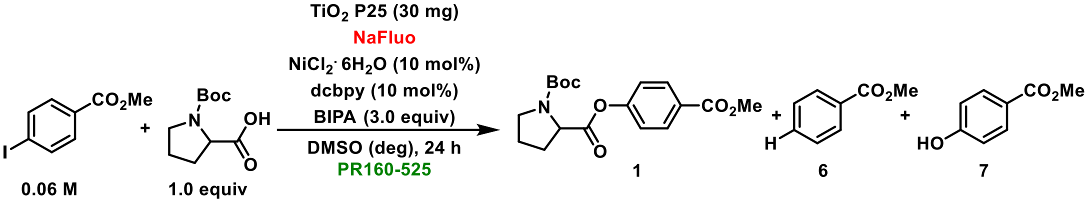

Entry	NaFluo [mol%]	Conversion [%][b]	1 [%][c]	6 [%][c]	7 [%][c]
1	2.50	56	41	7	3
2	2.00	66	52	7	5
3	1.50	79	64	6	4
4	1.25	77	66	6	5
5	1.00	74	64	5	4
6	0.75	47	40	traces	traces
7	0.50	40	35	traces	traces

[a] Reaction conditions: methyl 4-iodobenzoate (190.3 µmol), *N*-Boc proline (190.3 µmol), Fluorescein sodium, $NiCl_2 \cdot 6H_2O$ (19.0 µmol) and dcbpy (19.0 µmol) in DMSO (anhydrous, 3 mL), BIPA (570.8 µmol), TiO_2 (30 mg), 525 nm LED (25% power), 24 h. [b] Conversion of methyl 4-iodobenzoate determined by ^{1}H-NMR using 1,3,5-trimethoxybenzene as internal standard. [c] NMR yields determined by ^{1}H-NMR using 1,3,5-trimethoxybenzene as internal standard. NaFluo = Fluorescein sodium. dcbpy = 2,2′-bipyridine-4,4′-dicarboxylic acid. n.d. = not detected. BIPA = *N*-*tert*-butylisopropylamine. deg = degassed

Table S11. Optimization of the amount of *N*-Boc proline using the 525 nm LED setup.[a]

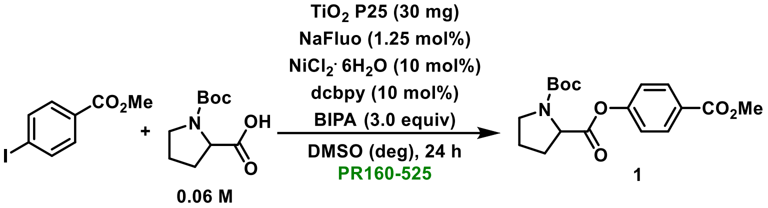

Entry	Methyl 4-iodobenzoate [equiv]	1 [%][b]
1	1.5	76
2	1.0	66

[a]Reaction conditions: methyl 4-iodobenzoate, *N*-Boc proline (190.3 µmol), Fluorescein sodium (2.4 µmol), NiCl₂·6H₂O (19.0 µmol) and dcbpy (19.0 µmol) in DMSO (anhydrous, 3 mL), BIPA (570.8 µmol), TiO₂ (30 mg), 525 nm LED (25% power), 24 h. [c]NMR yields determined by ^{1}H-NMR using 1,3,5-trimethoxybenzene as internal standard. NaFluo = Fluorescein sodium. dcbpy = 2,2′-bipyridine-4,4′-dicarboxylic acid. n.d. = not detected. BIPA = *N-tert*-butylisopropylamine. deg = degassed

Table S12. Optimized conditions and control studies using the 440 nm setup.[a]

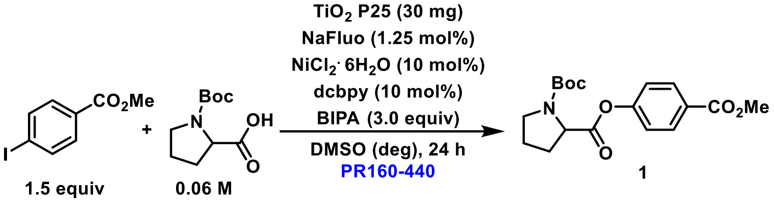

Entry	Deviation from standard conditions	**1** [%][b]
1	none	95
2	UV filter[c]	80
3	no NaFluo	15
4	no NaFluo, UV filter[c]	n.d.
5	no TiO_2	25
6	no TiO_2, UV filter[d]	20
7	No dcbpy	n.d.
8	no $NiCl_2 \cdot 6H_2O$	n.d.
9	no light	n.d.
10	no degassing	n.d.
11	no BIPA	n.d.

Reaction conditions: methyl 4-iodobenzoate (285.4 µmol), *N*-Boc proline (190.3 µmol), Fluorescein sodium (2.4 µmol), $NiCl_2 \cdot 6H_2O$ (19.0 µmol) and dcbpy (19.0 µmol) in DMSO (anhydrous, 3 mL), BIPA (570.8 µmol), TiO_2 (30 mg), 440 nm LED lamp (25% power), 24 h. [b]NMR yields determined by ^{1}H-NMR using 1,3,5-trimethoxybenzene as internal standard. [c]Reactions were carried out with a 425 nm cut-off filter (See Figure S13) between the light source and the reaction vessel NaFluo = Fluorescein sodium. dcbpy = 2,2′-bipyridine-4,4′-dicarboxylic acid. n.d. = not detected. BIPA = *N-tert*-butylisopropylamine. deg = degassed

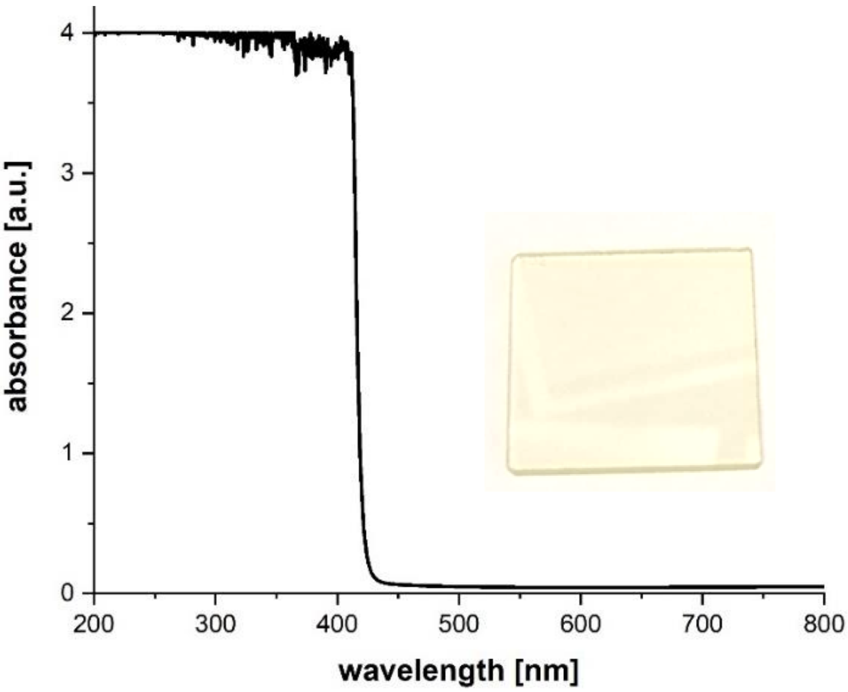

Fig. S12. Absorption spectrum of the 425 nm cut-off filter that was used for control studies using the PR160-440 setup.

Table S13. Optimized conditions and control studies using the 525 nm setup.[a]

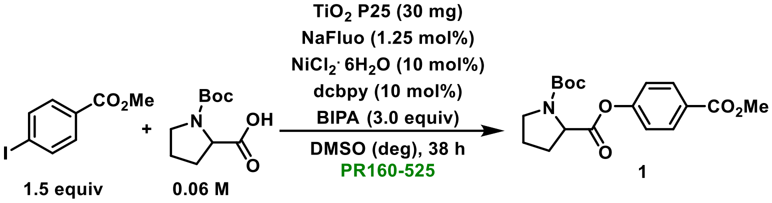

Entry	**Deviation from standard conditions**	**1 [%]**[b]
1	none	97
2	no TiO_2	n.d.
3	no NaFluo	n.d.
4	no dcbpy	traces
5	no $NiCl_2 \cdot 6H_2O$	n.d.
6	no light	n.d.
7	no degassing	n.d.
8	no BIPA	n.d.

[a] Reaction conditions: methyl 4-iodobenzoate (285.4 µmol), *N*-Boc proline (190.3 µmol), Fluorescein sodium (2.4 µmol), $NiCl_2 \cdot 6H_2O$ (19.0 µmol) and dcbpy (19.0 µmol) in DMSO (anhydrous, 3 mL), BIPA (570.8 µmol), TiO_2 (30 mg), 525 nm LED (25% power), 38h. [b] NMR yields determined by ^1H-NMR using 1,3,5-trimethoxybenzene as internal standard. NaFluo = Fluorescein sodium. dcbpy = 2,2′-bipyridine-4,4′-dicarboxylic acid. n.d. = not detected. BIPA = *N*-*tert*-butylisopropylamine. deg = degassed

Table S14. Dye screening using the 666 nm setup.[a]

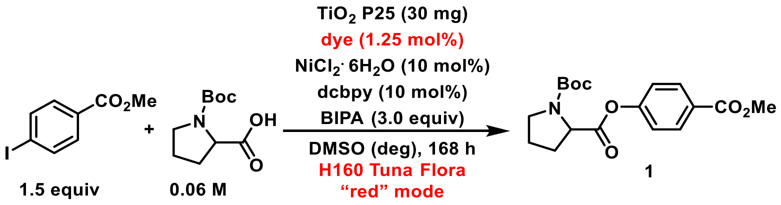

Entry	Dye	Variation	1 [%][b]
1	N3	--	95
2	N3	No TiO_2	n.d.
3	Z907	--	29
4	D149	--	n.d.

[a]Reaction conditions: methyl 4-iodobenzoate (285.4 µmol), *N*-Boc proline (190.3 µmol), Fluorescein sodium (2.4 µmol), $NiCl_2\cdot 6H_2O$ (19.0 µmol) and dcbpy (19.0 µmol) in DMSO (anhydrous, 3 mL), BIPA (570.8 µmol), TiO_2 (30 mg), 666 nm LED (100% power), 168h. [b]NMR yields determined by ^{1}H-NMR using 1,3,5-trimethoxybenzene as internal standard. NaFluo = Fluorescein sodium. dcbpy = 2,2′-bipyridine-4,4′-dicarboxylic acid. n.d. = not detected. BIPA = *N-tert*-butylisopropylamine. deg = degassed

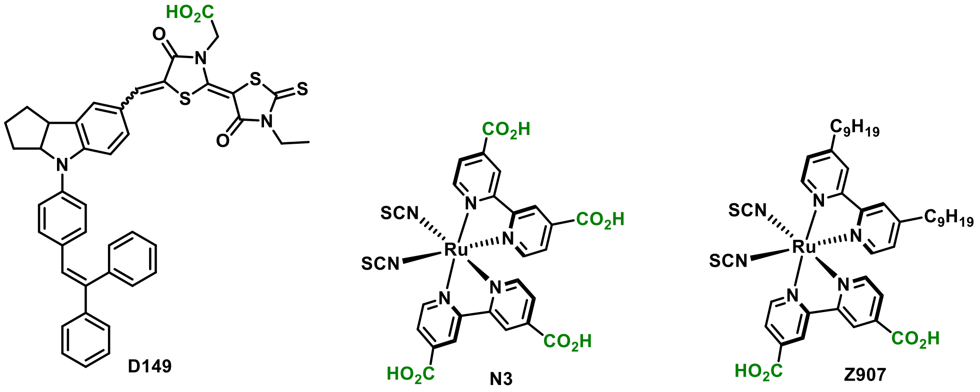

Fig. S13. Structures of dyes that were tested for experiments using the 666 nm setup. The functionalities that bind to the surface hydroxyl groups of TiO_2 are marked in green.

3.2 Experimental procedure for the optimized C-O arylation using *in situ* generation of DSMPs.

An oven dried vial (19 x 100 mm) equipped with a stir bar was charged with TiO_2 P25 (90 mg), *N*-Boc proline (122.7 mg, 570.0 µmol, 1.0 equiv), methyl 4-iodobenzoate (224.1 mg, 855.1 µmol, 1.5 equiv), fluorescein sodium or N3 (7.1 µmol, 1.25 mol%), $NiCl_2 \cdot 6H_2O$ (13.6 mg 57.1 µmol, 10 mol%) and 2,2′-bipyridine-4,4′-dicarboxylic acid (dcbpy, 13.9 mg 57.1 µmol, 10 mol%). Subsequently, DMSO (anhydrous, 6 mL) and *N*-tert-butylisopropylamine (BIPA, 271 µL, 1.71 mmol, 3 equiv) were added and the vial was sealed with a septum and Parafilm. The reaction mixture was sonicated for 5-10 min followed by stirring for 5 min to obtain a fine dispersion. The mixture was then degassed by bubbling Argon for 10 min. The mixture was irradiated using the 525 (fluorescein sodium) or 666 nm LED setup (N3) with rapid stirring (1400 rpm). After the respective reaction time, one equivalent of 1,3,5-trimethoxybenzene (internal standard, 96 mg, 570 µmol) was added and the mixture was stirred for 5 min. An aliquot of the reaction mixture (~200 µL) was filtered, diluted with DMSO-d_6 and subjected to ^{1}H-NMR analysis to determine NMR yields. Thereafter, the NMR sample was combined with the reaction mixture. The reaction mixture was diluted with H_2O (40 mL) and extracted with dichloromethane (3 x 30 mL). The combined organic phases were washed with brine (50 mL), dried over Na_2SO_4 and concentrated. The product was purified by flash column chromatography (SiO_2, Hexane/EtOAc elution gradient of 0-20%) on a Grace Reveleris system using a 12 g cartridge. In some cases, mixed fractions containing small amounts of the phenol byproduct and the desired product were observed. These could be easily purified by a basic extraction (DCM and 0.5 M NaOH), followed by drying the organic phase over Na_2SO_4 and solvent evaporation to maximize the reaction yield. The title compound was isolated as a yellowish solid.

Using fluorescein sodium and the 525 nm setup:

Reaction time: 38 h

Isolated yield: 90% (179.2 mg, 512.9 µmol)

Using N3 and the 666 nm setup:

Reaction time: 168 h

Isolated yield: 92% (183.2 mg, 524.4 µmol)

1-(tert-butyl) 2-(4-(methoxycarbonyl)phenyl) pyrrolidine-1,2-dicarboxylate 1: ^{1}H NMR (400 MHz, $CDCl_3$) rotameric mixture, δ 8.03 (m, 2H), 7.15 (m, 2H), 4.50 (dd, *J* = 8.6, 4.3 Hz, 0.4H), 4.42 (dd, *J* = 8.7, 4.3 Hz, 0.6H), 3.88 (m, 3H), 3.61 – 3.38 (m, 2H), 2.45 – 2.25 (m, 1H), 2.16 (m, 1H), 2.10 – 1.86 (m, 2H), 1.42 (m, 9H). ^{13}C NMR (151 MHz, $CDCl_3$) rotameric mixture, signals for minor rotamer are enclosed in parenthesis δ (170.86) 170.82, (166.01) 165.88, 154.15 (153.88), 153.15, 130.93 (130.80), 127.52 (127.36), (121.22) 121.86, 80.00 (79.80), 58.88 (58.79), 51.93 (51.87), (46.34) 46.15, 30.71 (29.66), 28.09, (24.25) 23.43. HRMS (ESI) m/z calcd for $C_{18}H_{23}NNaO_6$ [$(M+Na)^+$] 372.1423, found 372.1417.

These data are in full agreement with those previously published in the literature (*14*).

3.3 Experiments using *ex situ* prepared catalysts.

Table S15. C-O arylation with an nickel complex immobilized on TiO_2 (*ex situ* preparation), using the 440 nm setup.[a]

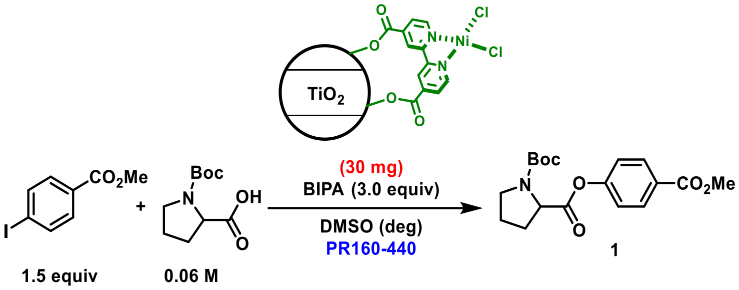

Entry	t [h]	1 [%][c]
1	38	29
2	168	67

[a]Reaction conditions: methyl 4-iodobenzoate (285.4 µmol), *N*-Boc proline (190.3 µmol), TiO_2-$NiCl_2$·dcbpy (30 mg) in DMSO (anhydrous, 3 mL), BIPA (570.8 µmol), 440 nm LED (25% power), 38 h. [c]NMR yields determined by ^{1}H-NMR using 1,3,5-trimethoxybenzene as internal standard. dcbpy = 2,2′-bipyridine-4,4′-dicarboxylic acid. n.d. = not detected. BIPA = *N*-*tert*-butylisopropylamine. deg = degassed

Table S16. C-O arylation with an *ex situ* prepared DSMP and reference systems using the 525 nm setup.[a]

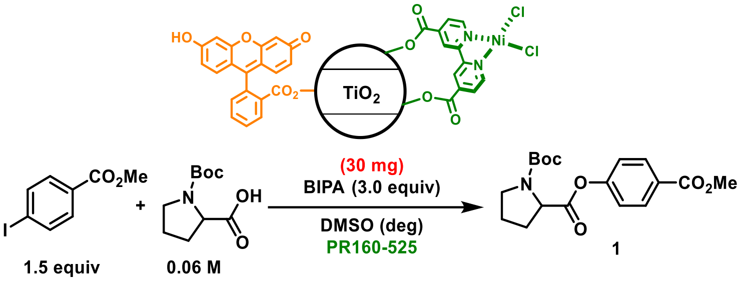

Entry	Catalyst	t [h]	1 [%][b]
1	Fluo-TiO_2-$NiCl_2$·dcbpy	38	63
2	Fluo-TiO_2 + $NiCl_2$·dcbpy[c]	24	63
3	Fluo-TiO_2 + $NiCl_2$·dtbbpy[c]	24	27

[a]Reaction conditions: methyl 4-iodobenzoate (285.4 µmol), *N*-Boc proline (190.3 µmol), NaFluo-TiO_2-$NiCl_2$·dcbpy (30 mg) in DMSO (anhydrous, 3 mL), BIPA (570.8 µmol), TiO_2 (30 mg), 525 nm LED (25% power), 38 h. [b]NMR yields determined by ^{1}H-NMR using 1,3,5-trimethoxybenzene as internal standard. The nickel salt and the ligand were added separately (19.0 µmol). NaFluo = Fluorescein sodium. dcbpy = 2,2′-bipyridine-4,4′-dicarboxylic acid. dtbbpy = 4,4′-di-tert-butyl-2,2′-dipyridyl. n.d. = not detected. BIPA = *N*-*tert*-butylisopropylamine. deg = degassed

4 C-S cross-coupling

4.1 Optimization studies using in situ generation of DSMPs.

An oven dried vial (19 x 100 mm) equipped with a stir bar was charged with TiO_2 P25 (30 mg), methyl 4-iodobenzoate (1 equiv), methyl 3-mercaptopropionate (2 equiv), a dye (1.25 mol%), $NiBr_2 \cdot 3H_2O$ (10 mol%), and the ligand (10 mol%). Subsequently, MeCN (anhydrous, 3 mL) and *N*-tert-butylisopropylamine (BIPA, 3 equiv) were added, and the vial was sealed with a septum and Parafilm. The reaction mixture was sonicated for 5-10 min followed by stirring for 5 min to obtain a fine dispersion. The mixture was then degassed by bubbling Argon for 10 min. The mixture was irradiated with the respective LED lamps with rapid stirring (1400 rpm). After the respective reaction time, one equivalent of 1,3,5-trimethoxybenzene was added. An aliquot of the reaction mixture (~200 µL) was filtered, diluted with DMSO-d_6 and subjected to ^1H-NMR analysis. For a representative NMR spectrum, see Fig. S14.

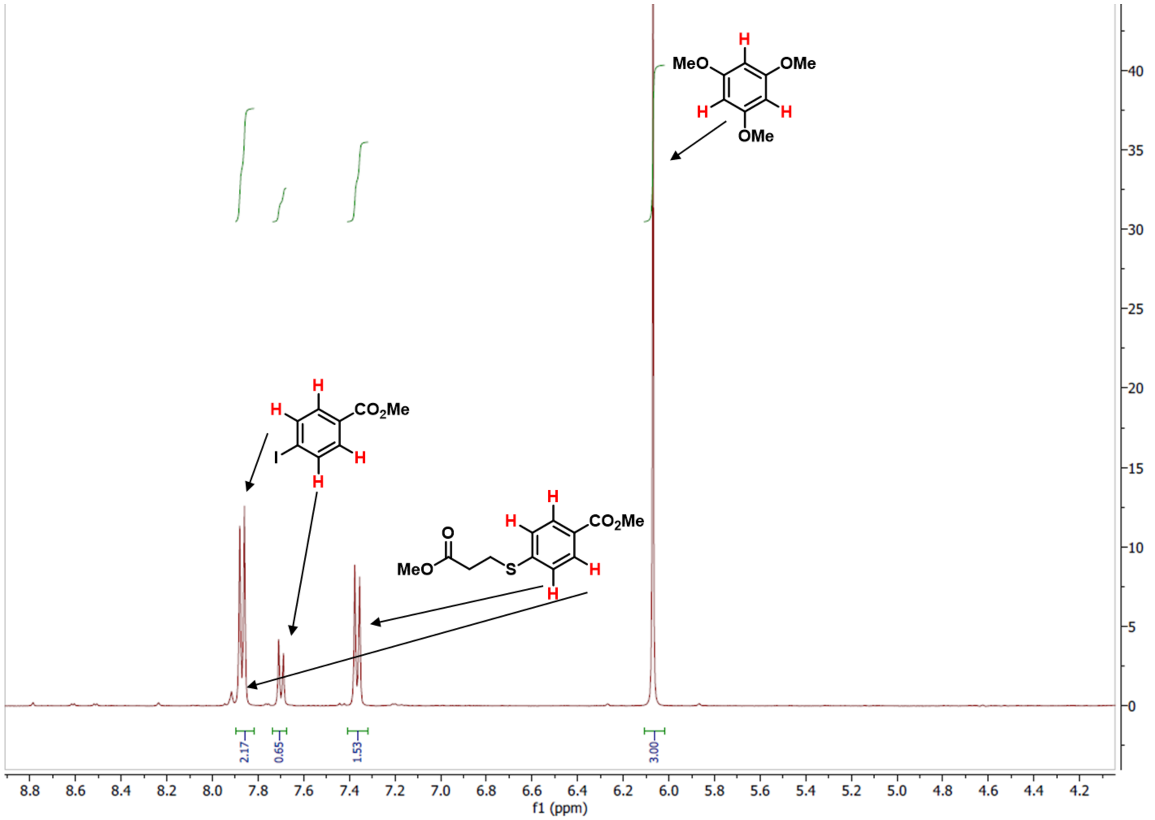

Fig. S14. Representative ^1H-NMR spectrum of a crude reaction mixture for determining NMR yields in the C-S arylation.

Table S17. Ligand screening in absence of a dye using the 440 nm LED setup.[a]

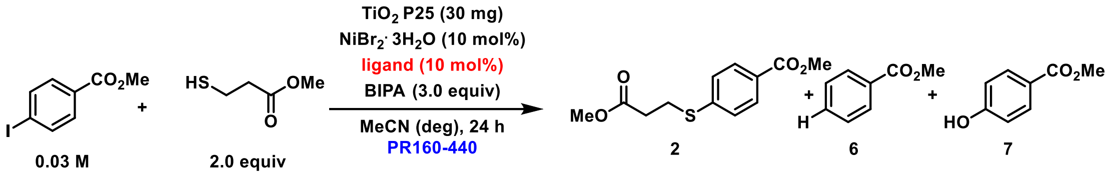

Entry	Ligand	Conversion [%][b]	2 [%][c]	6 [%][c]	7 [%][c]
1	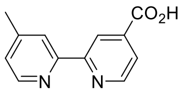	86	84	n.d.	n.d.
2	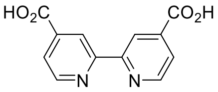	32	32	n.d.	n.d.

[a] Reaction conditions: methyl 4-iodobenzoate (300.0 µmol), methyl 3-mercaptopropionate (600.0 µmol), $NiBr_2 \cdot 3H_2O$ (30.0 µmol), ligand (30.0 µmol), BIPA (900 µmol) in MeCN (3 mL), and TiO_2 (30 mg), 440 nm LED (50% power), 24 h. [b] Conversion of methyl 4-iodobenzoate determined by ^1H-NMR using 1,3,5-trimethoxybenzene as internal standard. [c] NMR yields determined by ^1H-NMR using 1,3,5-trimethoxybenzene as internal standard. BIPA = *N*-*tert*-butylisopropylamine. n.d. = not detected. deg = degassed

Table S18. Dye screening using the 525 nm LED setup.[a]

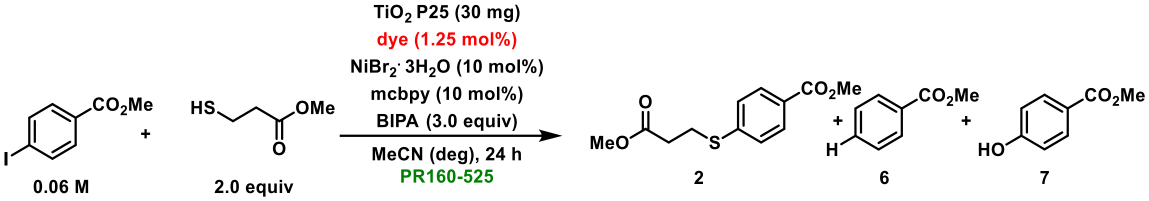

Entry	Dye	Conversion [%][b]	2 [%][c]	6 [%][c]	7 [%][c]
1	--	18	18	n.d.	n.d.
2	Coumarin 343	quant	99	n.d.	n.d.
3	Rose bengal	91	91	n.d.	n.d.
4	Rhodamin B	47	45	n.d.	n.d.
5	Brilliant blue R	5	n.d.	n.d.	n.d.
6	Alizarin red S	5	5	n.d.	n.d.
7	Methyl orange	4	n.d.	n.d.	n.d.
8	Congo Red	4	n.d.	n.d.	n.d.
9	Bromophenol blue	0	n.d.	n.d.	n.d.
10	Fluorescein sodium	0	n.d.	n.d.	n.d.

[a]Reaction conditions: methyl 4-iodobenzoate (190.3 µmol), methyl 3-mercaptopropionate (380.5 µmol), dye (2.4 µmol), $NiBr_2{\cdot}3H_2O$ (19.0 µmol) TiO_2 (30 mg), and mcbpy (19.0 µmol), BIPA (570.8 µmol) in MeCN (3 mL), 525 nm LED (50% power), 24 h. [b]Conversion of methyl 4-iodobenzoate determined by ^{1}H-NMR using 1,3,5-trimethoxybenzene as internal standard. [c]NMR yields determined by ^{1}H-NMR using 1,3,5-trimethoxybenzene as internal standard. For structures of the dyes, see Fig. S11. BIPA = *N*-*tert*-butylisopropylamine. mcbpy = 4'-methyl-2,2'-bipyridine-4-carboxylic acid . n.d. = not detected. deg = degassed. quant = quantitative.

Table S19. Optimized conditions and control studies using using the 440 nm LED setup.[a]

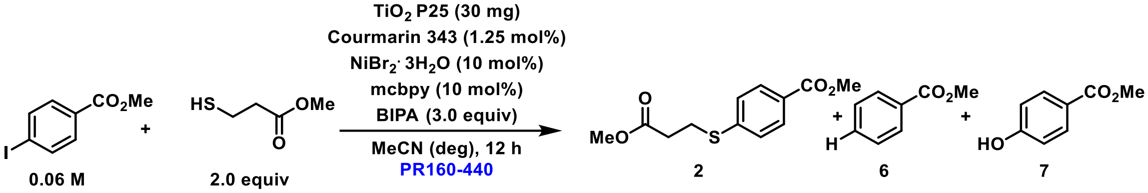

Entry	Deviation from standard conditions	Conversion [%][b]	2 [%][c]	6 [%][c]	7 [%][c]
1	--	quant	99	n.d.	n.d.
2	no degassing	40	35	n.d.	n.d.
3	no Coumarin 343	21	19	n.d.	n.d.
4	no BIPA	20	19	n.d.	n.d.
5	no light	5	n.d.	n.d.	n.d.
6	no $NiBr_2{\cdot}3H_2O$	4	traces	n.d.	n.d.
7	no TiO_2	3	n.d.	n.d.	n.d.
8	no mcbpy	0	n.d.	n.d.	n.d.

[a]Reaction conditions: methyl 4-iodobenzoate (190.3 µmol), methyl 3-mercaptopropionate (380.5 µmol), coumarin 343 (2.4 µmol), $NiBr_2{\cdot}3H_2O$ (19.0 µmol) and mcbpy (19.0 µmol), BIPA (570.8 µmol) in MeCN (3 mL), TiO_2 (30 mg), 440 nm LED (50% power), 12 h. [b]Conversion of methyl 4-iodobenzoate determined by ^{1}H-NMR using 1,3,5-trimethoxybenzene as internal standard. [c]NMR yields determined by ^{1}H-NMR using 1,3,5-trimethoxybenzene as internal standard. BIPA = *N*-*tert*-butylisopropylamine. mcbpy = 4'-methyl-2,2'-bipyridine-4-carboxylic acid. n.d. = not detected. deg = degassed. quant = quantitative.

Table S20. Optimized conditions and control studies using the 525 nm LED setup.[a]

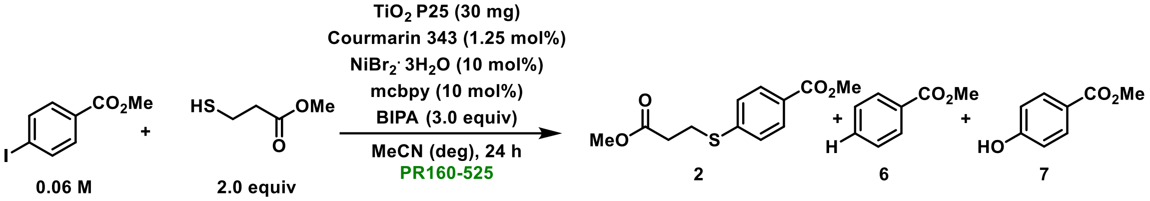

Entry	Deviation from standard conditions	Conversion [%][b]	2 [%][c]	6 [%][c]	7 [%][c]
1	--	quant.	99	n.d.	n.d.
2	no degassing	40	37	n.d.	n.d.
3	no BIPA	18	17	n.d.	n.d.
4	no Coumarin 343	17	17	n.d.	n.d.
5	no $NiBr_2·3H_2O$	8	traces	n.d.	n.d.
6	no TiO_2	6	traces	3	n.d.
7	no light	5	n.d.	n.d.	n.d.
8	no mcbpy	0	n.d.	n.d.	n.d.

[a] Reaction conditions: methyl 4-iodobenzoate (190.3 µmol), methyl 3-mercaptopropionate (380.5 µmol), Coumarin 343 (2.4 µmol), $NiBr_2·3H_2O$ (19.0 µmol) and mcbpy (19.0 µmol), BIPA (570.8 µmol) in MeCN (3 mL), TiO_2 (30 mg), 525 nm LED (50% power), 24 h. [b] Conversion of methyl 4-iodobenzoate determined by ^{1}H-NMR using 1,3,5-trimethoxybenzene as internal standard. [c] NMR yields determined by ^{1}H-NMR using 1,3,5-trimethoxybenzene as internal standard. BIPA = *N-tert*-butylisopropylamine. mcbpy = 4'-methyl-2,2'-bipyridine-4-carboxylic acid. n.d. = not detected. deg = degassed. quant = quantitative.

Table S21. Optimized conditions and control studies using the 666 nm setup.[a]

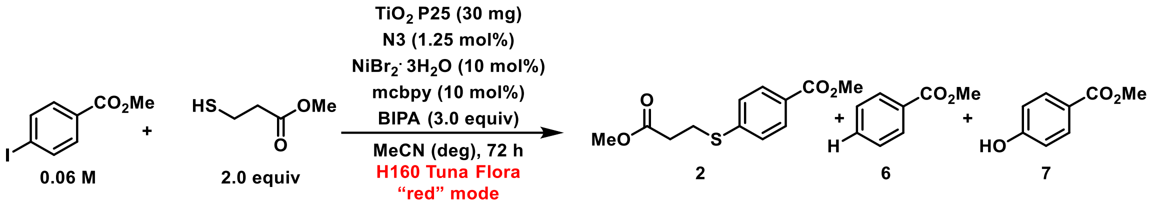

Entry	Deviation from standard conditions	Conversion [%][b]	2 [%][c]	6 [%][c]	7 [%][c]
1	--	quant	99	n.d.	n.d.
2	no TiO_2	20	20	n.d.	n.d.
3	no N3	10	10	n.d.	n.d.

[a]Reaction conditions: methyl 4-bromobenzoate (190.3 µmol), methyl 3-mercaptopropionate (380.5 µmol), N3 (2.4 µmol), $NiBr_2 \cdot 3H_2O$ (19.0 µmol) and mcbpy (19.0 µmol) BIPA (570.8 µmol) in MeCN (3 mL), TiO_2 (30 mg), 666 nm LED (100% power), 72 h. [b]Conversion of methyl 4-iodobenzoate determined by ^{1}H-NMR using 1,3,5-trimethoxybenzene as internal standard. [c]NMR yields determined by ^{1}H-NMR using 1,3,5-trimethoxybenzene as internal standard. BIPA = *N*-*tert*-butylisopropylamine. mcbpy = 4'-methyl-2,2'-bipyridine-4-carboxylic acid . n.d. = not detected. deg = degassed. quant = quantitative.

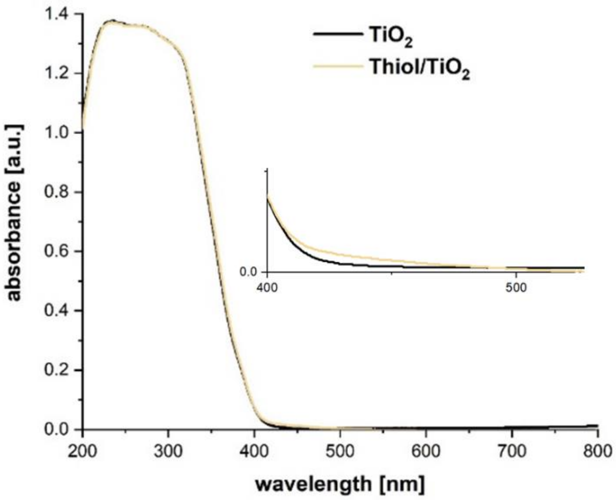

Fig. S15. UV/Vis absorption spectra of TiO_2 (black) and 3-mercaptopropionate-TiO_2 (yellow).

The absorption spectrum of TiO_2 P25 is extended to visible light due to surface complexation of the thiol starting material (*24*). This effect is responsible for background reactions.

4.2 Experimental procedure for the optimized C-S arylation using in situ generation of DSMPs.

An oven dried vial (19 x 100 mm) equipped with a stir bar was charged with TiO_2 P25 (90 mg), methyl 4-iodobenzoate (149.37 mg, 570.0 µmol, 1.0 equiv), methyl 3-mercaptopropionate (126.3 µL, 1.14 mmol, 2.0 equiv), Coumarin 343 or N3 (7.1 µmol, 1.25 mol%), $NiBr_2 \cdot 3H_2O$ (15.5 mg, 57.0 µmol, 10 mol%) and 4'-methyl-2,2'-bipyridine-4-carboxylic acid (12.2 mg, 57.0 µmol, 10 mol%). Subsequently, MeCN (anhydrous, 6 mL) and *N*-tert-butylisopropylamine (BIPA, 271 µL, 1.71 mmol, 3 equiv) were added and the vial was sealed with a septum and Parafilm. The reaction mixture was sonicated for 5-10 min followed by stirring for 5 min to obtain a fine dispersion. The mixture was then degassed by bubbling Argon for 10 min. The mixture was irradiated using the 525 (fluorescein sodium) or 666 nm LED setup (N3) with rapid stirring (1400 rpm). After the respective reaction time, one equivalent of 1,3,5-trimethoxybenzene (internal standard 96 mg, 570 µmol) was added and the mixture was stirred for 5 min. An aliquot of the reaction mixture (~200 µL) was filtered, diluted with DMSO-d_6 and subjected to ^{1}H-NMR analysis. Thereafter, the NMR sample was combined with the reaction mixture, diluted with H_2O (40 mL) and extracted with ethyl acetate (3 x 30 mL). The combined organic phases were washed with aqueous NaOH (1 M, 2x40 ml) and brine (40 mL), dried over Na_2SO_4 and concentrated. The product was purified by flash column chromatography (SiO_2, Hexane/EtOAc elution gradient of 0-10%) on a Grace Reveleris system using a 12 g cartridge. The title compound was isolated as a white solid.

Using Coumarin 343 and the 525 nm setup:

Reaction time: 24 h
Isolated yield: 95% (135.7 mg, 533.6 µmol)

Using N3 and the 666 nm setup:

Reaction time: 72 h
Isolated yield: 96% (137.3 mg, 540.0 µmol)

Methyl 4-((3-methoxy-3-oxopropyl)thio)benzoate 2: ^{1}H NMR (400 MHz, $CDCl_3$) δ 7.93 (d, J = 8.6 Hz, 2H), 7.31 (d, J = 8.6 Hz, 2H), 3.89 (s, 3H), 3.69 (s, 3H), 3.25 (t, J = 7.4 Hz, 2H), 2.68 (t, J = 7.4 Hz, 2H). ^{13}C NMR (101 MHz, $CDCl_3$) δ 171.98, 166.68, 142.68, 130.18, 127.41, 127.17, 52.21, 52.08, 33.83, 27.38. HRMS-EI (m/z) $[M^*]^+$ calcd for $C_{12}H_{14}O_4S$: 254.0613; found: 254.0617.

These data are in full agreement with those previously published in the literature (*25*).

5 C-N cross-coupling

5.1 Optimization studies using *in situ* generation of DSMPs.

General experimental procedure for screening experiments *via in situ* DSMP preparation. An oven dried vial (19 x 100 mm) equipped with a stir bar was charged with TiO_2 P25 (30 mg), methyl 4-bromobenzoate (1 equiv), pyrrolidine (3 equiv), a dye, $NiBr_2 \cdot 3H_2O$ (10 mol%), and a ligand (10 mol%). Subsequently, dimethylacetamide (anhydrous, 3 mL) was added and the vial was sealed with a septum and Parafilm. The reaction mixture was sonicated for 5-10 min, followed by stirring for 5 min to obtain a fine dispersion. The mixture was then degassed by bubbling Argon for 10 min. The mixture was irradiated with the respective LED lamps with rapid stirring (1400 rpm). After the respective reaction time, one equivalent of 1,3,5-trimethoxybenzene was added. An aliquot of the reaction mixture (~200 µL) was filtered, diluted with DMSO-d_6 and subjected to ^{1}H-NMR analysis. For a representative NMR spectrum, see Fig. S16.

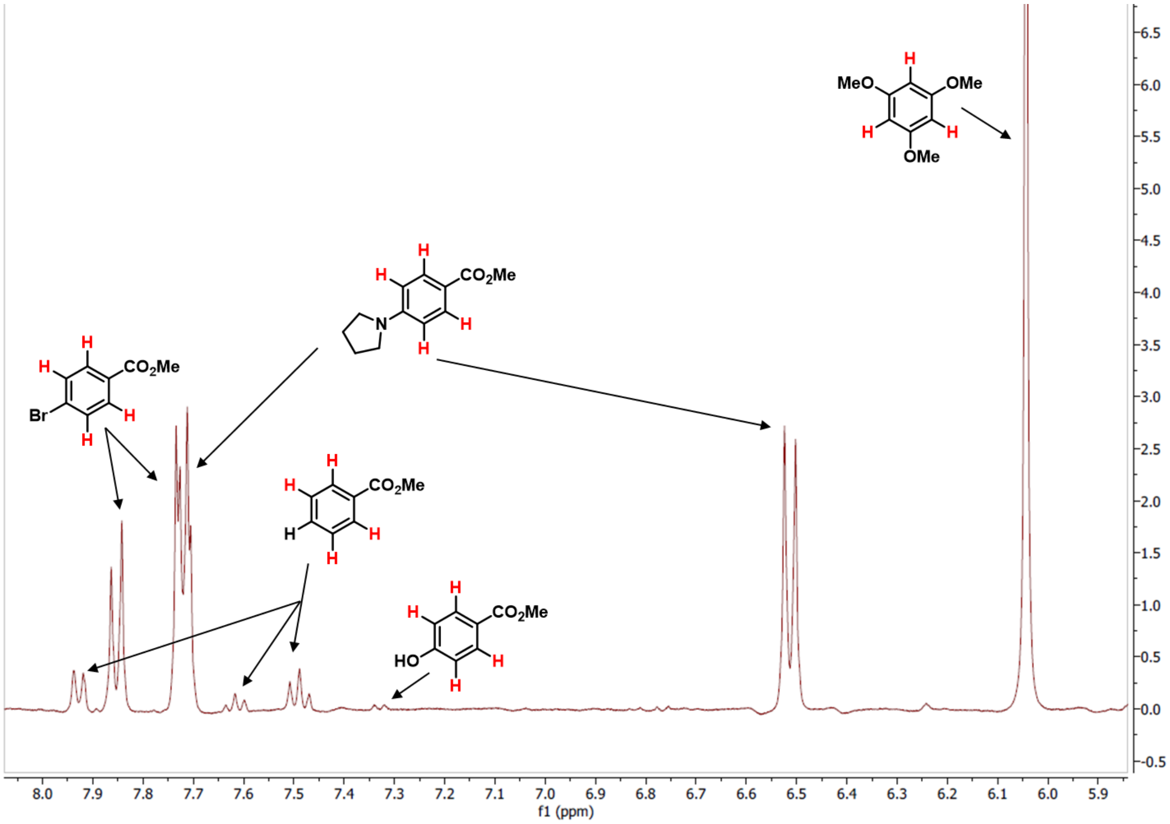

Fig. S16. Representative ^{1}H-NMR spectrum of a crude reaction mixture for determining NMR yields in the C-N arylation.

Table S22. Ligand screening in absence of a dye using the 440 nm LED setup.[a]

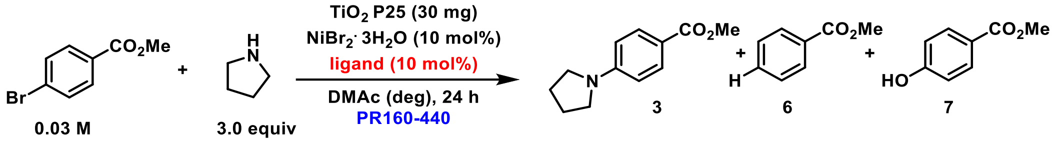

Entry	Ligand	Conversion [%][b]	3 [%][c]	6 [%][c]	7 [%][c]
1	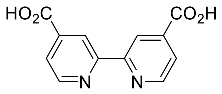	89	78	3	traces
2	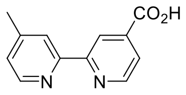	88	62	10	3

[a]Reaction conditions: methyl 4-bromobenzoate (300.0 µmol), pyrrolidine (900.0 µmol), $NiBr_2 \cdot 3H_2O$ (30.0 µmol) and ligand (30.0 µmol) in DMAc (3 mL), TiO_2 (30 mg), 440 nm, LED (50% power), 24 h. [b]Conversion of methyl 4-bromobenzoate determined by ^{1}H-NMR using 1,3,5-trimethoxybenzene as internal standard. [c]NMR yields determined by ^{1}H-NMR using 1,3,5-trimethoxybenzene as internal standard. DMAc = dimethylacetamied.

Table S23. Dye screening using the 525 nm LED setup.[a]

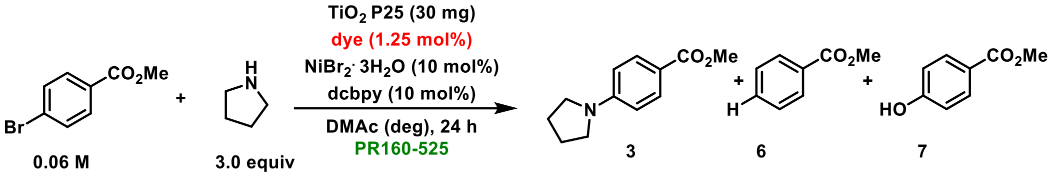

Entry	Dye	Conversion [%][b]	3 [%][c]	6 [%][c]	7 [%][c]
1	--	2	n.d.	n.d.	n.d.
2	Rose bengal	56	43	7	n.d.
3	Coumarin 343	50	32	14	n.d.
4	Rhodamin B	15	3	traces	n.d.
5	Fluorescein sodium	10	traces	6	n.d.
6	Bromophenol blue	7	n.d.	n.d.	n.d.
7	Congo red	5	n.d.	n.d.	n.d.
8	Alizarin red S	4	n.d.	n.d.	n.d.
9	Brilliant blue R	2	n.d.	n.d.	n.d.
10	Catechol	0	n.d.	n.d.	n.d.
14	Methyl orange	0	n.d.	n.d.	n.d.

[a]Reaction conditions: methyl 4-bromobenzoate (190.3 µmol), pyrrolidine (570.8 µmol), dye (2.4 µmol), $NiBr_2 \cdot 3H_2O$ (19.0 µmol) and dcbpy (19.0 µmol) in DMAc (3 mL), TiO_2 (30 mg), 525 nm LED (50% power), 24 h. [b]Conversion of methyl 4-bromobenzoate determined by ^{1}H-NMR using 1,3,5-trimethoxybenzene as internal standard. [c]NMR yields determined by ^{1}H-NMR using 1,3,5-trimethoxybenzene as internal standard. For structures of the dyes, see Fig. S11. dcbpy = 2,2′-bipyridine-4,4′-dicarboxylic acid. DMAc = dimethylacetamide. n.d. = not detected. deg = degassed.

Table S24. Optimization of the amount of dye and equivalents of pyrrolidine using the 525 nm setup.[a]

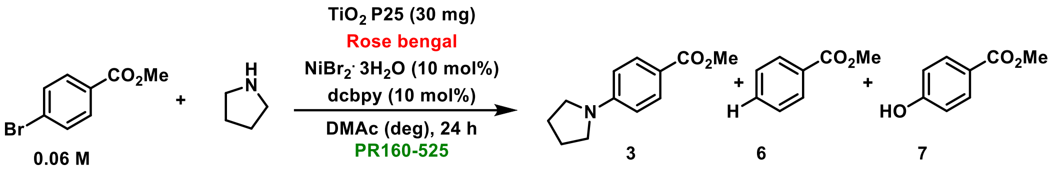

Entry	variations	Conversion [%][b]	3 [%][c]	6 [%][c]	7 [%][c]
1	0.50 mol% dye + 5 equiv pyrrolidine	quant	98	traces	n.d.
2	0.63 mol% dye + 5 equiv pyrrolidine	quant	85	6	n.d.
3	0.63 mol% dye + 3 equiv pyrrolidine	67	58	10	traces

[a] Reaction conditions: methyl 4-bromobenzoate (190.3 µmol), pyrrolidine, $NiBr_2 \cdot 3H_2O$ (19.0 µmol), Rose begal, and dcbpy (19.0 µmol) in DMAc (3 mL), TiO_2 (30 mg), 525 nm LED (50% power), 24 h. [b] Conversion of methyl 4-bromobenzoate determined by ^{1}H-NMR using 1,3,5-trimethoxybenzene as internal standard. [c] NMR yields determined by ^{1}H-NMR using 1,3,5-trimethoxybenzene as internal standard. dcbpy = 2,2′-bipyridine-4,4′-dicarboxylic acid. DMAc = dimethylacetamide n.d. = not detected. deg = degassed. quant = quantitative.

Table S25. Optimized conditions and control studies using the 440 nm setup.[a]

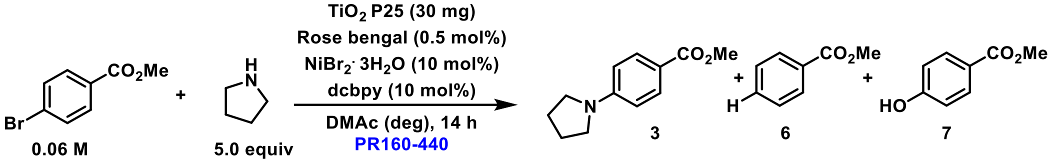

Entry	Deviation from standard conditions	Conversion [%][b]	3 [%][c]	6 [%][c]	7 [%][c]
1	--	quant	99	traces	n.d.
2	no dcbpy	67	65	n.d.	n.d.
3	no Rose Bengal	20	19	n.d.	n.d.
4	no light	2	n.d.	n.d.	n.d.
5	no $NiBr_2·3H_2O$	0	n.d.	n.d.	n.d.
6	no TiO_2	0	n.d.	n.d.	n.d.
7	no degassing	0	n.d.	n.d.	n.d.

[a] Reaction conditions: methyl 4-bromobenzoate (190.3 µmol), pyrrolidine (951.6 µmol), Rose Bengal (1.0 µmol), $NiBr_2·3H_2O$ (19.0 µmol) and dcbpy (19.0 µmol) in DMAc (3 mL), TiO_2 (30 mg), 440 nm blue LED (50% power) for 14 h. [b] Conversion of methyl 4-bromobenzoate determined by ^{1}H-NMR using 1,3,5-trimethoxybenzene as internal standard. [c] NMR yields determined by ^{1}H-NMR using 1,3,5-trimethoxybenzene as internal standard. dcbpy = 2,2′-bipyridine-4,4′-dicarboxylic acid. DMAc = dimethylacetamide n.d. = not detected. deg = degassed. quant = quantitative

Table S26. Optimized conditions and control studies using the 525 nm setup.[a]

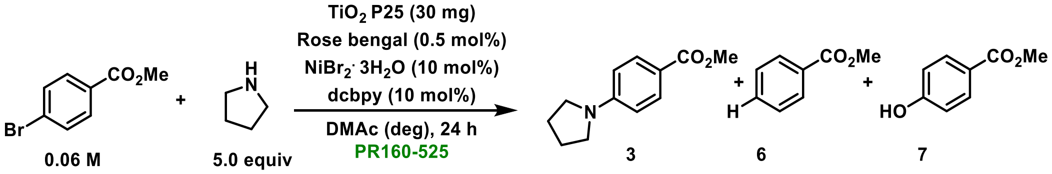

Entry	Deviation from standard conditions	Conversion [%][b]	3 [%][c]	6 [%][c]	7 [%][c]
1	--	quant	99	traces	n.d.
2	no dcbpy	70	69	n.d.	n.d.
3	no Rose Bengal	2	traces	n.d.	n.d.
4	no light	2	n.d.	n.d.	n.d.
5	no $NiBr_2 \cdot 3H_2O$	0	n.d.	n.d.	n.d.
6	no TiO_2	0	n.d.	n.d.	n.d.
7	no degassing	0	n.d.	n.d.	n.d.

[a] Reaction conditions: methyl 4-bromobenzoate (190.3 µmol), pyrrolidine (951.4 µmol), Rose Bengal (1.0 µmol), $NiBr_2 \cdot 3H_2O$ (19.0 µmol) and dcbpy (19.0 µmol) in DMAc (3 mL), TiO_2 (30 mg), 525 nm LED (50% power), 24 h. [b] Conversion of methyl 4-bromobenzoate determined by ^{1}H-NMR using 1,3,5-trimethoxybenzene as internal standard. [c] NMR yields determined by ^{1}H-NMR using 1,3,5-trimethoxybenzene as internal standard. dcbpy = 2,2′-bipyridine-4,4′-dicarboxylic acid. DMAc = dimethylacetamide n.d. = not detected. deg = degassed. quant = quantitative

Table S27. Optimized conditions and control studies using the 666 nm setup.[a]

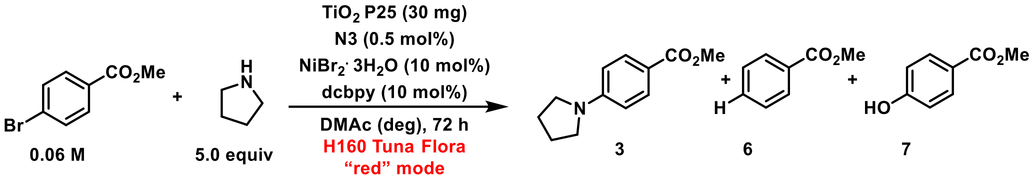

Entry	Deviation from standard conditions	Conversion [%][b]	3 [%][c]	6 [%][c]	7 [%][c]
1	--	quant.	95	4	n.d.
2	no TiO_2	2	n.d.	n.d.	n.d.
3	No N3	3	n.d.	n.d.	n.d.

[a] Reaction conditions: methyl 4-bromobenzoate (190.3 µmol), pyrrolidine (951.4 µmol), Rose Bengal (1.0 µmol), $NiBr_2·3H_2O$ (19.0 µmol) and dcbpy (19.0 µmol) in DMAc (3 mL), TiO_2 (30 mg), 666 nm red LED (100% power), 72 h. [b] Conversion of methyl 4-bromobenzoate determined by ^{1}H-NMR using 1,3,5-trimethoxybenzene as internal standard. [c] NMR yields determined by ^{1}H-NMR using 1,3,5-trimethoxybenzene as internal standard. dcbpy = 2,2′-bipyridine-4,4′-dicarboxylic acid. DMAc = dimethylacetamide n.d. = not detected. deg = degassed. quant = quantitative

5.2 Experimental procedure for the optimized C-N arylation using in situ generation of DSMPs.

An oven dried vial (19 x 100 mm) equipped with a stir bar was charged with TiO_2 (90 mg), pyrrolidine (121.6 mg, 142.7 µl, 1.71 mmol, 5.0 equiv), and 4-bromomethylbenzoate (122.6 mg, 570.0 µmol, 1.0 equiv), Rose Bengal or N3 (2.9 µmol, 0.50 mol%), $NiBr_2 \cdot 3H_2O$ (57.0 µmol, 10 mol%) and 2,2′-bipyridine-4,4′-dicarboxylic acid (57.0 µmol, 10 mol%). Subsequently, DMAc (anhydrous, 6 mL) was added and the vial was sealed with a septum and Parafilm. The reaction mixture was sonicated for 5-10 min followed by stirring for 5 min to obtain a fine dispersion. The mixture was then degassed by bubbling Argon for 10 min. The mixture was irradiated using the 525 (Rose Bengal) or 666 nm LED setup (N3) with rapid stirring (1400 rpm). After the respective reaction time, one equivalent of 1,3,5-trimethoxybenzene (internal standard 96 mg, 570 µmol) was added and the mixture was stirred for 5 min. An aliquot of the reaction mixture (~200 µL) was filtered, diluted with DMSO-d_6 and subjected to ^{1}H-NMR analysis. Thereafter, the NMR sample was combined with the reaction mixture, diluted with H_2O (40 mL) and extracted with ethyl acetate (3 x 30 mL). The combined organic phases were washed with H_2O (40 mL), $NaHCO_3$ solution (40 ml) and brine (40 mL), dried over Na_2SO_4 and concentrated. The product was purified by flash column chromatography (SiO_2, Hexane/EtOAc elution gradient of 0-10%) on a Grace Reveleris system using a 12 g cartridge. The title compound was isolated as a white solid.

Using Rose Bengal and the 525 nm setup:

Reaction time: 72 h

Isolated yield: 94% (109.9 mg, 535.8 µmol)

Using N3 and the 666 nm setup:

Reaction time: 72 h

Isolated yield: 96% (112.2 mg, 547,0 µmol)

1-(4-methylbenzoate)pyrrolidine 3: ^{1}H NMR (400 MHz, $CDCl_3$) δ 7.90 (d, J = 8.7 Hz, 2H), 6.47 (d, J = 8.7 Hz, 2H), 3.84 (s, 3H), 3.42 – 3.09 (m, 4H), 2.05 – 1.86 (m, 4H). ^{13}C NMR (101 MHz, $CDCl_3$) δ 167.76, 150.95, 131.49, 116.37, 110.76, 51.55, 47.62, 25.58. HRMS (ESI-TOF) m/z calcd. for $C_{12}H_{16}NO_2$ [(M+H)$^+$]: 206.1176; found: 206.1187.

These data are in full agreement with those previously published in the literature (*26*).

6 C-C cross-coupling

6.1 Synthesis of 1-((trimethylsilyl)methyl)piperidine

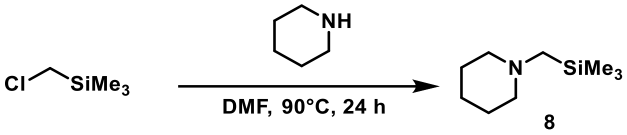

A 100 mL round bottom flask equipped with a stir bar was charged with (chloromethyl)trimethylsilane (3.07 g, 25 mmol, 1 equiv), DMF (25 mL) and piperidine (6.38 g, 7.41 mL, 75 mmol, 3.0 equiv). The mixture was heated to 90ºC in an oil bath (overnight) under an argon atmosphere. Reaction progress was assessed by NMR. When the reaction was completed, the mixture was cooled to room temperature and was diluted with deionized H_2O (~50 mL). The mixture was extracted with Et_2O (75 mL). The layers were separated, and the aqueous layer was extracted with Et_2O (2 × 50 mL). The combined organic layers were washed with deionized H_2O (2 ×100 mL) and brine (150 mL). The organic layer was dried (Na_2SO_4), and the solvent was removed. Further purification was accomplished by vacuum distillation (bp 60-62 °C @ 1 mmHg) giving clear colorless oil (2.57 g, 60%).

1-((trimethylsilyl)methyl)piperidine 8: ^{1}H NMR (400 MHz, $CDCl_3$) δ. 0.02 (s, 9H), 1.29 -1.38 (m, 2H), 1.47 -1.56 (m, 4H), 1.85 (s, 2H), 2.19 -2.38 (m, 4H). ^{13}C NMR (101 MHz, $CDCl_3$) δ -0.97 (CH_3), 23.96 (CH_2), 26.45 (CH_2), 51.82 (CH_2), 58.58 (CH_2). HRMS (ESI-TOF) m/z calcd. for C_9H_2NSi [$(M+H)^+$]: 172.1516; found: 172.1515.

These data are in full agreement with those previously published in the literature (*17*).

6.2 Optimization studies using *in situ* generation of DSMPs.

General experimental procedure for screening experiments *via in situ* DSMP preparation. An oven dried vial (19 x 100 mm) equipped with a stir bar was charged with TiO_2 P25 (30 mg), 4-bromobenzonitrile (1 equiv), 1-((trimethylsilyl)methyl)piperidine (1.2 equiv), a dye (1.25 mol%), $NiBr_2 \cdot$glyme (10 mol%), and a ligand (10 mol%). Subsequently, the solvent (anhydrous, 3 mL) was added and the vial was sealed with a septum and Parafilm. The reaction mixture was sonicated for 5-10 min followed by stirring for 5 min to obtain a fine dispersion. The mixture was then degassed by bubbling Argon for 10 min. The mixture was irradiated with the respective LED lamps with rapid stirring (1400 rpm). After the respective reaction time, an aliquot of the reaction mixture (~200 µL) was extracted with diethyl ether and the solvent was removed. The remaining reaction mixture , diluted with $CDCl_3$ and subjected to ^{1}H-NMR analysis to determine substrate-to-product rations. For a representative NMR spectrum, see Fig. S17.

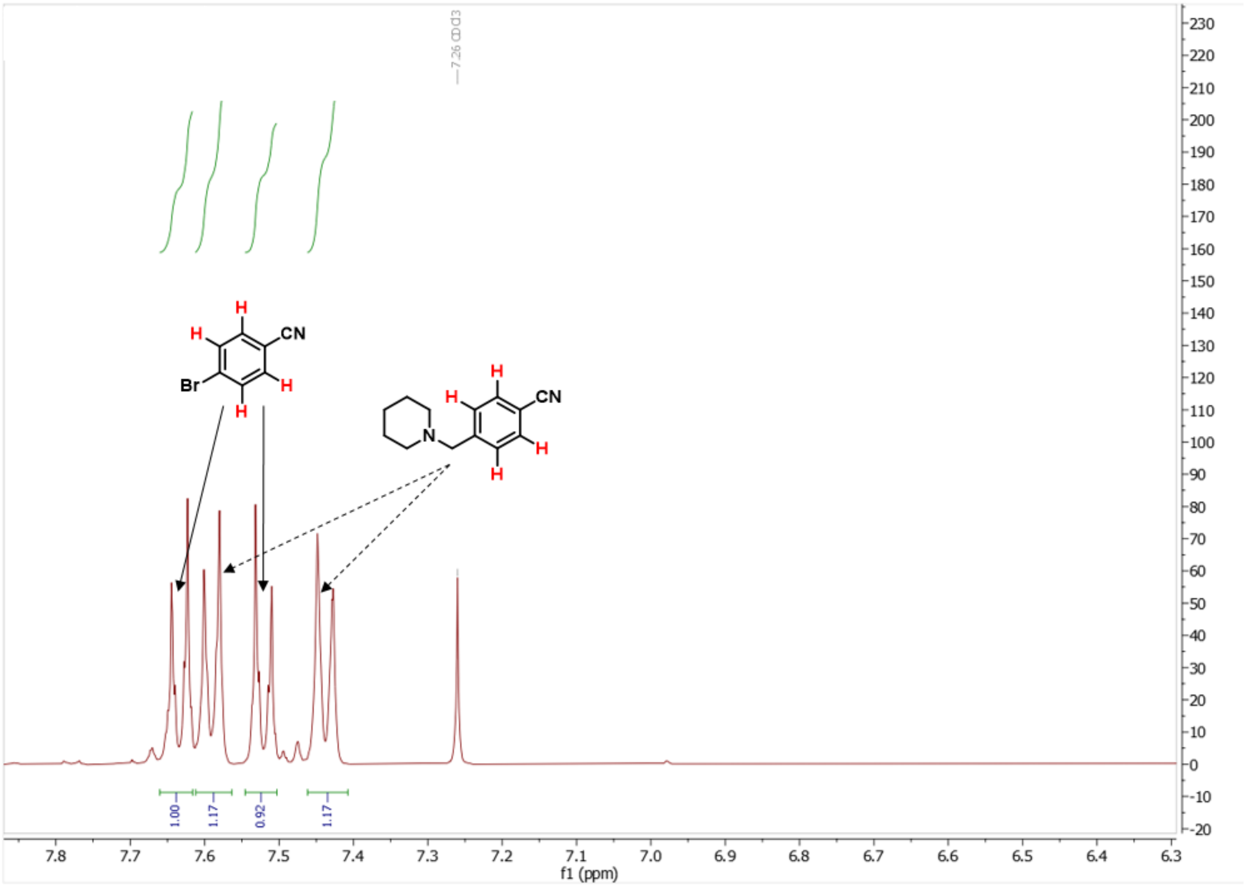

Fig. S17. Representative ^{1}H-NMR spectrum of a crude reaction mixture for determining substrate-to-product ratios yields in the C-C cross-coupling.

Table S28. Ligand screening in absence of a dye using the 440 nm LED setup.[a]

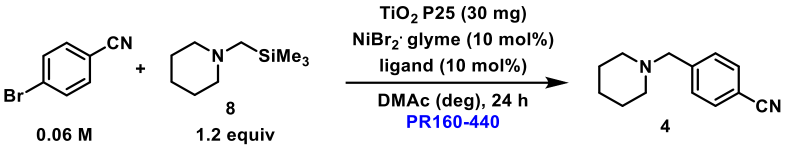

Entry	Ligand	Ar-Br:4[b]
1	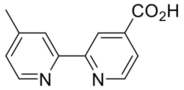	19:1
2	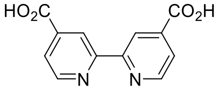	1:0

[a]Reaction conditions: 4-bromobenzonitrile (190.3 µmol), 1-((trimethylsilyl)methyl)piperidine (228.3 µmol), $NiBr_2 \cdot 3H_2O$ (19.0 µmol) and ligand (19.0 µmol) in DMAc (3 mL), TiO_2 (30 mg), 440 nm LED (100% power), 24 h. [c]Determined by ^{1}HNMR. DMAc = dimethylacetamide. glyme = 1,2-dimethoxyethane. n.d. = not detected. deg = degassed.

Table S29. Dye screening using the 440 nm LED setup.[a]

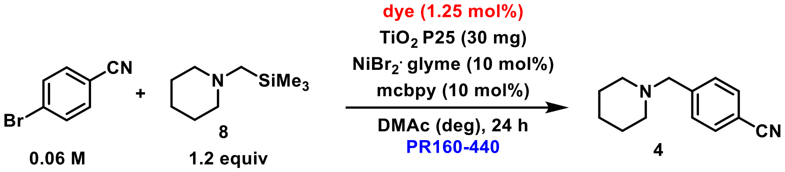

Entry	**Sensitizer**	**Ar-Br:4[b]**
1	Coumarin 343	1.8:1
2	Rose bengal	1.4:1
3	Rhodamin B	3:1
4	Fluorescein sodium	3.4:1

[a] Reaction conditions: 4-bromobenzonitrile (190.3 µmol), 1-((trimethylsilyl)methyl)piperidine (228.3 µmol), Sensitizer (1.25 mol%), $NiBr_2$·glyme (19.0 µmol) and mcbpy (19.0 µmol) in DMAc (3 mL), TiO_2 (30 mg), 440 nm LED (100% power), 24 h. [b] Determined by ^{1}HNMR. For structures of the dyes, see Fig. S11. DMAc = dimethylacetamide. glyme = 1,2-dimethoxyethane. mcbpy = 4'-methyl-2,2'-bipyridine-4-carboxylic acid. n.d. = not detected. deg = degassed.

Table S30. Optimized conditions and control studies using the 440 nm setup.[a]

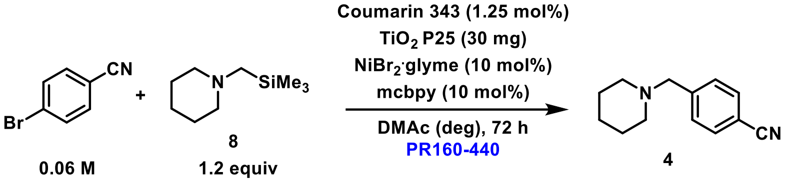

Entry	Deviation from standard conditions	Ar-Br:4[b]
1	--	0:1
2	no mcbpy	4:1
3	no Coumarin 343	10:1
4	no light	1:0
5	no TiO_2	9:1
6	no $NiBr_2$·glyme	1:0
7	no degassing	13:1

[a]Reaction conditions: 4-bromobenzonitrile (190.3 µmol), 1-((trimethylsilyl)methyl)piperidine (228.3 µmol), Coumarin 343 (1.25 mol%), $NiBr_2$·glyme (19.0 µmol) and mcbpy (19.0 µmol) in DMAc (3 mL), TiO_2 (30 mg), 440 nm LED (100% power), 72 h. [b]Determined by ^{1}HNMR. DMAc = dimethylacetamide. glyme = 1,2-dimethoxyethane. mcbpy = 4'-methyl-2,2'-bipyridine-4-carboxylic acid. n.d. = not detected. deg = degassed.

Table S31. Optimized conditions and control studies using the 525 nm setup.[a]

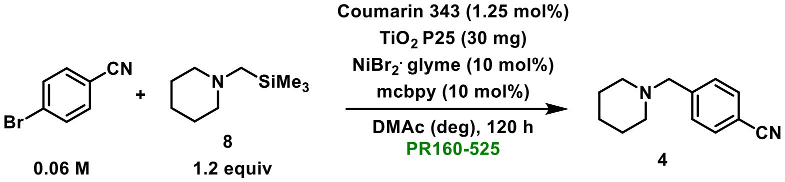

Entry	Deviation from standard conditions	Ar-Br:4[b]
1	none	0:1
2	no mcbpy	7:1
3	no Coumarin 343	1:0
4	no light	1:0
5	no TiO_2	12:1
6	no $NiBr_2$·glyme	1:0
7	no degassing	19:1

[a] Reaction conditions: 4-bromobenzonitrile (190.3 µmol), 1-((trimethylsilyl)methyl)piperidine (228.3 µmol), Coumarin 343 (1.25 mol%), $NiBr_2$·glyme (19.0 µmol) and mcbpy (19.0 µmol) in DMAc (3 mL), TiO_2 (30 mg), 525 nm LED (100% power), 120 h. [b] Determined by ^{1}HNMR. DMAc = dimethylacetamide. glyme = 1,2-dimethoxyethane. mcbpy = 4'-methyl-2,2'-bipyridine-4-carboxylic acid. n.d. = not detected. deg = degassed.

Table S32. Optimized conditions and control studies using the 666 nm setup.[a]

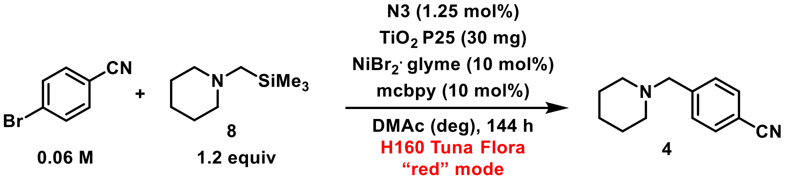

Entry	Deviation from standard conditions	Ar-Br:4[b]
1	none	0:1
2	no N3	1:0
3	no TiO_2	1:0

[a] Reaction conditions: 4-bromobenzonitrile (190.3 µmol), 1-((trimethylsilyl)methyl)piperidine (228.3 µmol), N3 (1.25 mol%), $NiBr_2$·glyme (19.0 µmol) and mcbpy (19.0 µmol) in DMAc (3 mL), TiO_2 (30 mg), 666 nm LED (100% power), 144 h. [b] Determined by ^{1}HNMR. DMAc = dimethylacetamide. glyme = 1,2-dimethoxyethane. mcbpy = 4'-methyl-2,2'-bipyridine-4-carboxylic acid. n.d. = not detected. deg = degassed.

6.3 Experimental procedure for the optimized C-C coupling using *in situ* generation of DSMPs.

An oven dried vial (19 x 100 mm) equipped with a stir bar was charged with TiO_2 (30 mg), 1-((trimethylsilyl)methyl)piperidin (139.8 µL, 685.0 µmol, 1.2 equiv), 4-bromobenzonitrile (103.9 mg, 570.0 µmol, 1.0 equiv), Coumarin 343 (7.1 µmol, 1.25 mol%), $NiBr_2$·gylme (57.0 µmol, 10 mol%) and 4'-methyl-2,2'-bipyridine-4-carboxylic acid (57.0 µmol, 10 mol%). Subsequently, DMAc (anhydrous, 6 mL) was added and the vial was sealed with a septum and Parafilm. The reaction mixture was sonicated for 5-10 min followed by stirring for 5 min to obtain a dispersion. The mixture was then degassed by bubbling Argon for 10 min. The mixture was irradiated using the 440, 525 (Rose Bengal) or 666 nm LED setup (N3) with rapid stirring (1400 rpm). After the respective reaction time, an aliquot of the reaction mixture was extracted with diethyl ether. The solvent was removed and remaining reaction mixture diluted with $CDCl_3$ and subjected to ^{1}H-NMR analysis (See Table S13). Thereafter, the NMR sample was combined with the reaction mixture, diluted with H_2O (40 mL) and 2M NaOH (10 mL) and extracted with Et_2O (3 x 30 mL). The combined organic phases were washed with brine (50 mL), dried over Na_2SO_4 and concentrated. The product was purified by flash column chromatography (SiO_2, DCM/MeOH elution gradient of 0-2%) on a Grace Reveleris system using a 12 g cartridge. The title compound was isolated as a yellowish oil.

Using Coumarin 343 and the 440 nm setup:

Reaction time: 72 h

Isolated yield: 68% (77.7 mg, 388.0µmol)

Using Coumarin 343 and the 525 nm setup:

Reaction time: 120 h

Isolated yield: 75% (85.6 mg, 427.4 µmol)

Using N3 and the 666 nm setup:

Reaction time: 144 h

Isolated yield: 81% (92.4 mg, 461,3 µmol)

4-(Piperidin-1-ylmethyl)benzonitrile 4: ^{1}H NMR (400 MHz, $CDCl_3$) δ 7.60 (d, *J* = 8.2 Hz, 2H), 7.46 (d, *J* = 8.0 Hz, 2H), 3.52 (s, 2H), 2.46 - 2.29 (m, 4H), 1.64 – 1.51 (m, 4H), 1.50 – 1.38

(m, 2H). ^{13}C NMR (101 MHz, $CDCl_3$) δ 144.79, 132.13, 129.66, 119.17, 110.80, 63.31, 54.71, 26.01, 24.29. HRMS (ESI-TOF) m/z calcd. for $C_{13}H_{16}N_2$ $[(M+H)^+]$: 200.1386; found: 200.1397.

These data are in full agreement with those previously published in the literature (*17*).

7 Catalyst recycling experiments

Experimental procedure for catalyst recycling experiments of the C-O arylation with the 525 nm setup using Fluo-TiO_2-$NiCl_2$·dcbpy generated *in situ*. An oven dried vial (19 x 100 mm) equipped with a stir bar was charged with TiO_2 P25 (30 mg), *N*-Boc proline (40.9 mg, 190.3 µmol, 1.0 equiv), methyl 4-iodobenzoate (74.8 mg, 285.4 µmol, 1.5 equiv), fluorescein sodium (2.4 µmol, 1.25 mol%), $NiCl_2 \cdot 6H_2O$ (4.5 mg 19.0 µmol, 10 mol%) and 2,2′-bipyridine-4,4′-dicarboxylic acid (dcbpy, 4.6 mg 19.0 µmol, 10 mol%). Subsequently, DMSO (anhydrous, 3 mL) and *N*-tert-butylisopropylamine (BIPA, 90.4 µL, 570.8 µmol, 3 equiv) were added and the vial was sealed with a septum and Parafilm. The reaction mixture was sonicated for 5-10 min followed by stirring for 5 min to obtain a fine dispersion. The mixture was then degassed by bubbling Argon for 10 min. The mixture was irradiated using the 525 nm LED setup with rapid stirring (1400 rpm). After the respective reaction time, the reaction mixture was centrifuged and washed twice with 3 mL DMSO. The remaining DSMPs was lyophilized overnight and reused in the next reaction

Table S33. Catalyst Recycling experiments of the C-O arylation with the 525 nm setup using an *in situ* generated DSMP.[a]

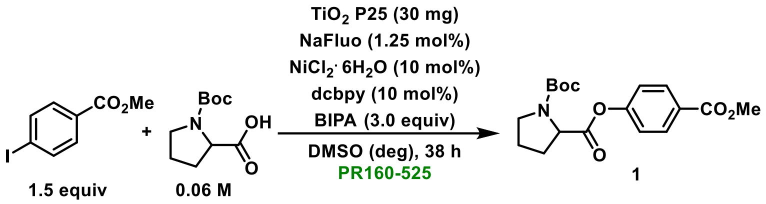

Entry	Cycle	1 [%][c]
1	1	95
2	2	67
3	3	58
4	4	26
5	5	n.d.
6	+NaFluo (1.25 mol%)[d]	98
7	+$NiCl_2·6H_2O$ (10 mol%)[e]	75

[a] Reaction conditions: methyl 4-iodobenzoate (285.4 µmol), *N*-Boc proline (190.3 µmol), Fluorescein sodium (2.4 µmol), $NiCl_2·6H_2O$ (19.0 µmol) and dcbpy (19.0 µmol) in DMSO (anhydrous, 3 mL), BIPA (570.8 µmol), TiO_2 (30 mg), 525 nm LED (25% power), 38h. [b] Conversion of methyl 4-iodobenzoate determined by ^{1}H-NMR using 1,3,5-trimethoxybenzene as internal standard. [c] NMR yields determined by ^{1}H-NMR using 1,3,5-trimethoxybenzene as internal standard. [d] Fluorescein sodium (2.4 µmol) was added to a reaction mixture using the material recovered from entry 5. [e] The nickel salt (19.0 µmol) was added to a reaction mixture using the material recovered from entry 5. NaFluo = Fluorescein sodium. dcbpy = 2,2′-bipyridine-4,4′-dicarboxylic acid. n.d. = not detected. BIPA = *N-tert*-butylisopropylamine. deg = degassed

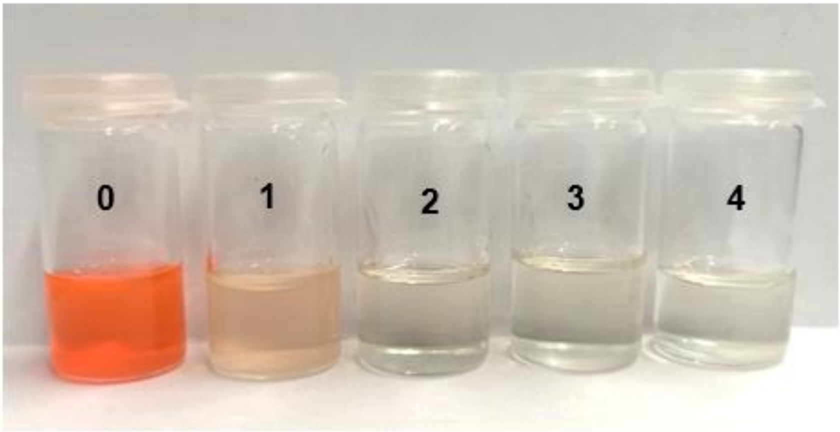

Fig. S18. Reaction mixtures (see Table S33) by centrifugation.

Table S34. ICP-OES measurements of the nickel content the DSMP and the recovered DSMP after 5 cycles.

Sample	Ni [mg/g catalyst]
TiO_2	0.02
Fluo-TiO_2-$NiCl_2$·dcbpy (*in situ*)	7.43
Fluo-TiO_2-$NiCl_2$·dcbpy (after) [a]	0.71

[a] Fluo-TiO_2-$NiCl_2$·dcbpy after 5 reaction cycles

Experimental procedure for catalyst recycling experiments of the C-O arylation with the 525 nm setup using Fluo-TiO_2-$NiCl_2$·dcbpy generated *in ex situ*.

An oven dried vial (19 x 100 mm) equipped with a stir bar was charged with TiO_2 P25 (30 mg), *N*-Boc proline (40.9 mg, 190.3 µmol, 1.0 equiv), methyl 4-iodobenzoate (74.8 mg, 285.4 µmol, 1.5 equiv) and Fluo-TiO_2-$NiCl_2$·dcbpy (for preparation, see section 2). Subsequently, DMSO (anhydrous, 3 mL) and *N*-tert-butylisopropylamine (BIPA, 90.4 µL, 570.8 µmol, 3 equiv) were added and the vial was sealed with a septum and Parafilm. The reaction mixture was sonicated for 5-10 min followed by stirring for 5 min to obtain a fine dispersion. The mixture was then degassed by bubbling Argon for 10 min. The mixture was irradiated using the 525 nm LED setup with rapid stirring (1400 rpm). After the respective reaction time, the reaction mixture was centrifuged and washed twice with 3 mL DMSO. The remaining DSMPs was lyophilized overnight and reused in the next reaction.

Table S35. Catalyst Recycling experiments of the C-O arylation with the 525 nm setup using an *ex situ* prepared DSMP.[a]

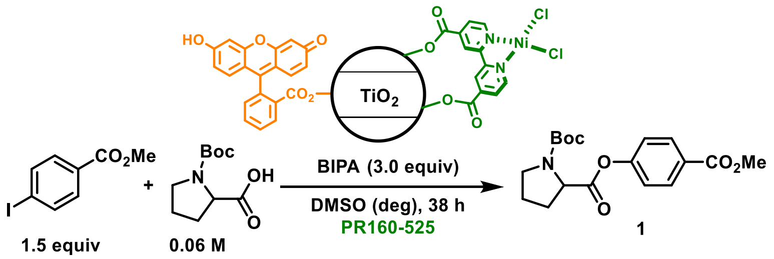

Entry	Cycles	1 [%][c]
1	*ex situ* prepared	63
2	1	21
3	2	4

[a]Reaction conditions: methyl 4-iodobenzoate (285,4 µmol), *N*-Boc proline (190.3 µmol) in DMSO (anhydrous, 3 mL), BIPA (570.8 µmol), catalyst (30 mg; for preparation procedure see 2.1), 525 nm LED (25% power), 38h. [b]Conversion of methyl 4-iodobenzoate determined by ^{1}H-NMR using 1,3,5-trimethoxybenzene as internal standard. [c]NMR yields determined by ^{1}H-NMR using 1,3,5-trimethoxybenzene as internal standard. dcbpy = 2,2′-bipyridine-4,4′-dicarboxylic acid. n.d. = not detected. BIPA = *N-tert*-butylisopropylamine. deg = degassed

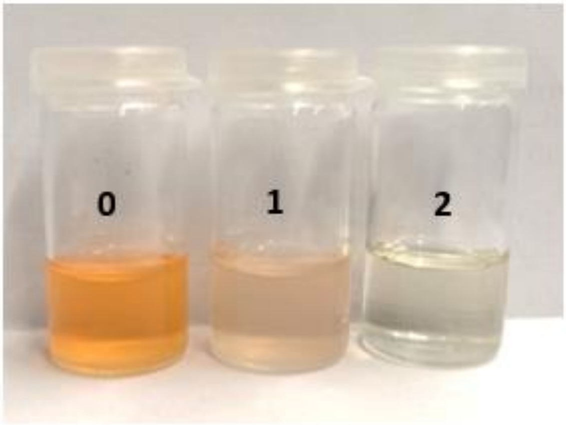

Fig. S19. Reaction mixtures (see Table S35) after catalyst separation by centrifugation.

Table S36. ICP-OES measurements of the nickel content on the new and recovered catalyst

Sample	Ni [mg/g catalyst]
TiO_2	0.02
Fluo-DSMP (*ex situ*)	6.50
Fluo-DSMP (after)[a]	1.66
Fluo-TiO_2	0.041
TiO_2-$NiCl_2$·dcbpy	5.45

[a] Fluo-TiO_2-$NiCl_2$·dcbpy after 5 reaction cycles

8 Experiments with insulating metal oxides and diffusion controlled metallaphotocatalysis.

The reactions were carried out according to the optimized experimental procedures for the individual couplings (see Section 3.2.; 4.2; 5.2 and 6.2) using different metal oxides and ligands.

Table S37. C-O cross-couplings with different metal oxides using the 525 nm setup.[a]

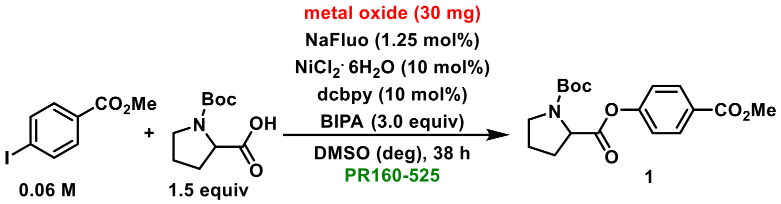

Entry	Metal oxide	1 [%][b]
1	TiO_2	97
2	SiO_2	50
3	Al_2O_3	39
4	ZnO	33
5	-	n.d.

[a]Reaction conditions: methyl 4-iodobenzoate (285.4 µmol), *N*-Boc proline (190.3 µmol), Fluorescein sodium (2.4 µmol), $NiCl_2 \cdot 6H_2O$ (19.0 µmol) and dcbpy (19.0 µmol), BIPA (570.8 µmol), and metal oxide (30 mg) in DMSO (anhydrous, 3 mL), 525 nm LED (25% power) for 38h. [b]NMR yields determined by ^1H-NMR using 1,3,5-trimethoxybenzene as internal standard. NaFluo = Fluorescein sodium. dcbpy = 2,2′-bipyridine-4,4′-dicarboxylic acid. n.d. = not detected. BIPA = *N-tert*-butylisopropylamine. deg = degassed

Table S38. C-O cross-couplings with different metal oxides and a non-binding nickel complex using the 525 nm setup.[a]

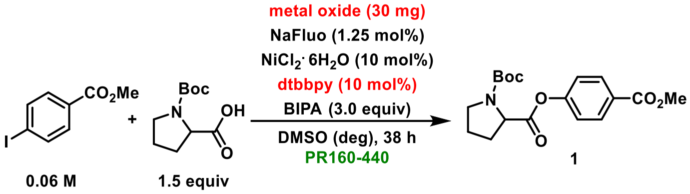

Entry	Metal oxide	1 [%][b]
1	TiO_2	65
2	SiO_2	n.d.
3	Al_2O_3	n.d.
4	ZnO	traces
5	-	n.d.

[a]Reaction conditions: methyl 4-iodobenzoate (285.4 µmol), *N*-Boc proline (190.3 µmol), Fluorescein sodium (2.4 µmol), $NiCl_2·6H_2O$ (19.0 µmol), dtbbpy (19.0 µmol), BIPA (570.8 µmol), and metal oxide (30 mg) in DMSO (anhydrous, 3 mL), 525 green LED (25% power) for 38h. [b]NMR yields determined by ^{1}H-NMR using 1,3,5-trimethoxybenzene as internal standard. NaFluo = Fluorescein sodium. dtbbpy = 4,4′-di-tert-butyl-2,2′-dipyridyl. n.d. = not detected. BIPA = *N-tert*-butylisopropylamine. deg = degassed

Table S39. C-O cross-couplings with different metal oxides using the 666 nm setup.[a]

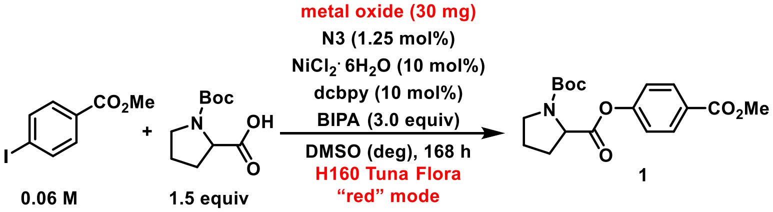

Entry	Metal oxide	1 [%][c]
1	TiO_2	95
2	SiO_2	48
3	Al_2O_3	37

[a]Reaction conditions: methyl 4-iodobenzoate (285.4 µmol), *N*-Boc proline (190.3 µmol), Fluorescein sodium (2.4 µmol), $NiCl_2·6H_2O$ (19.0 µmol) and dcbpy (19.0 µmol) in DMSO (anhydrous, 3 mL), BIPA (570.8 µmol), semiconductor (30 mg), 666 nm LED (100% power) for 168h.. [c]NMR yields determined by ^{1}H-NMR using 1,3,5-trimethoxybenzene as internal standard. NaFluo = Fluorescein sodium. dcbpy = 2,2′-bipyridine-4,4′-dicarboxylic acid. n.d. = not detected. BIPA = *N-tert*-butylisopropylamine. deg = degassed

Table S40. C-S cross-couplings with different metal oxides using the 525 nm setup.[a]

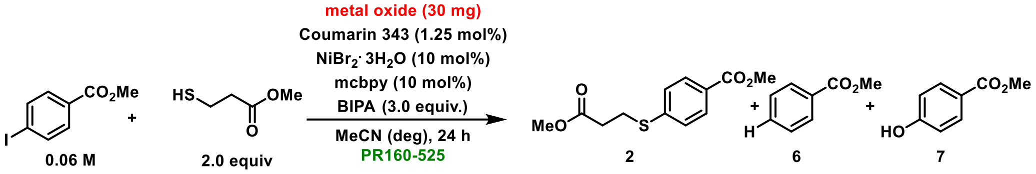

Entry	Metal oxide	2 [%][b]	6 [%][b]	7 [%][b]
1	TiO_2	99	n.d.	n.d.
2	Al_2O_3	99	n.d.	n.d.
3	SiO_2	48	n.d.	n.d.
4	-	traces	n.d.	n.d.

[a]Reaction conditions: methyl 4-bromobenzoate (190.3 µmol), methyl 3-mercaptopropionate (380.5 µmol), Coumarin 343 (2.4 µmol), $NiBr_2 \cdot 3H_2O$ (19.0 µmol), mcbpy (19.0 µmol) and metal oxide (30 mg) in MeCN (3 mL), 525 nm LED (50% power) for 24 h. [b]NMR yields determined by ^1H-NMR using 1,3,5-trimethoxybenzene as internal standard. BIPA = *N*-*tert*-butylisopropylamine. mcbpy = 4'-methyl-2,2'-bipyridine-4-carboxylic acid . n.d. = not detected. deg = degassed. quant = quantitative.

Table S41. C-S cross-couplings with different metal oxides and a non-binding nickel complex using the 525 nm setup.[a]

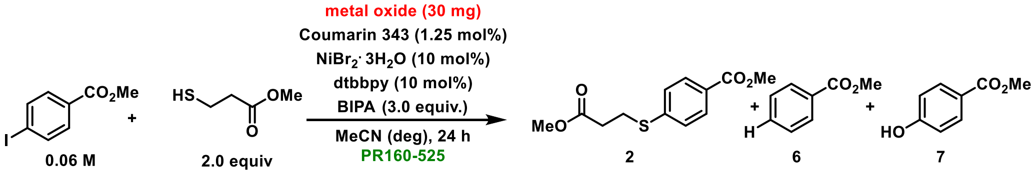

Entry	Metal oxide	2 [%][b]	6 [%][b]	7 [%][b]
1	TiO_2	80	n.d.	n.d.
2	Al_2O_3	10	n.d.	n.d.
3	SiO_2	5	n.d.	n.d.
4	-	traces	n.d.	n.d.

[a]Reaction conditions: methyl 4-bromobenzoate (190.3 µmol), methyl 3-mercaptopropionate (380.5 µmol), Coumarin 343 (2.4 µmol), $NiBr_2 \cdot 3H_2O$ (19.0 µmol), dtbbpy (19.0 µmol) and metal oxide (30 mg) in MeCN (3 mL), 525 green LED (50% power) for 24 h. [b]NMR yields determined by ^1H-NMR using 1,3,5-trimethoxybenzene as internal standard. BIPA = *N*-*tert*-butylisopropylamine. dtbbpy = 4,4′-di-tert-butyl-2,2′-dipyridyl. n.d. = not detected. deg = degassed. quant = quantitative.

Table S42. C-N cross-couplings with different metal oxides using the 525 nm setup.[a]

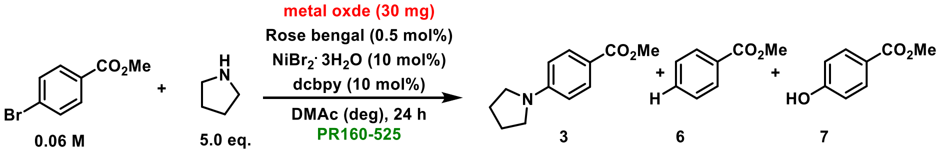

Entry	Metal oxide	3 [%][b]	6 [%][b]	7 [%]b
1	TiO_2	99	n.d.	n.d.
2	Al_2O_3	99	n.d.	n.d.
3	SiO_2	48	n.d.	n.d.
4	-	n.d.	n.d.	n.d.

[a] Reaction conditions: methyl 4-bromobenzoate (190.3 µmol), pyrrolidine (951.4 µmol), Rose Bengal (0.5 mol%) $NiBr_2\cdot 3H_2O$ (19.0 µmol) and dcbpy (19.0 µmol) in DMAc (3 mL), metal oxide (30 mg), 525 nm green LED (50% power) for 24 h. [b]Conversion of methyl 4-bromobenzoate determined by ^{1}H-NMR using 1,3,5-trimethoxybenzene as internal standard. [c]NMR yields determined by ^{1}H-NMR using 1,3,5-trimethoxybenzene as internal standard. dcbpy = 2,2′-bipyridine-4,4′-dicarboxylic acid. DMAc = dimethylacetamide n.d. = not detected. deg = degassed. quant = quantitative

Table S43. C-N cross-couplings with different metal oxides and a non-binding nickel complex using the 525 nm setup.[a]

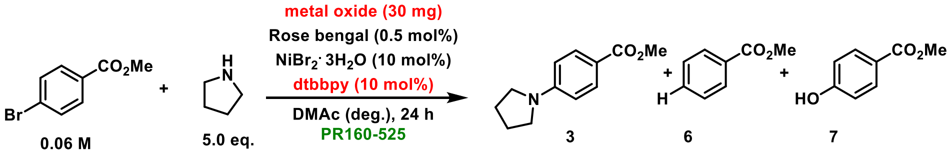

Entry	Metal oxide	3 [%][b]	6 [%][b]	7 [%][b]
1	TiO_2	12	n.d.	n.d.
2	Al_2O_3	n.d.	n.d.	n.d.
3	SiO_2	n.d.	n.d.	n.d.
4	-	n.d.	n.d.	n.d.

[a] Reaction conditions: methyl 4-bromobenzoate (190.3 µmol), pyrrolidine (951.4 µmol), Rose Bengal (0.5 mol%) $NiBr_2\cdot 3H_2O$ (19.0 µmol) and dtbbpy (19.0 µmol), metal oxide (30 mg), in DMAc (3 mL), 525 nm LED (50% power) for 24 h. [b]NMR yields determined by ^{1}H-NMR using 1,3,5-trimethoxybenzene as internal standard. dtbbpy = 4,4′-di-tert-butyl-2,2′-dipyridyl. DMAc = dimethylacetamide n.d. = not detected. deg = degassed. quant = quantitative

Table S44.C-C cross-couplings with different metal oxides using the 525 nm setup.[a]

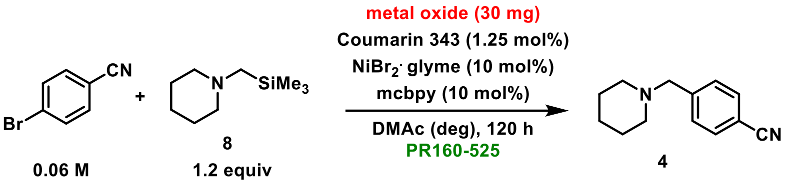

Entry	Metal oxide	Ar-Br:4[b]
1	TiO_2	0:1
2	Al_2O_3	1.5:1
3	SiO_2	1.6:1
4	-	1:traces

[a]Reaction conditions: 4-bromobenzonitrile (190.3 µmol), 1-((trimethylsilyl)methyl)piperidine (228,3 µmol), N3 (1.25 mol%), $NiBr_2$·glyme (19.0 µmol) metal oxide (30 mg), and mcbpy (19.0 µmol) in DMAc (3 mL), 666 nm LED (100% power), 144 h. [b]Determined by ^{1}HNMR. DMAc = dimethylacetamide. glyme = 1,2-dimethoxyethane. mcbpy = 4'-methyl-2,2'-bipyridine-4-carboxylic acid. n.d. = not detected. deg = degassed.

Table S45. C-C cross-couplings with different metal oxides and a non-binding nickel complex using the 525 nm setup.[a]

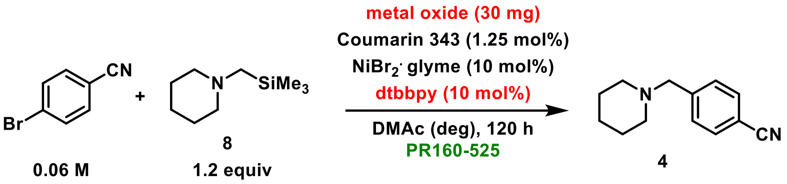

Entry	semiconductor	Ar-Br:4[b]
1	TiO_2	0:1
2	Al_2O_3	1:0
3	SiO_2	1:0
4	-	1:0

[a]Reaction conditions: 4-bromobenzonitrile (190.3 µmol), 1-((trimethylsilyl)methyl)piperidine (228,3 µmol), N3 (1.25 mol%), $NiBr_2$·glyme (19.0 µmol) metal oxide (30 mg), and mcbpy (19.0 µmol) in DMAc (3 mL), 666 nm LED (100% power), 144 h. [b]Determined by ^{1}HNMR. DMAc = dimethylacetamide. glyme = 1,2-dimethoxyethane. dtbbpy = 4,4′-di-tert-butyl-2,2′-dipyridyl. n.d. = not detected. deg = degassed.

9 Spectrophotometric titrations

Incremental amounts of $NiCl_2$·dcbpy or $NiCl_2$·dtbbpy were added while the concentration of Fluo-TiO_2 or Fluo-SiO_2 was kept constant. The fluorescence signals were corrected for re-absorption effects at the excitation wavelength and quantitatively analyzed.

Spectrophotometric titrations were conducted to analyze the electronic interactions between Fluo-MO (with MO = TiO_2 or SiO_2) and a nickel complex ($NiCl_2$·dcbpy or $NiCl_2$·dtbbpy) dispersed in DMSO. To this end, the absorption and emission features were monitored in dispersions with a constant concentration of Fluo-MO upon adding varying amounts of a nickel complex. The prominent absorption feature related to Fluo-MO with a maximum at 521 nm diminishes gradually upon stepwise addition of a nickel complex. The Fluo-MO related fluorescence, excited at 505 nm, is gradually quenched upon addition of the nickel complex (Fig. S27). The I_0/I relationship shows linear trends in all experiments except for the titration of Fluo-TiO_2 with $NiCl_2$·dcbpy, where a drastic increase of the slope was observed for $NiCl_2$·dcbpy concentrations > 7.3×10^{-7} M. A positive deviation from the initial linear relationship is typically described as mixed static and dynamic quenching, i.e. complex formation occurs to a certain degree. Association were determined from the linear parts of the I_0/I relationships and are summarized inTable S46.

Table S46. Association constants determined by spectrophotometric titrations.

	K_{ass} (dynamic) L mol^{-1}	**K_{ass} (static) L mol^{-1}**
Fluo-TiO_2 - $NiCl_2$·dcbpy	6.2×10^6	6.2×10^7
Fluo-TiO_2 - $NiCl_2$·dtbbpy	6.2×10^6	
Fluo-SiO_2 - $NiCl_2$·dcbpy	1.5×10^5	
Fluo-SiO_2 - $NiCl_2$·d*t*bbpy	7.0×10^4	

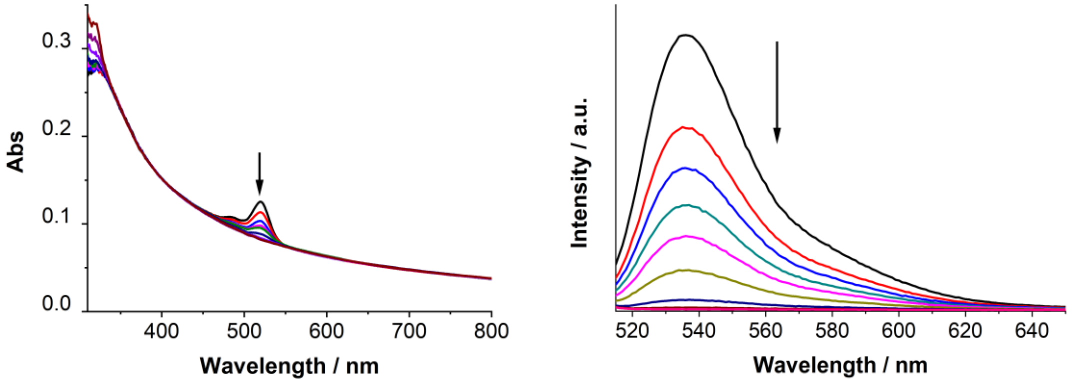

Fig. S20. Left: absorption spectra of Fluo-TiO_2 dispersed in DMSO during the course of a titration with $NiCl_2$·dcbpy (black to purple, 0 – 2.6 × 10^{-6} M); Right: steady-state fluorescence spectra of Fluo-TiO_2 dispersed in DMSO during the course of a titration with $NiCl_2$·dcbpy (black to purple, 0 – 2.6 × 10^{-6} M);

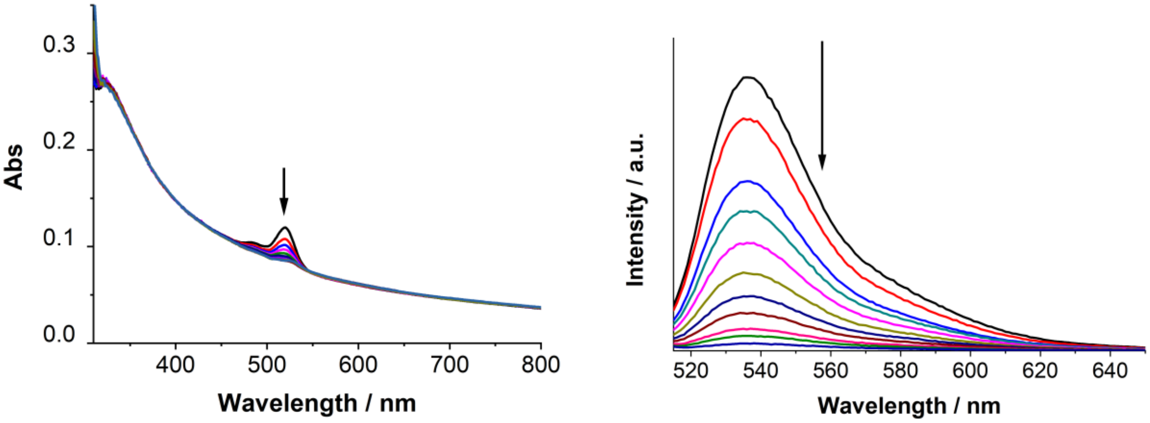

Fig. S21. Left: absorption spectra of Fluo-TiO_2 dispersed in DMSO during the course of a titration with $NiCl_2$·dtbbpy (black to purple, 0 – 2.6 × 10^{-6} M);Right: steady-state fluorescence spectra (λ_{ex} = 505 nm) of Fluo-TiO_2 dispersed in DMSO during the course of a titration with $NiCl_2$·dtbbpy (black to purple, 0 – 2.6 × 10^{-6} M).

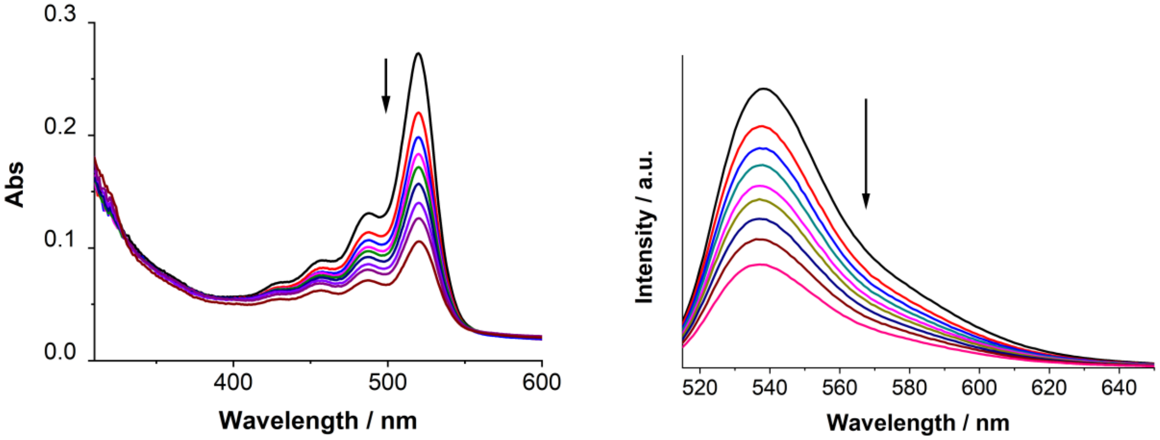

Fig. S22. Left: absorption spectra of Fluo-SiO$_2$ dispersed in DMSO during the course of a titration with NiCl$_2$·dcbpy (black to purple, 0 – 1.6 × 10^{-6} M); Right: steady-state fluorescence spectra (λ_{ex} = 505 nm) of Fluo-SiO$_2$ dispersed in DMSO during the course of a titration with NiCl$_2$·dcbpy (black to purple, 0 – 1.6 × 10^{-6} M).

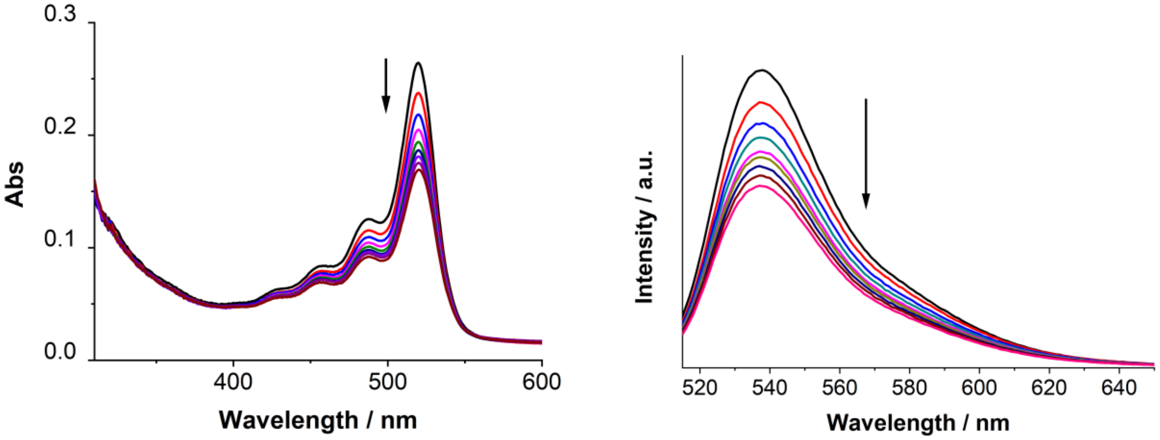

Fig. S23. Left: absorption spectra of Fluo-SiO$_2$ dispersed in DMSO during the course of a titration with NiCl$_2$·dtbbpy (black to purple, 0 – 1.6 × 10^{-6} M); Right: steady-state fluorescence spectra (λ_{ex} = 505 nm) of Fluo-SiO$_2$ dispersed in DMSO during the course of a titration with NiCl$_2$·dtbbpy (black to purple, 0 – 1.6 × 10^{-6} M).

10 Comparison of metallaphotocatalyst systems for the C-O arylation of cinnamic acid.

An oven dried vial (19 x 100 mm) equipped with a stir bar was charged with *trans* cinnamic acid (84.5 mg, 570 µmol, 1.0 equiv), 4-iodobenzotrifluoride (125.6 µL, 855 µmol, 1.5 equiv), $NiCl_2 \cdot 6H_2O$ (57 µmol, 10 mol%) and 2,2′-bipyridine-4,4′-dicarboxylic acid (57 µmol, 10 mol%). Three different homogeneous photocatalysts ($Ir[dF(Me)ppy]_2$ (dtbbpy))PF_6 (5.17 µmol, 1.00 mol%), $Ir[dF(CF_3)ppy]_2$(dtbpy))PF_6 (5.17 µmol, 1.00 mol%), $Ir(ppy)_3$ (5.17 µmol, 1.00 mol%)) and the DSMP system (Fluorescein sodium (7.14 µmol, 1.25 mol%) + TiO_2 (90 mg)) were studied in individual reactions. DMSO (anhydrous, 6 mL) and *N*-tert-butylisopropylamine (BIPA, 271 µL, 1.2 mmol, 3 equiv) were added and the vial was sealed with a septum and Parafilm. The reaction mixture was sonicated for 5-10 min followed by stirring for 5 min to obtain a fine dispersion of the solids. The mixture was then degassed by bubbling Argon for 10 min. The mixture was irradiated with the respective LED lamp with rapid stirring (1400 rpm). After the respective reaction time, one equivalent of 1,3,5-trimethoxybenzene (internal standard 96 mg, 570 µmol) was added and the mixture was stirred for 5 min. An aliquot of the reaction mixture (~200 µL) was filtered, diluted with $CDCl_3$, extracted with 1M HCl and subjected to ^{1}H-NMR analysis. For representative NMR spectra, see Fig. S24.

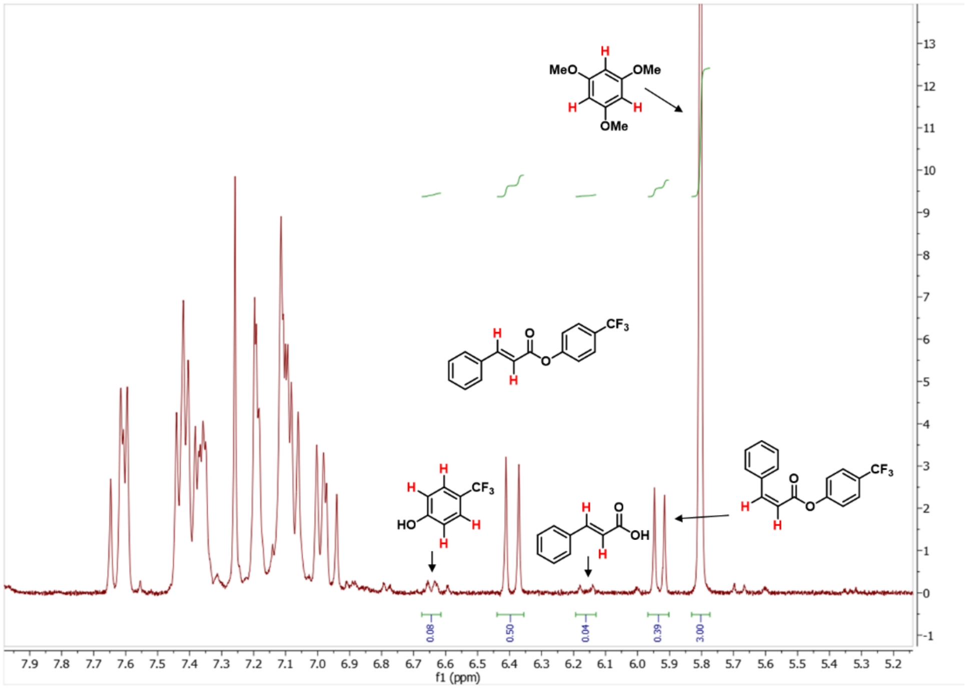

Fig. S24. Representative ^{1}H-NMR spectrum of a crude reaction mixture for determining NMR yields in the DSMP catalyzed C-O arylation of cinnamic acid.

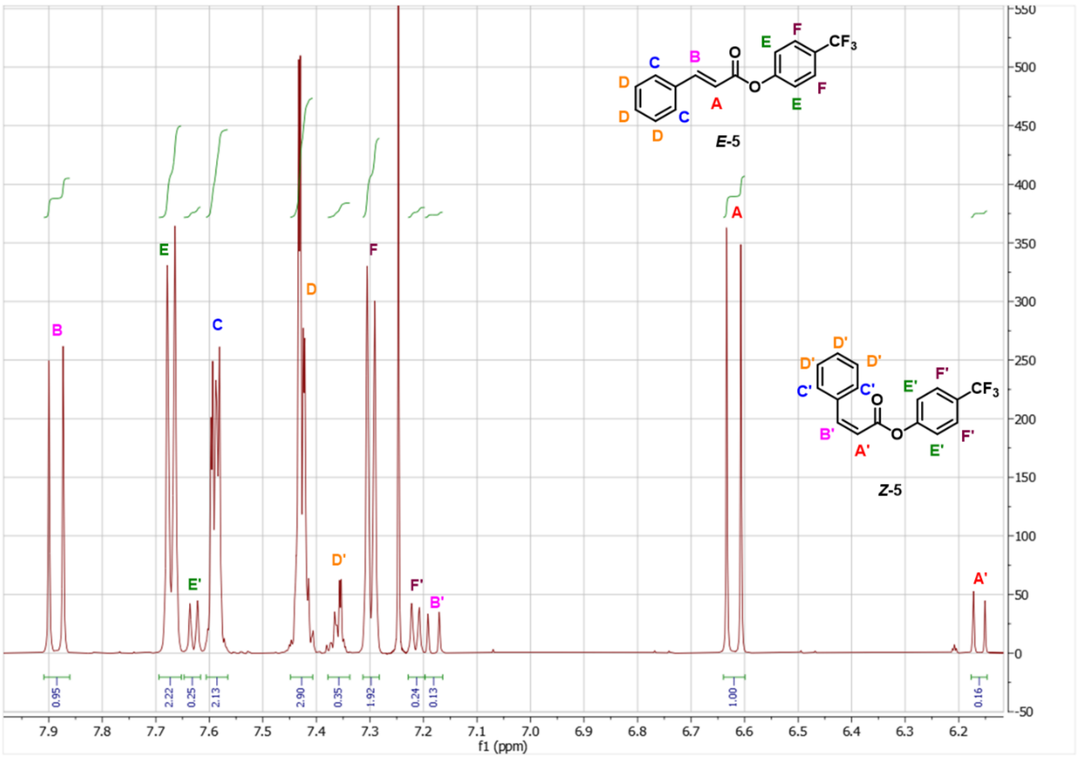

Fig. S25. Representative ^{1}H-NMR spectrum of a crude reaction mixture of *E*- and *Z*- cinnamic acid.

Table S47. Comparison of metallaphotocatalyst systems for the C-O arylation of cinnamic acid.[a]

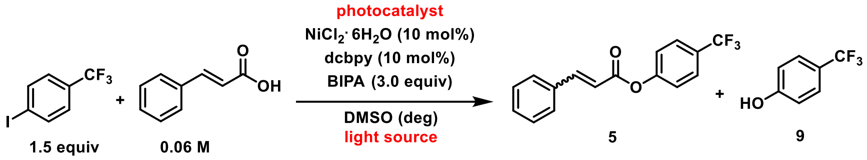

Entry	photocatalyst	Light source [nm]	Time [h]	*E*-5 [%][c]	*Z*-5 [%][c]	9 [%][c]
1	TiO_2 (30 mg) + NaFluo (1.25 mol%)	**525**	**72**	**95**	**n.d.**	**3**
2	TiO_2 (30 mg) + NaFluo (1.25 mol%)	**440**	**35**	**74**	**24**	**6**
3	$Ir[dF(Me)ppy]_2(dtbbpy))PF_6$ (1.00 mol%)	440	1	52	36	9
4	$Ir[dF(CF_3)ppy]_2(dtbpy))PF_6$ (1.00 mol%)	440	1	48	38	16
5	$Ir(ppy)_3$ (1.00 mol%)	440	1	70	22	20
6	$Ir(ppy)_3$ (1.00 mol%)	525	2	78	24	6

[a]Reaction conditions: 4-Iodobenzotrifluoride (285,4 µmol), *trans* cinnamic acid (190.3 µmol), Ir catalyst (1.90 µmol), Fluorescein sodium (2.4 µmol),), TiO_2 (30 mg), $NiCl_2 \cdot 6H_2O$ (19.0 µmol) and dcbpy (19.0 µmol) in DMSO (anhydrous, 3 mL), BIPA (570.8 µmol), 440 nm blue LED (100% power) at RT. [c]NMR yields determined by ^1H-NMR using 1,3,5-trimethoxybenzene as internal standard. [d] 525 nm LED (100%) instead of 440 nm LED. NaFluo = Fluorescein sodium.dcbpy = 2,2′-bipyridine-4,4′-dicarboxylic acid. BIPA = *N*-*tert*-butylisopropylamine. n.d. = not detected. deg = degassed

The reaction from table S47, Entry 1 was isolated on a larger scale for product characterization: An oven dried vial (19 x 100 mm) equipped with a stir bar was charged with *trans* cinnamic acid (84.5 mg, 570 µmol, 1.0 equiv), 4-iodobenzotrifluoride (125.6 µL, 855 µmol, 1.5 equiv), $NiCl_2 \cdot 6H_2O$ (13.6 mg, 57 µmol, 10 mol%), 2,2′-bipyridine-4,4′-dicarboxylic acid (dcbpy. 13.9 mg, 57 µmol, 10 mol%), fluorescein sodium (7.14 µmol, 1.25 mol%), and TiO_2 (90 mg). DMSO (anhydrous, 6 mL) and *N*-tert-butylisopropylamine (BIPA, 271 µL, 1.2 mmol, 3 equiv) were added and the vial was sealed with a septum and Parafilm. The reaction mixture was sonicated for 5-10 min followed by stirring for 5 min to obtain a fine dispersion of the solids. The mixture was then degassed by bubbling Argon for 10 min. The mixture was irradiated with the respective LED lamp with rapid stirring (1400 rpm). After the respective reaction time, one equivalent of 1,3,5-trimethoxybenzene (internal standard 96 mg, 570 µmol) was added and the mixture was stirred for 5 min. An aliquot of the reaction mixture (~200 µL) was filtered, diluted with $CDCl_3$, extracted with 1M HCl and subjected to ^{1}H-NMR analysis. The NMR sample was combined with the reaction mixture, diluted with H_2O (40 mL) and extracted with dichloromethane (3 x 30 mL). The combined organic phases were washed with brine (50 mL), dried over Na_2SO_4 and concentrated. The product was purified by flash column chromatography (SiO_2, Hexane/EtOAc elution gradient of 0-20%) on a Grace Reveleris system using a 12 g cartridge. The title compound was isolated as a white solid in 90% yield (Reaction time: 72 h, 149.92 mg, 513.0 µmol).

***E*-4-(Trifluoromethyl)phenyl cinnamate *E*-5:** ^{1}H NMR (400 MHz, $CDCl_3$) δ. 7.92 (d, J = 16.0 Hz, 1H), 7.69 (d, J = 8.4 Hz, 2H), 7.61 (dt, J = 6.7, 2.3 Hz, 2H), 7.45 (dd, J = 5.1, 2.0 Hz, 3H), 7.32 (d, J = 8.2 Hz, 2H), 6.65 (d, J = 16.0 Hz, 1H). ^{13}C NMR (101 MHz, $CDCl_3$) δ 164.92, 153.42, 147.53, 134.05, 131.10, 129.17, 128.51, 128.26 (s, J = 32.74 Hz), 126.89 (q, J = 3.8 Hz), 125.39 (s, J = 272.17 Hz), 122.27, 116.7. ^{19}F NMR (377 MHz, $CDCl_3$) δ -62.21 ppm. HRMS-EI (m/z) $[M^*]^+$ calcd for $C_{16}H_{11}F_3O_2$: 292.0711; found: 292.0718.

These data are in full agreement with those previously published in the literature (*27*).

Table S48. Control studies isomerization of 4-(Trifluoromethyl)phenyl cinnamate.[a]

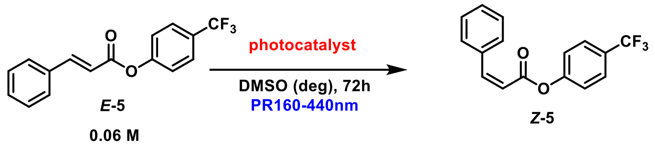

Entry	photocatalyst	***E*-5 : *Z*-5**[c]
1	--	1 : 0.16
2	NaFluo (1.25 mol%)	1 : 0.11
3	TiO_2 (30 mg)	1 : 0.12

[a] Reaction conditions: *E*-4-(Trifluoromethyl)phenyl cinnamate (190.3 µmol), Fluorescein sodium (2.4 µmol),), TiO_2 (30 mg), in DMSO (anhydrous, 3 mL), 440 nm blue LED (100% power), 72h. [c] Determined by ^{1}HNMR. NaFluo = Fluorescein sodium. n.d. = not detected. deg = degassed

11 References

1. J. A. Milligan, J. P. Phelan, S. O. Badir, G. A. Molander, Alkyl Carbon-Carbon Bond Formation by Nickel/Photoredox Cross-Coupling. *Angew. Chem. Int. Ed.* **58**, 6152-6163 (2019).
2. J. Twilton *et al.*, The merger of transition metal and photocatalysis. *Nat. Rev. Chem.* **1**, 1-18 (2017).
3. C. Cavedon, P. H. Seeberger, B. Pieber, Photochemical Strategies for Carbon–Heteroatom Bond Formation. *Eur. J. Org. Chem.* **10**, 1379-1392 (2020).
4. J. Lu *et al.*, Donor–Acceptor Fluorophores for Energy-Transfer-Mediated Photocatalysis. *J. Am. Chem. Soc.* **140**, 13719-13725 (2018).
5. F. Glaser, C. Kerzig, O. S. Wenger, Multi-Photon Excitation in Photoredox Catalysis: Concepts, Applications, Methods. *Angew. Chem. Int. Ed.* **59**, 2-21 (2020).
6. B. D. Ravetz *et al.*, Photoredox catalysis using infrared light via triplet fusion upconversion. *Nature.* **565**, 343-346 (2019).
7. B. D. Ravetz *et al.*, *https://doi.org/10.26434/chemrxiv.12124215.v1*. (2020).
8. N. A. Romero, D. A. Nicewicz, Organic Photoredox Catalysis. *Chem. Rev.* **116**, 10075-10166 (2016).
9. A. Hagfeldt, G. Boschloo, L. Sun, L. Kloo, H. Pettersson, Dye-Sensitized Solar Cells. *Chem. Rev.* **110**, 6595-6663 (2010).
10. J. Willkomm *et al.*, Dye-sensitised semiconductors modified with molecular catalysts for light-driven H2 production. *Chem. Soc. Rev.* **45**, 9-23 (2016).
11. A. Hagfeldt, M. Graetzel, Light-Induced Redox Reactions in Nanocrystalline Systems. *Chem. Rev.* **95**, 49-68 (1995).
12. E. R. Welin, C. Le, D. M. Arias-Rotondo, J. K. McCusker, D. W. C. MacMillan, Photosensitized, energy transfer-mediated organometallic catalysis through electronically excited nickel(II). *Science* **355**, 380-385 (2017).
13. X. Zhu *et al.*, Lead halide perovskites for photocatalytic organic synthesis. *Nat. Commun.* **10**, 2843 (2019).
14. B. Pieber *et al.*, Semi-heterogeneous Dual Nickel/Photocatalysis using Carbon Nitrides: Esterification of Carboxylic Acids with Aryl Halides. *Angew. Chem. Int. Ed.* **58**, 9575-9580 (2019).
15. M. S. Oderinde, M. Frenette, D. W. Robbins, B. Aquila, J. W. Johannes, Photoredox Mediated Nickel Catalyzed Cross-Coupling of Thiols With Aryl and Heteroaryl Iodides via Thiyl Radicals. *J. Am. Chem. Soc.* **138**, 1760-1763 (2016).
16. E. B. Corcoran *et al.*, Aryl amination using ligand-free Ni(II) salts and photoredox catalysis. *Science* **353**, 279-283 (2016).

17. C. Remeur, C. B. Kelly, N. R. Patel, G. A. Molander, Aminomethylation of Aryl Halides Using α-Silylamines Enabled by Ni/Photoredox Dual Catalysis. *ACS Catalysis* **7**, 6065-6069 (2017).
18. T. Lei *et al.*, General and Efficient Intermolecular [2+2] Photodimerization of Chalcones and Cinnamic Acid Derivatives in Solution through Visible-Light Catalysis. *Angew. Chem. Int. Ed.* **56**, 15407-15410 (2017).
19. P. Shu *et al.*, Synthesis of (Z)-Cinnamate Derivatives via Visible-Light-Driven E-to-Z Isomerization. *SynOpen* **03**, 103-107 (2019).
20. K. Neuthe *et al.*, Phosphonic acid anchored ruthenium complexes for ZnO-based dye-sensitized solar cells. *Dyes Pigments* **104**, 24-33 (2014).
21. Y. Shigeta, A. Kobayashi, M. Yoshida, M. Kato, Crystal Engineering of Vapochromic Porous Crystals Composed of Pt(II)-Diimine Luminophores for Vapor-History Sensors. *Crys. Growth. Des.* **18**, 3419-3427 (2018).
22. H. C. Brown, J. V. B. Kanth, P. V. Dalvi, M. Zaidlewicz, Molecular Addition Compounds. 15. Synthesis, Hydroboration, and Reduction Studies of New, Highly Reactive tert-Butyldialkylamine−Borane Adducts. *J. Org. Chem.* **64**, 6263-6274 (1999).
23. https://www.kessil.com/photoreaction/index.php
24. S. Gisbertz, B. Pieber, Heterogeneous Photocatalysis in Organic Synthesis. *ChemPhotoChem*. **4**, 1-21 (2020).
25. C. Cavedon, A. Madani, P. H. Seeberger, B. Pieber, Semiheterogeneous Dual Nickel/Photocatalytic (Thio)etherification Using Carbon Nitrides. *Org. Lett.* **21**, 5331-5334 (2019).
26. S. Gisbertz, S. Reischauer, B. Pieber, Overcoming Limitations in Dual Photoredox/Nickel catalyzed C–N Cross-Couplings due to Catalyst Deactivation. *Nat. Catal.* in press. *doi: 10.1038/s41929-020-0473-6*
27. J. S. E. Ahlin, P. A. Donets, N. Cramer, Nickel(0)-Catalyzed Enantioselective Annulations of Alkynes and Arylenoates Enabled by a Chiral NHC Ligand: Efficient Access to Cyclopentenones. *Angew. Chem. Int. Ed.* **53**, 13229-13233 (2014).

12 Copies of NMR spectra

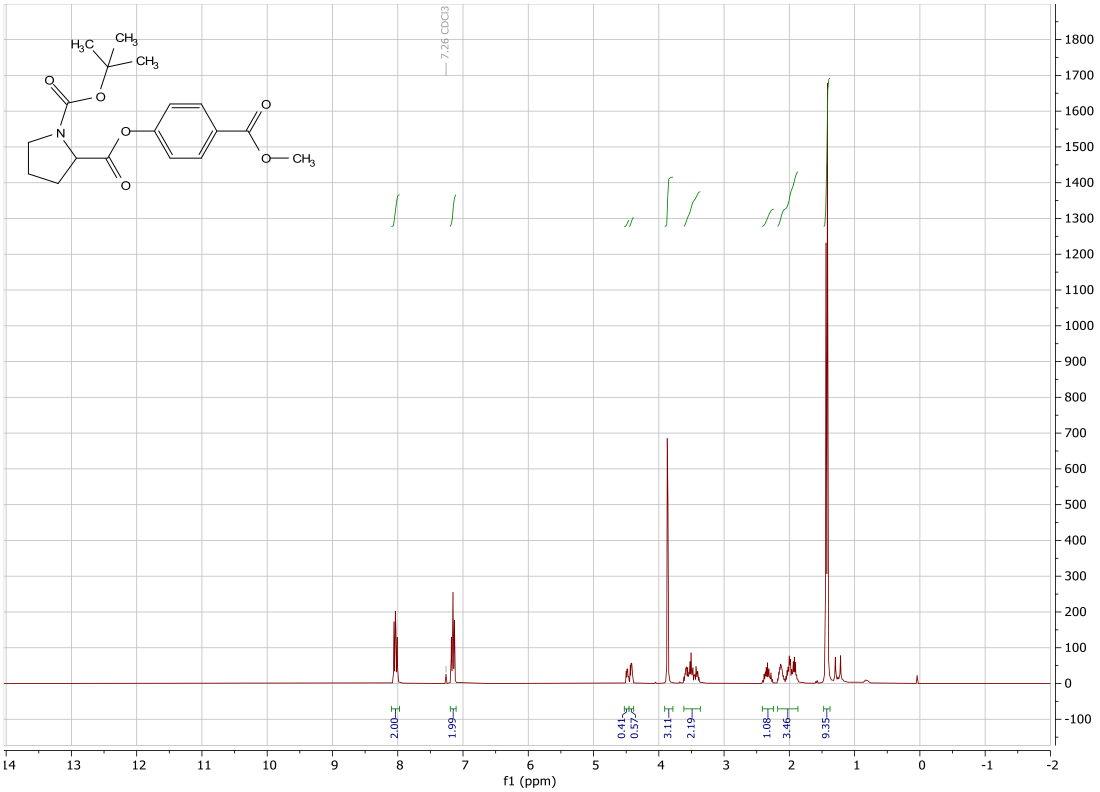

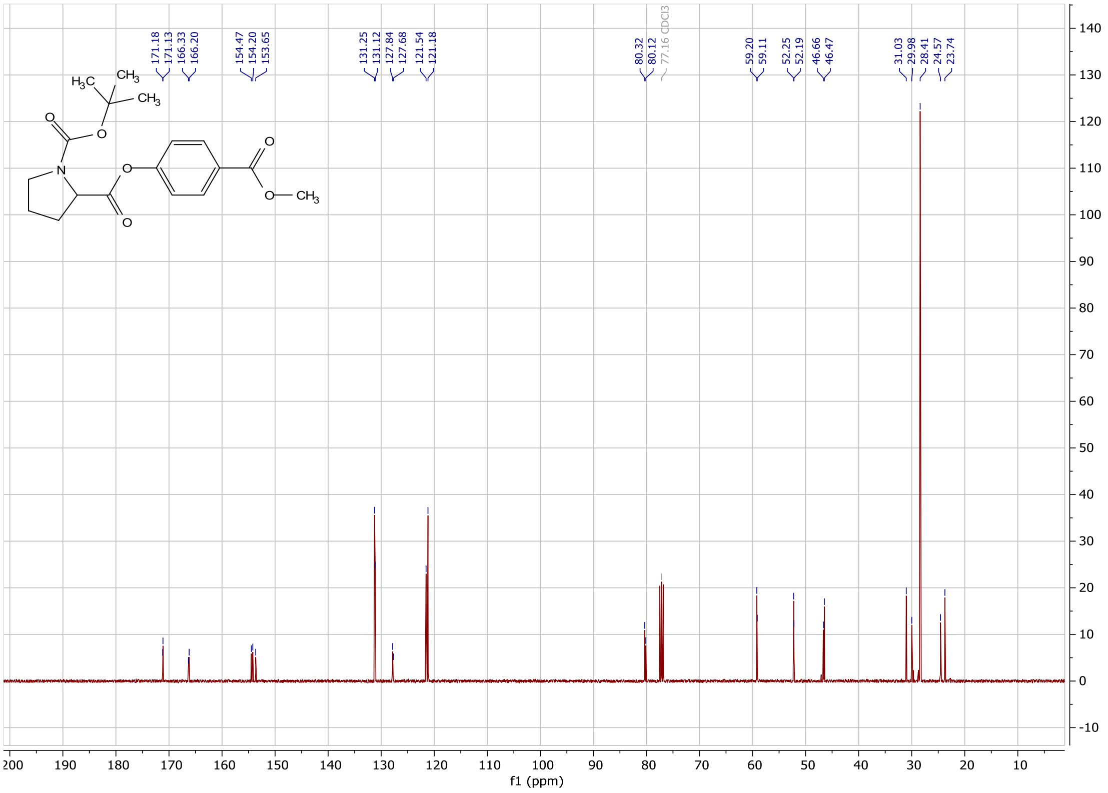

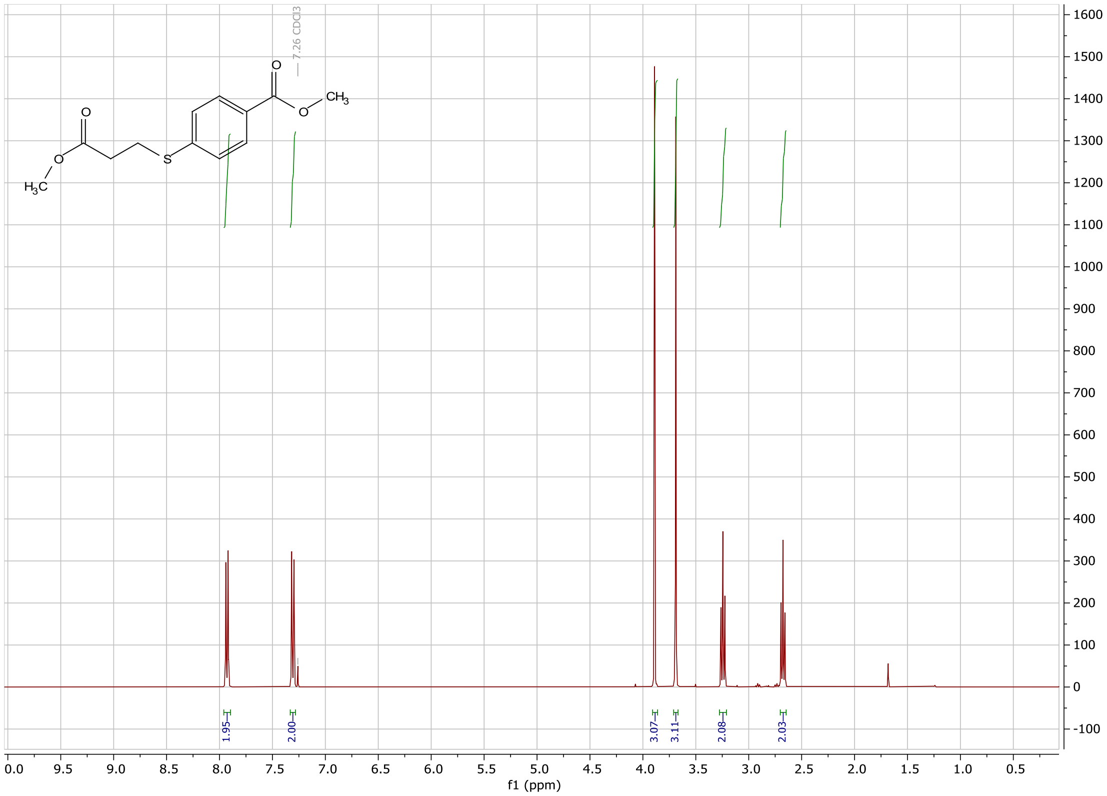

7.26 CDCl3
1.95
2.00
3.07
3.11
2.08
2.03
f1 (ppm)
0.0 9.5 9.0 8.5 8.0 7.5 7.0 6.5 6.0 5.5 5.0 4.5 4.0 3.5 3.0 2.5 2.0 1.5 1.0 0.5
1600 1500 1400 1300 1200 1100 1000 900 800 700 600 500 400 300 200 100 0 -100
O
O
CH3
S
O
O
H3C

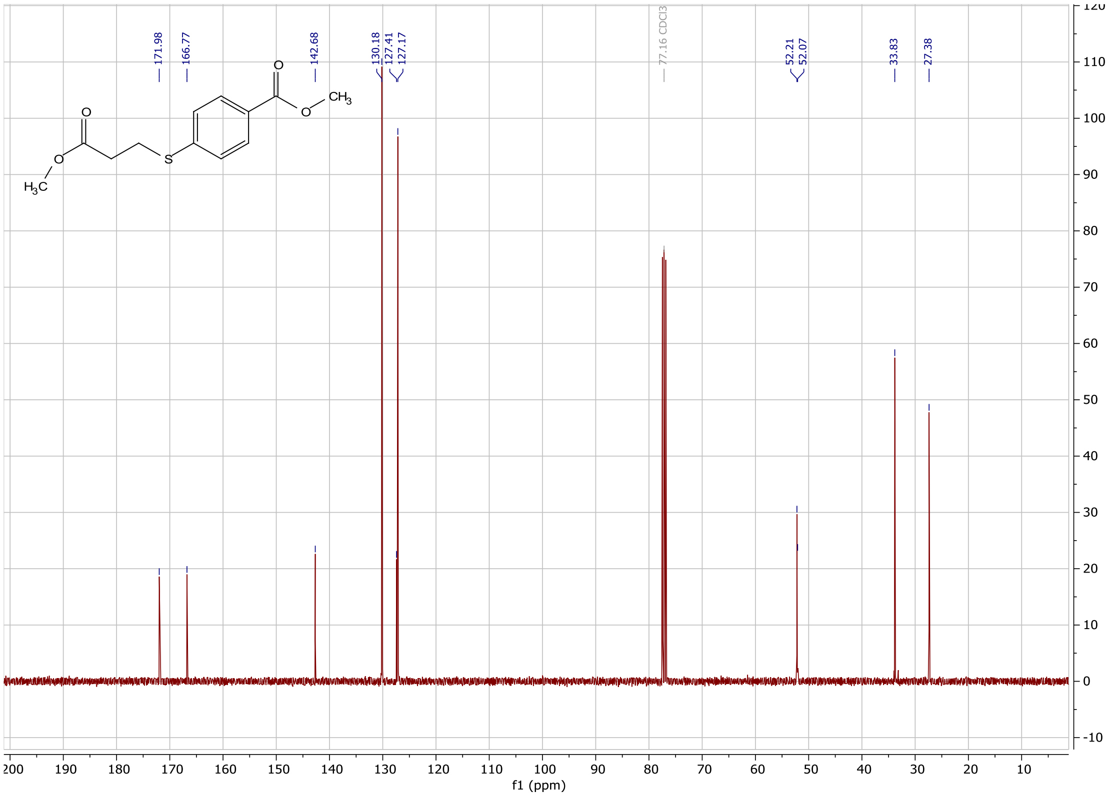

171.98
166.77
142.68
130.18
127.41
127.17
77.16 CDCl3
52.21
52.07
33.83
27.38
f1 (ppm)
200 190 180 170 160 150 140 130 120 110 100 90 80 70 60 50 40 30 20 10
120 110 100 90 80 70 60 50 40 30 20 10 0 -10
O
O
CH3
S
O
O
H3C

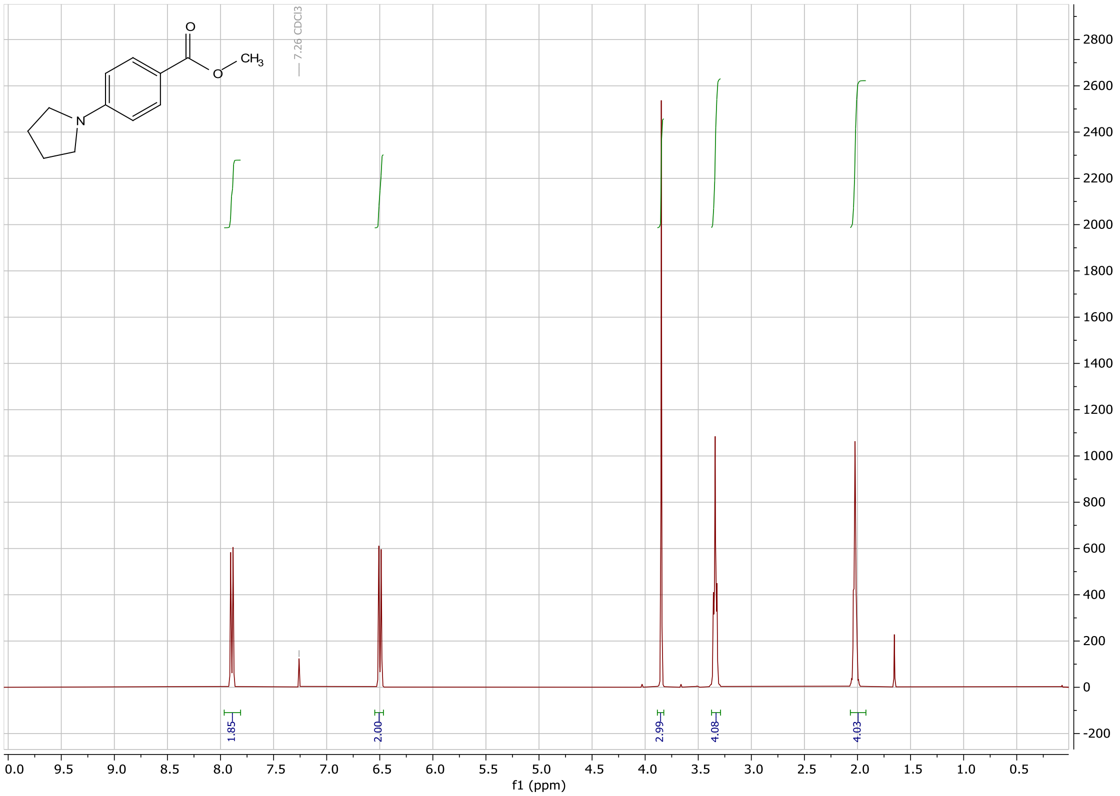

O
CH3
O
N
7.26 CDCl3
1.85
2.00
2.99
4.08
4.03
f1 (ppm)
0.0
9.5
9.0
8.5
8.0
7.5
7.0
6.5
6.0
5.5
5.0
4.5
4.0
3.5
3.0
2.5
2.0
1.5
1.0
0.5
2800
2600
2400
2200
2000
1800
1600
1400
1200
1000
800
600
400
200
0
-200

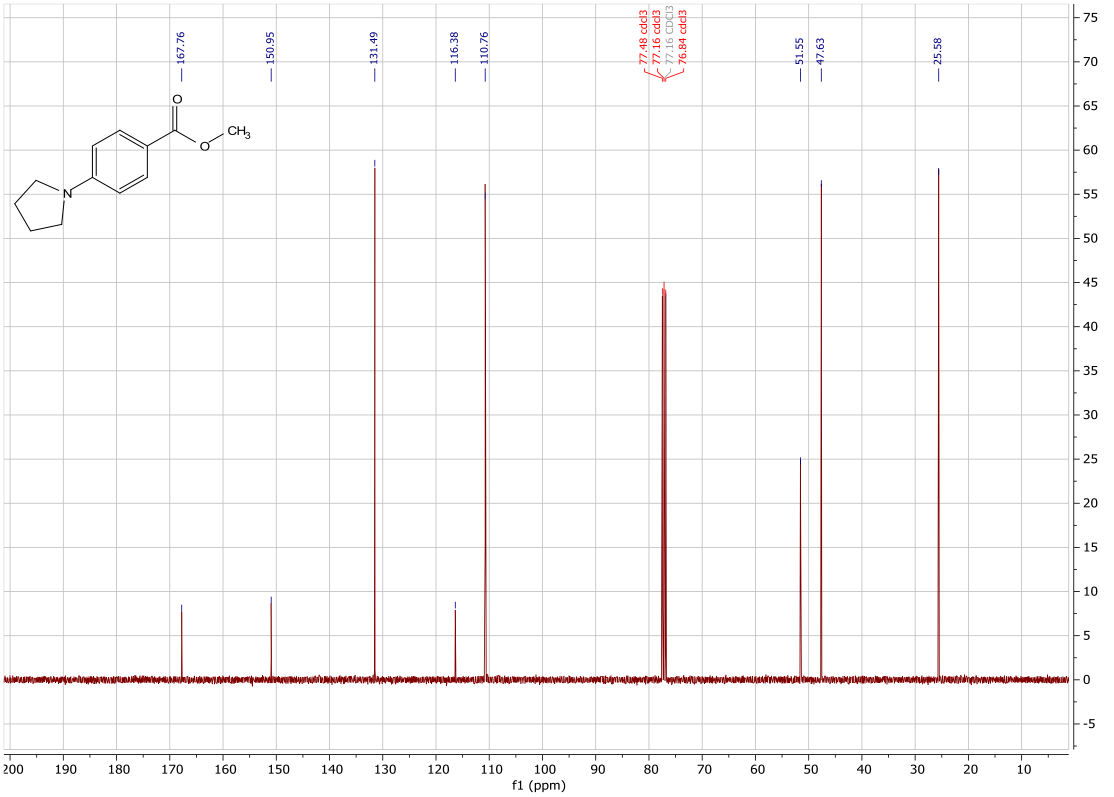

167.76
150.95
131.49
116.38
110.76
77.48 cdcl3
77.16 cdcl3
77.16 CDCl3
76.84 cdcl3
51.55
47.63
25.58
O
CH3
O
N
f1 (ppm)
200
190
180
170
160
150
140
130
120
110
100
90
80
70
60
50
40
30
20
10
75
70
65
60
55
50
45
40
35
30
25
20
15
10
5
0
-5

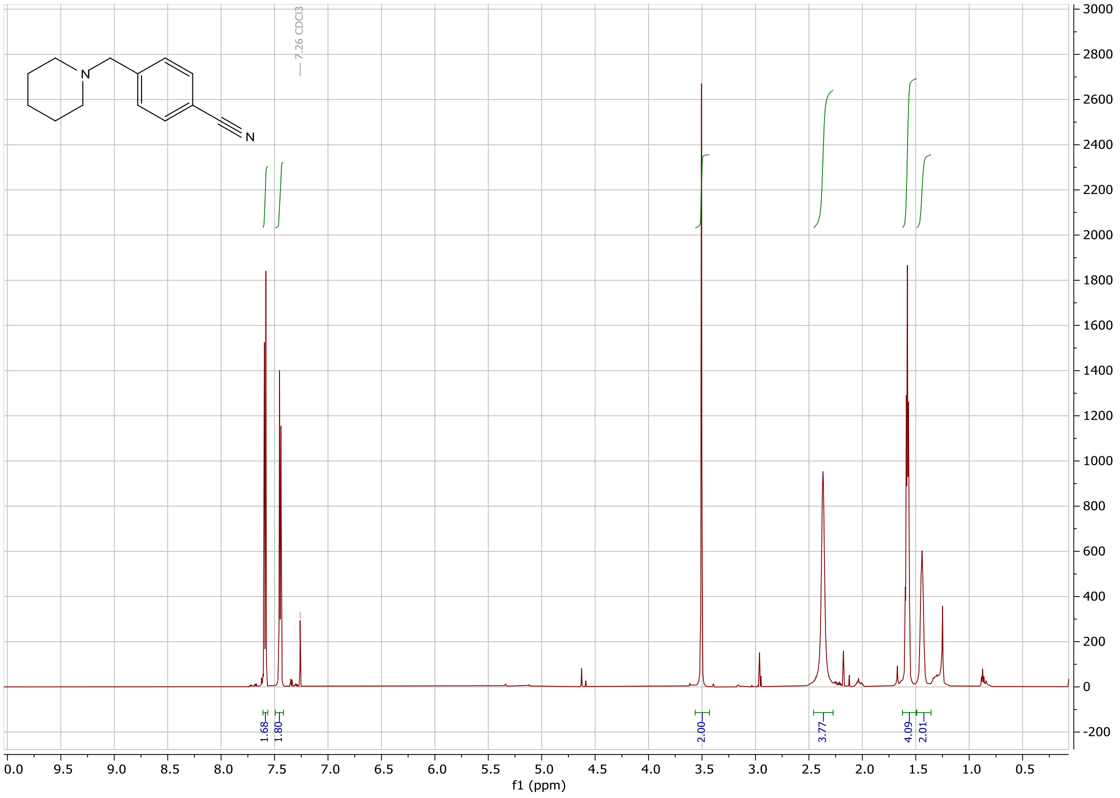
N
N
7.26 CDCl3
1.68
1.80
2.00
3.77
4.09
2.01
10.0 9.5 9.0 8.5 8.0 7.5 7.0 6.5 6.0 5.5 5.0 4.5 4.0 3.5 3.0 2.5 2.0 1.5 1.0 0.5
f1 (ppm)
3000 2800 2600 2400 2200 2000 1800 1600 1400 1200 1000 800 600 400 200 0 -200

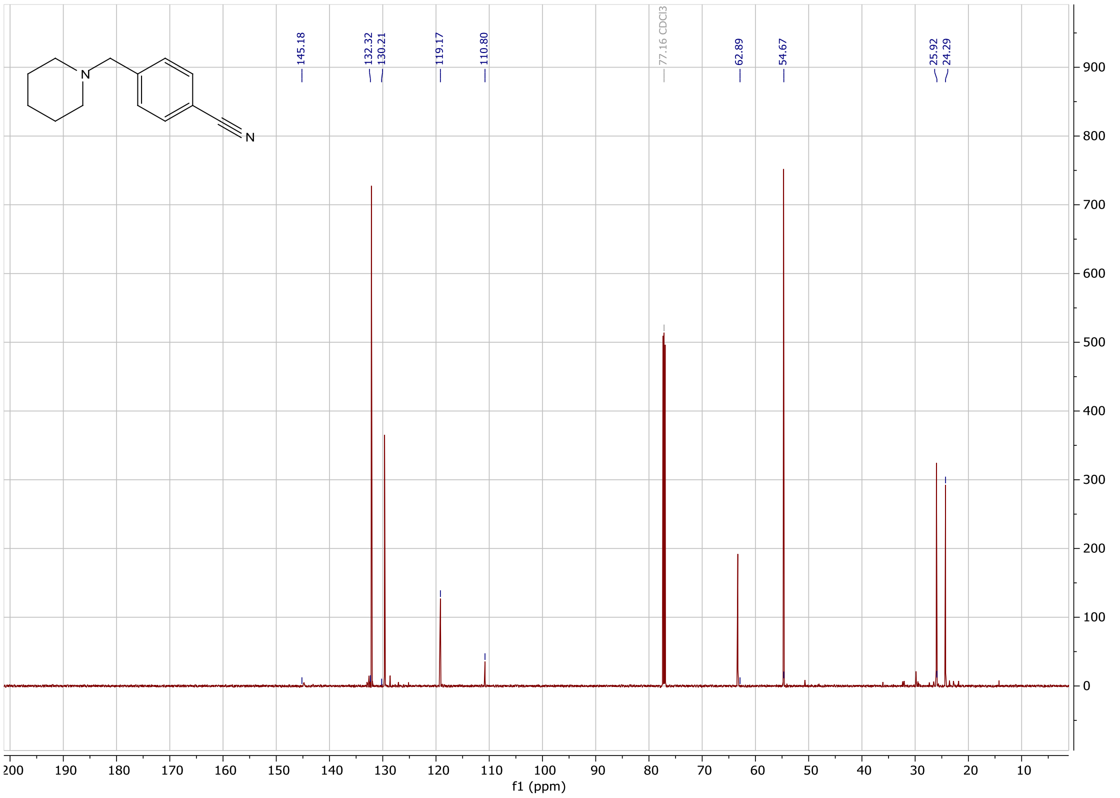
N
N
145.18
132.32
130.21
119.17
110.80
77.16 CDCl3
62.89
54.67
25.92
24.29
200 190 180 170 160 150 140 130 120 110 100 90 80 70 60 50 40 30 20 10
f1 (ppm)
900 800 700 600 500 400 300 200 100 0

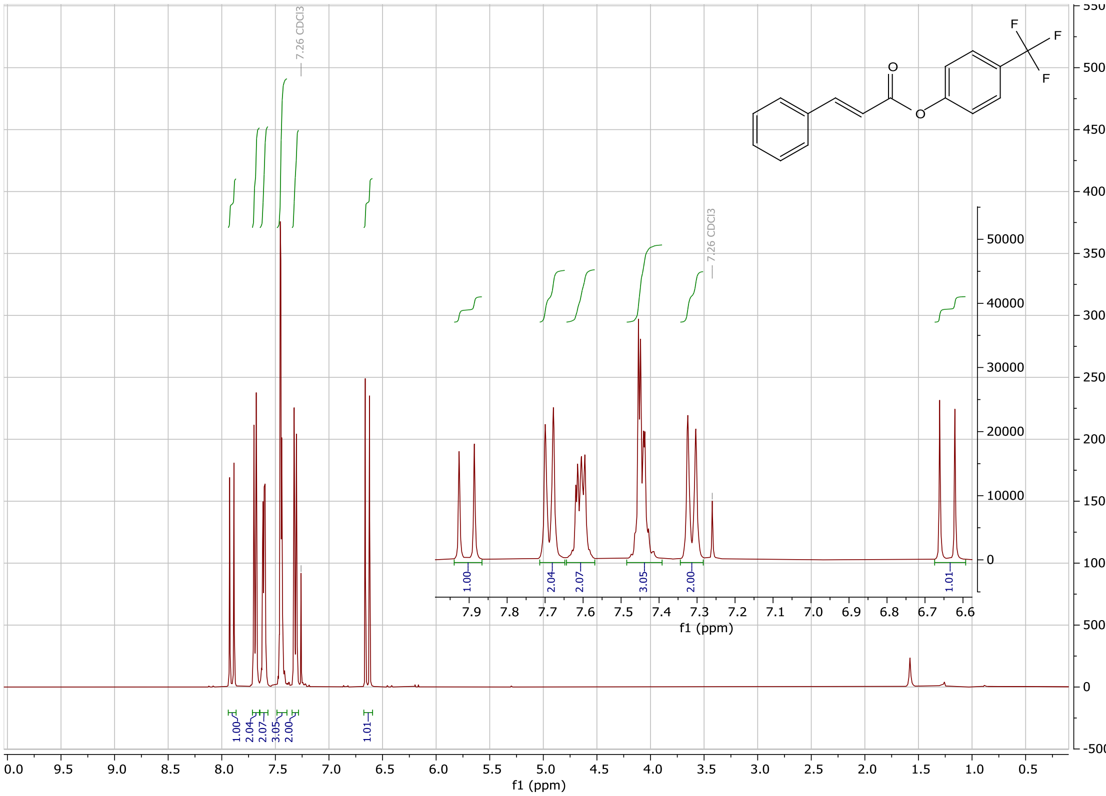
7.26 CDCl3
1.00
2.04
2.07
3.05
2.00
1.01
f1 (ppm)
F
F
F
O
O

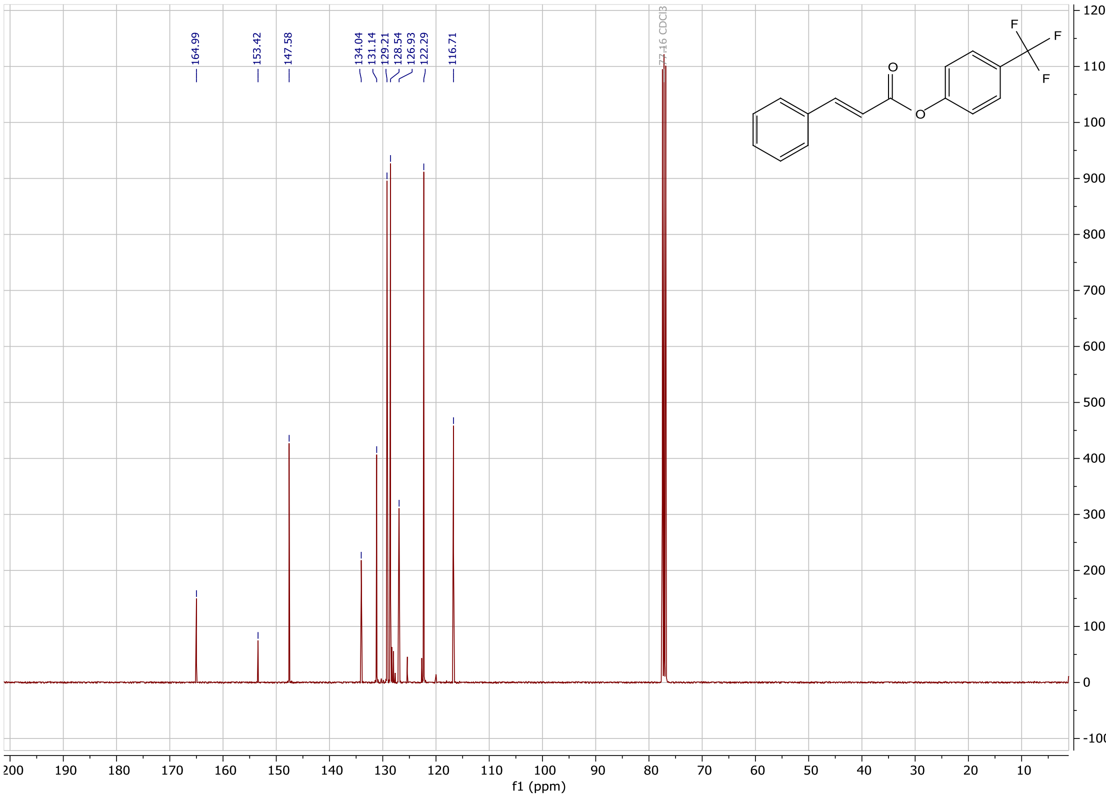
164.99
153.42
147.58
134.04
131.14
129.21
128.54
126.93
122.29
116.71
77.16 CDCl3
f1 (ppm)
F
F
F
O
O

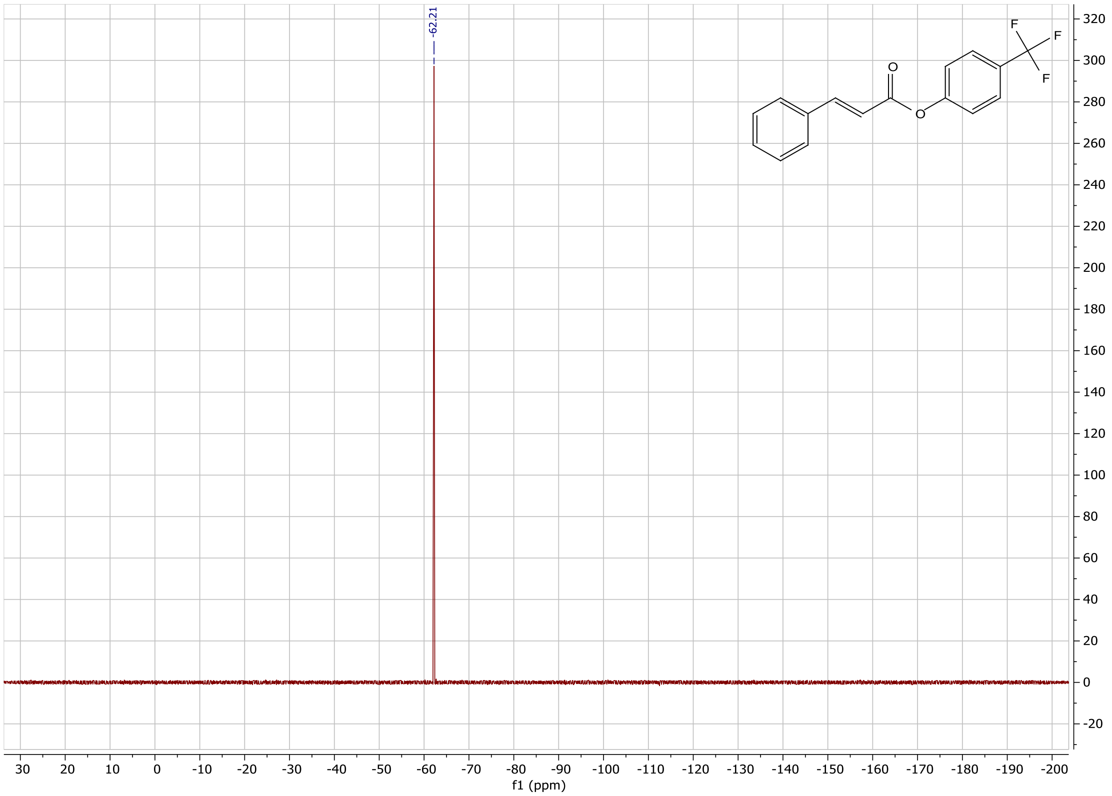
-62.21
O
O
F
F
F
320
300
280
260
240
220
200
180
160
140
120
100
80
60
40
20
0
-20
30 20 10 0 -10 -20 -30 -40 -50 -60 -70 -80 -90 -100 -110 -120 -130 -140 -150 -160 -170 -180 -190 -200
f1 (ppm)